PLASMA STERILIZATION TECHNOLOGY

FOR SPACECRAFT APPLICATIONS

FINAL REPORT

September 1975

Prepared for

CALIFORNIA INSTITUTE OF TECHNOLOGY
JET PROPULSION LABORATORY
Contract Number 953647

"This work was performed for the Jet Propulsion Laboratory, California Institute of Technology, as sponsored by the National Aeronautics and Space Administration under contract NAS7-100."

Prepared by

S. J. Fraser
R. L. Olson, Ph.D.
W. M. Leavens, Ph.D.

BOEING AEROSPACE COMPANY
(a Division of The Boeing Company)
Seattle, Washington

ABSTRACT

PLASMA STERILIZATION TECHNOLOGY FOR SPACECRAFT APPLICATIONS

This contract consisted of four study phases that provided information on the application of plasma gas technology for solving problems associated with planetary quarantine.

The first phase determined that helium plasma, generated at reduced pressure (0.2 mm Hg) was the most efficient for killing microbial spores.

Phase II expanded the types of organisms tested for evaluation of helium plasma, and the results demonstrated that all of the organisms tested were susceptible to plasma. Plasma diagnostics determined that the primary kill mechanism was energetic ultraviolet irradiation. High electron temperatures were responsible for physical disruption of microbial cells.

During Phase III, helium plasma was demonstrated to be effective for sterilizing long capillary tubes of varied diameters. Plasma gas was shown to be an efficient surface sterilizer.

Phase IV analyzed the effect of plasma on spacecraft materials. The results showed that the plasma process was compatible with most tested materials.

Results of the four completed phases demonstrated that plasma gas, specifically helium plasma, is a highly effective sterilant and,as such, is a technique that can be applied to remedy specific planetary quarantine, and other, sterilizing problems.

TABLE OF CONTENTS

SECTION 1

PLASMA STERILIZATION TECHNOLOGY FOR SPACECRAFT APPLICATIONS

SUMMARY

PLASMA STERILIZATION TECHNOLOGY
FOR SPACECRAFT APPLICATIONS

This is the final report submitted by The Boeing Company to the Jet Propulsion Laboratory on JPL Contract Number 953647. Four research phases were conducted for the contract that extended from May 1973 through September 1975. These phases are discussed separately in this report in Sections II, III, IV and V respectively. A detailed design of the plasma generating apparatus is included in Section VI. A summary of the total contract effort is presented in Section I.

INTRODUCTION

Traditionally, sterilization and decontamination of spacecraft components have been accomplished by heat or by chemical solutions. Certain materials and complex equipment often suffer a loss in reliability due to heat damage or chemical incompatibility. In addition, these traditional methods are not readily adaptable for use in space, i.e., on interplanetary sample return missions.

Plasma cleaning and sterilization involves exciting a gas and passing it over the material to be sterilized. The apparatus used includes a gas exciter (radio frequency), a sterilization chamber and vacuum pump. In operation, specimens are placed in the sterilization chamber, pressure reduced, and excited gas is introduced. Sterilization occurs. The plasma process does not appear to degrade materials which have been tested to date and, in addition, does not significantly raise the temperature of the object being sterilized. The objective of this investigation was to develop and apply plasma gas sterilization technology to problems associated with planetary quarantine.

The program consisted of four phases. The approach of Phase I was to obtain data that defined the effective sterilizing ranges of four separate gases with respect to power and pressure. The second phase was conducted to determine the lethal constituents of a plasma environment. The effectiveness of plasma against a diverse group of microorganisms was also investigated. The third and fourth phases respectively determined the penetrating efficiency of plasmas for sterilization and the compatibilities of spacecraft materials with a plasma environment.

Also included in this documentation is a detailed design of the plasma sterilizer used throughout the study.

PHASE I

RADIO FREQUENCY GENERATED PLASMAS OF ARGON, NITROGEN, OXYGEN, AND HELIUM

Specific test matrices were designed to define optimum radio frequency (rf) power, the "best" single gas, and chamber pressure required for plasma sterilization.

Plasmas of argon, nitrogen, oxygen and helium were generated at pressures of 0.2 through 1.0 mm Hg. RF power ranged from 50 to 300 watts.

Spores of the organism Bacillus subtilis var. niger were exposed at timed intervals to the plasmas and analysis for survivors followed.

The data showed that helium gas, ionized with 300 watts rf at 0.2 mm Hg chamber pressure, was the most efficient combination for killing B. subtilis spores. Also, plasma environment measurements indicated that ultraviolet irradiation that resulted during recombination of the ionized gases was a dominant kill mechanism in plasma.

PHASE II

PLASMA GAS CHARACTERISTICS

Data obtained from Phase I was used to expand the range of microorganisms tested for evaluation of plasma sterilizing properties. In addition, plasmas of mixed gases were studied. Measurements to characterize plasma and to define the lethal constituents were developed.

A variety of typical spacecraft organisms, in addition to fungal spores were selected and exposed to helium plasma for varied time intervals. Analysis for survivors showed that, although death rates varied between microbial types, all of the microorganisms tested were susceptible to the lethal effects of plasma.

The primary mechanism responsible for killing microorganisms was theorized to be energetic ultraviolet irradition, particularly the 21.2 eV resonance line. In support of this, measurements of plasma constituents revealed that high electron temperatures were present and most probably resulted in physical disruption of the integrity of a cell.

Plasma diagnostics were developed that enabled correlation of increased microbial death with increased plasma density (electron temperature).

Plasmas of mixed gases were shown to be less effective in killing bacterial spores than the single gas helium.

PHASE III

PLASMA GAS PENETRATION

Different geometric configurations were exposed to plasma to determine the effectiveness of ionized gas for contacting and sterilizing all surfaces. Contaminated capillary tubing of varied internal diameters (I.D.), and lengths, and mated surfaces were exposed to helium plasma. Analysis for survivors showed that tubing of 0.07 cm I.D. and 12.0 cm in length was sterilized. The initial spore contamination level of 10^4 was reduced to 0 within one hour of plasma treatment. Results of contaminated mated surfaces showed a slight reduction from original numbers, but the helium plasma was unable to penetrate and sterilize mated surfaces at the exposure levels tested.

PHASE IV

EFFECT OF PLASMA GAS ON SELECTED SPACECRAFT MATERIALS

Spacecraft materials were subjected to a plasma environment to determine material compatibility with the process. Specific analyses were conducted for comparisons of before and after plasma treated specimens. These included reflectance, transmission, mechanical testing, electrical resistivity, and visual appearance.

The analyses showed that, overall, helium and oxygen plasmas did not alter the measured properties of most test materials. Exceptions were noted for three films tested for mechanical tension and in a black coating analyzed for reflectance after plasma exposure. The degree of changes ranged from slight to marked.

Evaluation of compatibility of materials with plasma should be determined by comparison of alterations in similar properties of a material after other sterilization methods and by the predicted usage of the material.

SECTION II

PHASE I

RADIO FREQUENCY GENERATED PLASMAS OF ARGON, NITROGEN, OXYGEN AND HELIUM

PHASE I

TABLE OF CONTENTS

PHASE I

1.0 PURPOSE

This phase of the program was concerned with defining and comparing the effective sterilizing ranges for different single gases as related to radio frequency power (rf) and vacuum pressure. Also, theories concerning the physical nature of plasma were formulated from experimental measurements developed during this phase.

2.0 INTRODUCTION

Previous preliminary Boeing data showed the feasibility of using an argon plasma, generated at low pressure, to kill Bacillus subtilis var. niger spores. RF power values were also shown to affect the rate of spore death. In addition, a study "Evaluation of Plasma Cleaning and Electron Spectroscopy for Reduction of Organic Contamination" (1972, JPL PO GU-561461) demonstrated that plasma was an effective technique for the removal of microorganisms and organic films from surfaces.

3.0 PROCEDURE

Phase I was designed to define, via specific test matrices, optimum rf power and the "best" single gas and chamber pressure required for plasma sterilization. Also, formulation of the theoretical physics of plasmas was initiated. A description of the two tasks that comprised Phase I follows.

3.1 TASK 1 - PLASMA OF SINGLE GASES

The objective of this task was to determine the relative effectiveness of different gas plasmas for sterilizing. Plasmas of argon, helium, nitrogen and oxygen were generated by radio frequency electrodeless excitation. Samples of microorganisms were exposed to the plasma environment and analyses for survivors were performed.

The test equipment used in this study is diagrammed in Figure 1. Gas, monitored by a flowmeter, passed into the discharge region. External copper electrodes excited the gas and initiated ionization. RF power provided the energy coupling into the gas at 13.56 megahertz (FCC requirements). After rf excitation, the gas passed out of the electrode region and the "active" species were carried through the glass sterilization chamber and eventually exhausted. The electronics package, pictured in Figure 2, consisted of an a-c power supply #516F-2, transmitter #32S-3A, rf linear amplifier 30S-1, antenna tuner #180S-1, and a directional wattmeter #302C-3 (Collins Radio Company, Cedar Rapids,Iowa).

In operation, test samples were positioned in the sterilization chamber, the pressure reduced, test gas flow adjusted, and then power applied to excite the gas via the external rf coupled electrodes. The configuration of the plasma sterilizer was such that ionized gas flowed over the samples through the chamber (Figure 3).

Parametric values for rf power, chamber pressure, gas flow and exposure time were varied. The test matrix is shown in Table 1. The gases, argon and helium, were each tested under these variables. The gases, oxygen and nitrogen, were found to produce less effective sterilizing plasmas during equipment checkout. Therefore, only the longest test exposure, 15 minutes, was studied. Both of these latter gases were tested as shown in Table 2.

The effectiveness of plasma gas for sterilizing was determined by exposing a controlled number of the sporeformer Bacillus subtilis var. niger to the plasma and analyzing for survivors. Test samples were prepared by inoculating sterile, stainless steel planchets, 1 inch in diameter, with

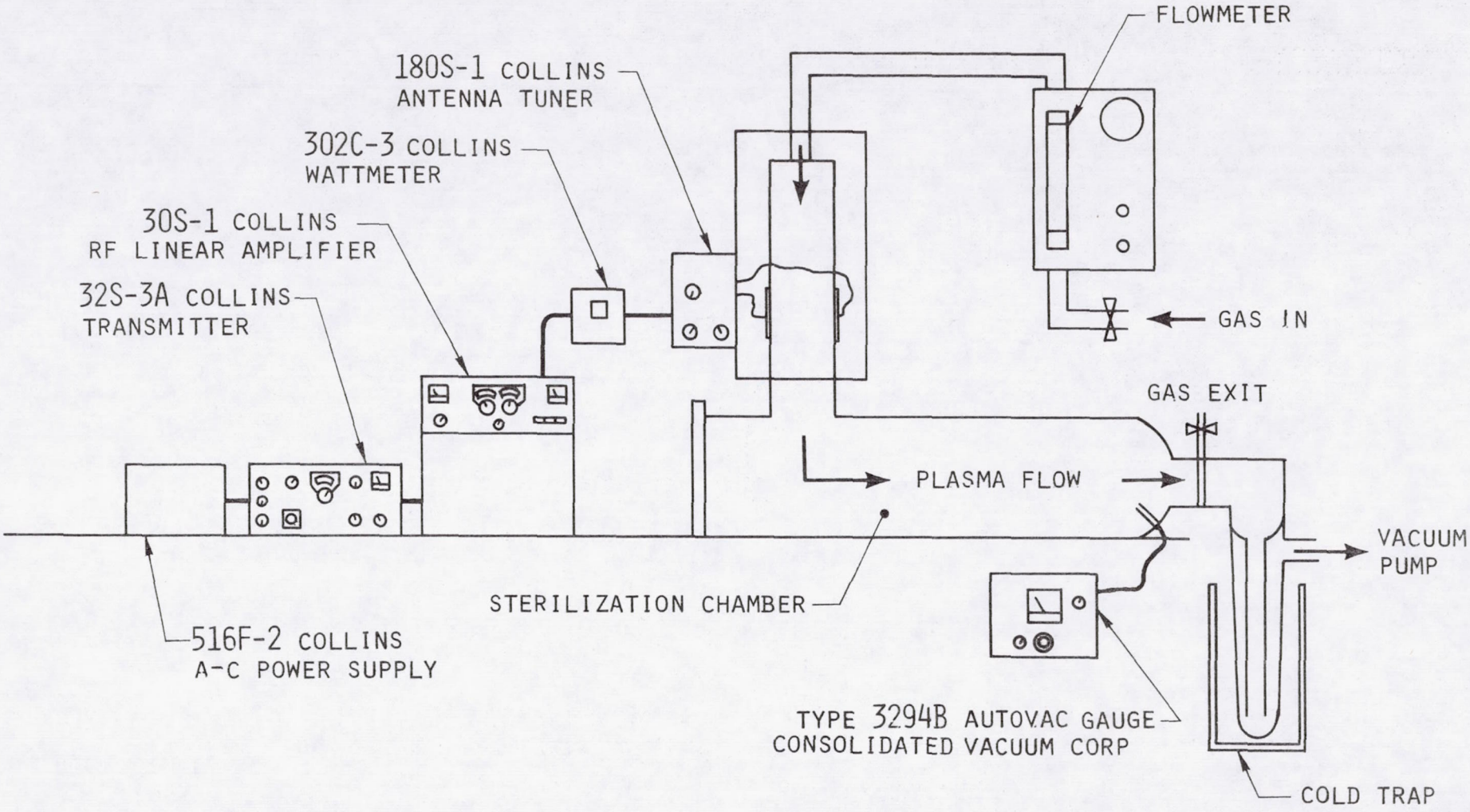

FIGURE 1: PLASMA STERILIZER RESEARCH UNIT

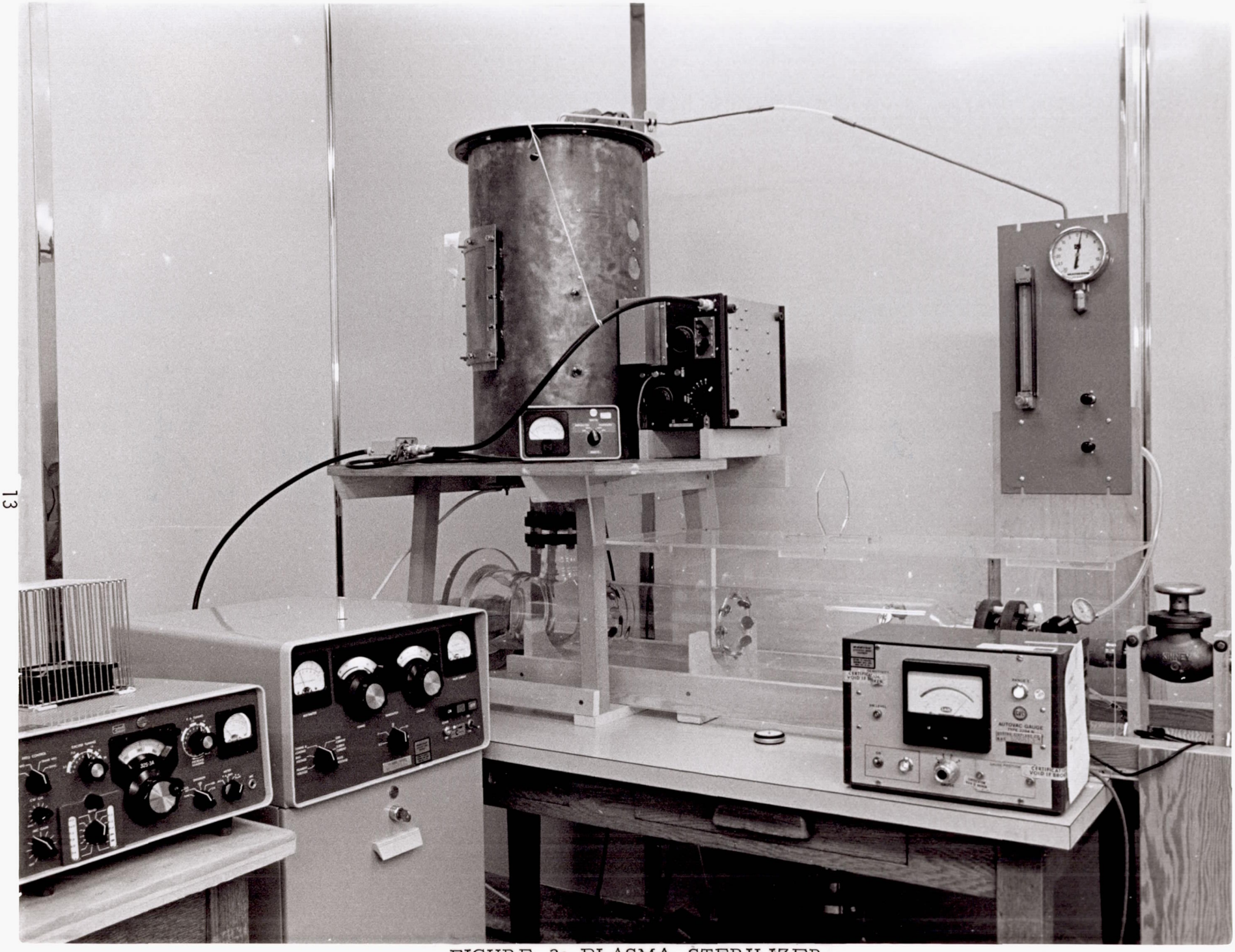

FIGURE 2: PLASMA STERILIZER

Page intentionally left blank

TABLE 1: TEST MATRIX FOR ARGON AND HELIUM

RF POWER WATTS	EXPOSURE TIME, MINUTES	CHAMBER PRESSURE, MM Hg					
		0.2		0.5		1.0	
		GAS FLOW CC/MIN.					
		10	20	10	20	10	20
50	5	A-1*	A-4	B-7	B-10	C-13	C-16
	10	A-2	A-5	B-8	B-11	C-14	C-17
	15	A-3	A-6	B-9	B-12	C-15	C-18
150	5	D-19	D-22	E-25	E-28	F-31	F-34
	10	D-20	D-23	E-26	E-29	F-32	F-35
	15	D-21	D-24	E-27	E-30	F-33	F-36
300	5	G-37	G-40	H-43	H-46	J-49	J-52
	10	G-38	G-41	H-44	H-47	J-50	J-53
	15	G-39	G-42	H-45	H-48	J-51	J-54

* Test Number

TABLE 2: TEST MATRIX FOR OXYGEN AND NITROGEN

RF POWER, WATTS	EXPOSURE TIME, MINUTES	CHAMBER PRESSURE, MM Hg					
		0.2		0.5		1.0	
		GAS FLOW CC/MIN					
		10	20	10	20	10	20
50	15		A-6*		B-12		C-18
150	15		D-24		E-30		F-36
300	15		G-42		H-48		J-54

* Test Number

approximately 10^5 spores. The aqueous suspension of spores was spread evenly in each planchet, which then was allowed to dry overnight in the air flow of a clean bench.

The test configuration for each plasma test consisted of locating the inoculated samples at three positions in the sterilizing chamber (Figure 4). At each position a glass ring held six test planchets and two sterile control planchets. Therefore, each complete test, or loaded chamber, was composed of 18 inoculated test planchets and six sterile controls.

Appropriate ambient die-off and procedural test controls were conducted for each test. Analyses of the exposed samples and controls were performed per standardized microbial recovery procedures. These procedures were adapted from NASA Standard Procedures for the Microbial Examination of Space Hardware NHB 5340.1A, and included sample inoculation and drying in a Class 100 clean bench, microbial removal by sonication, and enumeration with Trypticase Soy Agar pour plates.

An additional analysis was conducted during Task 1. For all test variables of the test matrices, temperatures at the three chamber positions were measured and recorded immediately following a 15 minute plasma exposure. Temperature probes consisted of stainless steel planchets soldered to thermocouples.

3.2 TASK 2 - PLASMA PHYSICS

The plasma used in these experiments is generated by an rf discharge in low pressure gas. It consists of free electrons, positive ions, and (in some cases) negative ions. In polyatomic gas species, the ions may be atomic or molecular. The plasma is much less dense than the gas; for every ion or electron there may be millions of neutral gas atoms or molecules.

The neutral gas is flowing from an inlet on one side of the rf discharge, through the test chamber, to a vacuum pump. The plasma is carried along by the gas. Once outside the rf discharge region, the plasma decays as

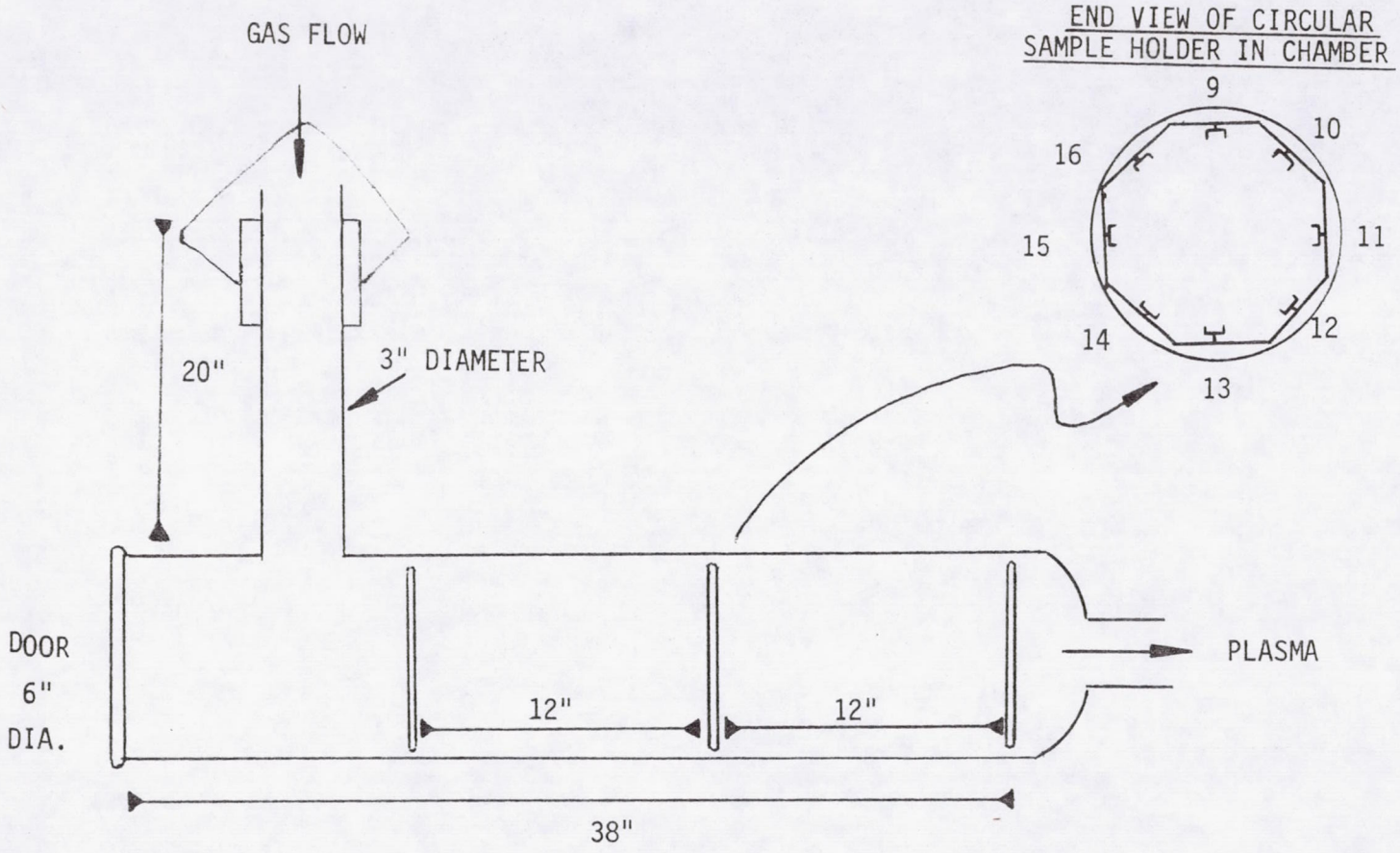

FIGURE 4: CHAMBER CONFIGURATION

electrons and ions recombine, and at each recombination event, the ionization energy is released, usually as light, often in the far ultraviolet (uv) region.

3.2.1 Langmuir Probe Characteristics

Plasma characteristics were determined by Langmuir probe measurements. An electrode or "probe" in the plasma was connected to an external power supply and the current collected by the probe was measured as a function of the applied voltage (Figure 5).

3.2.2 Plasma Kill Mechanisms

The two most likely microbial kill mechanisms in plasmas are ultraviolet irradiation from the recombining plasma, or sputtering of the cell wall by ion bombardment. Experiments were performed to obtain data on these two possible mechanisms.

3.2.2.1 Ultraviolet Irradiation

One mechanism by which a plasma sterilizes may be due to the production of ultraviolet irradiation. The recombination of ions and electrons may provide a source of intense "flowing" uv.

Helium and argon are good uv sources. Most of the volume recombination in argon and helium at low pressures will be two-body radiative recombination. Much of the recombination energy will appear in uv lines with the resonance line at 58 nanometers. There will also be a lower energy uv continuum (60-110 nanometers) due to a three-body radiative recombination, a neutral atom being the third body. The uv spectrum from surface recombination is not known, but is probably similar to the three-body recombination spectrum. In helium, some of the continuum can pass through most uv windows (sapphire, quartz), but the line radiation cannot. Nitrogen should be a poor uv source, since recombination of negative and positive ions will tend to radiate the recombination energy in long wavelength molecular bands. Task 3.2.2.1 was to screen for the presence of lethal uv in helium plasma.

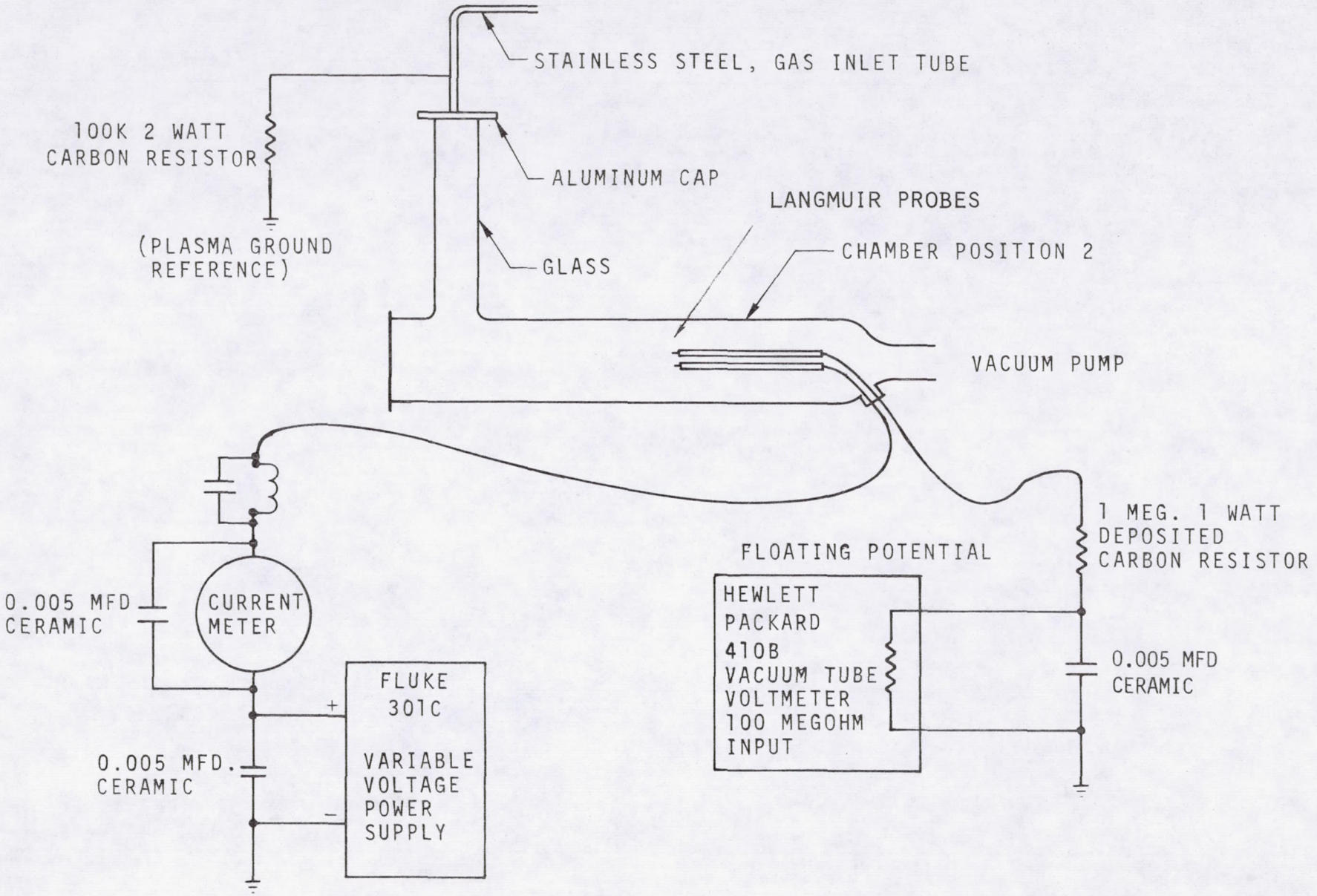

FIGURE 5: LANGMUIR PROBE SYSTEM

Ultraviolet cannot pass through "green" glass. The transmittance of green glass does not begin until approximately wavelength 350 nanometers. This is well above the uv spectral region. On the other hand, a sapphire window will transmit at 140 nanometers. This filter allows uv to pass.

The experimental approach was to protect B. subtilis spores from us and the plasma constituents. This was accomplished by covering three sample planchets with green glass. In addition, spores were exposed to uv by covering three samples with sapphire windows. These samples also were protected from the plasma constituents.

Uncovered spore samples were included and these were exposed to the complete plasma environment: ions, electrons, and recombination uv.

3.2.2.2 Sputtering

Sputtering was suggested as a kill mechanism, especially for the argon plasma, because the ion bombardment energy is sufficient to cause sputtering. This would require opening the cell wall to allow outgassing of the cell. Sputtering rates are not known for organic materials. For inorganics there is some data on sputtering by argon ions, and similar sputtering rates could damage cell walls significantly. Sputtering has a mass-dependent threshold. At the available ion energies, argon might sputter effectively, whereas helium could not sputter most materials at all. The only significant exception being that helium ions might sputter the hydrogen atoms in organic materials.

Several experiments were conducted to distinguish between the kill mechanisms. These experiments were conducted in helium plasma. The planchets were connected to power supplies, and kill was measured with the planchet voltage set at several points on the probe curves. Sample spore planchets were not normally connected to any outside voltage, so the spores were usually at floating potential. By putting the planchet at ground potential, we increase the bombarding ion energy, but not the flux (Section 4.2.1 for Definition).

Similarly, at voltages near ground potential the same flux of ions strikes the surface of planchets with less energy. Sputtering kill would drop drastically; uv kill should stay approximately constant. Just above space potential, the ions can no longer reach the planchet surface, and both sputtering and the surface recombination contribution to uv kill should stop.

4.0 RESULTS AND DISCUSSION

This section documents the results of Phase I. It consists of Tasks 1 and 2.

4.1 TASK 1 - PLASMAS OF SINGLE GASES

Plasmas of the gases argon, nitrogen, oxygen and helium were tested for their sterilizing effectiveness. Data obtained are presented.

4.1.1 Argon Plasma

The number of B. subtilis spores that survived exposure to argon plasma were recovered. Calculations for percent microbial survival were made and are recorded in Table 3.

From these data it is noted that:

(1) Percent survivors decreased as chamber pressure decreased. A pressure of 0.2 mm Hg resulted in more microbial kill.

(2) A power input of 150 watts (rf) appeared to excite argon to a more effective sterilizing state than 300 watts (rf).

(3) Using Position 3 as a conservative reference point, optimum kill through the chamber occurred at operating conditions of 150 watts and 0.2 mm Hg pressure for argon plasma.

(4) Variation in the volume of argon gas (10 and 20 cc per min.) did not appear to significantly influence the percent microbial survival.

Sample temperatures, recorded after 15 minute argon plasma tests, ranged from 21^{o} to $70^{o}C$ (Table 4). Chamber positions 2 and 3 experienced no temperatures in excess of $30^{o}C$ at all test conditions.

TABLE 3. PERCENT SURVIVAL OF BACILLUS SUBTILIS SPORES DUE TO ARGON PLASMA EXPOSURE[a]

RF POWER, WATTS	ARGON FLOW, CC/MIN.	PLASMA EXPOSURE, MINUTES	CHAMBER PRESSURE, MM HG								
			0.2			0.5			1.0		
			POS.1	POS.2	POS.3	POS.1	POS.2	POS.3	POS.1	POS.2	POS.3
			[b]								
50	10	5	0.15	51.02	89.80	38.78	89.80	73.47	100.00	100.00	100.00
		10	0.24	63.27	100.00	28.57	75.51	89.80	95.92	100.00	100.00
		15	0.18	13.67	79.59	6.53	97.60	95.92	91.84	91.84	100.00
	20	5	0.09	26.53	95.92	30.61	100.00	100.00	100.00	100.00	100.00
		10	0.39	24.49	79.59	1.65	95.92	97.96	81.63	100.00	100.00
		15	0.33	3.88	79.59	0.27	75.51	87.76	85.71	100.00	100.00
150	10	5	0.18	0.45	20.41	0.29	67.35	91.84	51.02	89.80	100.00
		10	0.07	0.19	3.67	0.22	59.19	65.31	7.55	93.88	100.00
		15	0.05	0.29	4.69	0.03	13.67	73.47	0.22	83.67	89.80
	20	5	0.19	0.17	4.08	0.29	8.37	93.88	1.14	81.63	85.71
		10	0.14	0.12	0.24	0.22	0.22	65.31	0.18	61.22	85.71
		15	0.09	0.05	0.31	0.06	0.27	63.27	0.18	83.67	75.51
300	10	5	0.15	11.63	55.10	20.41	89.80	100.00	79.59	89.70	93.88
		10	0.05	12.23	61.22	2.65	91.84	97.60	77.55	83.67	81.63
		15	0.05	10.41	77.55	0.31	83.67	87.76	30.61	46.94	38.78
	20	5	0.07	1.27	71.43	3.27	81.63	93.88	75.51	85.71	87.76
		10	0.12	0.35	79.59	0.24	75.51	81.63	55.10	53.06	79.59
		15	0.08	0.01	65.31	0.11	67.35	87.76	48.98	97.96	85.71

[a] 5×10^4 spores at 0 time

[b] Mean of 6 replicates.

TABLE 4: TEMPERATURE OF STAINLESS STEEL PLANCHETS IMMEDIATELY AFTER 15 MINUTES EXPOSURE TO ARGON PLASMA - ^{o}Centigrade

RF POWER, WATTS	ARGON FLOW, CC/MIN.	CHAMBER PRESSURE, MM HG											
		0.2				0.5				1.0			
		POSITION				POSITION				POSITION			
		1	2	3	A[a]	1	2	3	A	1	2	3	A
50	10	47	29	26	21	47	23	23	19	26	22	21	19
	20	51	28	27	19	46	23	23	19	26	23	22	19
150	10	66	30	26	21	51	26	25	21	27	22	21	19
	20	54	29	26	21	51	26	24	21	28	24	23	21
300	10	67	27	25	19	70	26	23	19	29	22	21	19
	20	59	29	25	19	66	28	23	19	32	25	23	19

[a] Probe outside chamber - ambient.

4.1.2 Nitrogen Plasma

Generally, B. subtilis spores were not affected to any great degree by exposure to nitrogen plasma for 15 minutes (Table 5). Sample temperatures during plasma exposure ranged from 22° to 38°C (Table 6).

4.1.3 Oxygen Plasma

Oxygen plasma was found to be a relatively weak sterilizing agent (Table 7). Some lethality was noted at the two lower chamber pressures (0.2 and 0.5 mm Hg). Under the test conditions for plasma production it appears that oxygen plasma was slightly more lethal than nitrogen, but nowhere near as efficient as argon plasma. Sample temperatures during oxygen plasma production were comparable to those recorded in nitrogen plasma.

4.1.4 Helium Plasma

Table 8 is the survival data obtained from exposing B. subtilis spores to helium plasma. From these data it is noted that:

(1) The number of survivors decreased as the chamber pressure decreased. A greater total spore kill was observed at 0.2 mm Hg than 1.0 mm Hg.

(2) A power input of 300 watts (rf) excited the helium to a very effective sterilizing level.

(3) Using Position 3 as the most conservative reference point, the greatest spore reduction occurred at operating conditions of 300 watts and 0.2 mm Hg pressure for helium plasma.

(4) Differences in helium flow did not greatly change plasma sterilizing effectiveness.

(5) Helium plasma was generally more efficient as a sterilizing agent than argon, oxygen, or nitrogen. Microbial kill was noted at most of the operating conditions of the test matrix.

Sample temperatures during helium plasma production ranged from 19° to 50°C (Table 9).

TABLE 5: PERCENT SURVIVAL OF BACILLUS SUBTILIS SPORES DUE TO 15 MINUTE NITROGEN PLASMA EXPOSURE [a]

RF POWER, WATTS	CHAMBER PRESSURE, MM HG								
	0.2			0.5			1.0		
	POS.1	POS.2	POS.3	POS.1	POS.2	POS.3	POS.1	POS.2	POS.3
50	88.9[b]	88.9	86.7	100.0	97.8	100.0	100.0	80.0	100.0
150	6.9	75.1	88.9	82.2	93.3	97.8	73.3	80.0	91.1
300	0.0	64.4	82.2	60.0	93.3	100.0	75.6	80.0	82.2

[a] 5×10^4 spores at 0 time

[b] Mean of 6 replicates

TABLE 6: TEMPERATURE OF STAINLESS STEEL PLANCHETS IMMEDIATELY AFTER 15 MINUTE EXPOSURE TO NITROGEN PLASMA - °Centigrade

RF POWER, WATTS	NITROGEN FLOW, CC/MIN	CHAMBER PRESSURE, MM HG											
		0.2				0.5				1.0			
		POSITION				POSITION				POSITION			
		1	2	3	A[a]	1	2	3	A	1	2	3	A
50	10	23	23	23	21	28	27	26	23	24	23	22	21
	20	24	24	24	21	24	23	24	21	24	23	22	21
150	10	31	26	24	22	27	25	25	23	26	23	22	21
	20	28	24	24	21	26	23	23	21	26	23	22	21
300	10	38	24	24	22	29	27	26	24	28	26	24	23
	20	38	24	24	22	27	24	23	21	26	23	22	21

[a] Probe outside chamber - ambient

TABLE 7: PERCENT MIRCORIBAL SURVIVAL AFTER 15 MINUTE EXPOSURE TO OXYGEN PLASMA [a]

RF POWER, WATTS	CHAMBER PRESSURE, MM HG								
	0.2			0.5			1.0		
	POS.1	POS.1	POS.3	POS.1	POS.2	POS.3	POS.1	POS.2	POS.3
50	35.5	74.2	71.0	64.5	80.6	83.9	TEST NOT APPLICABLE		
150	0.0	74.2	74.2	35.5	77.6	73.9	100.0	100.0	100.0
300	0.0	9.7	64.5	0.1	71.0	67.3	77.6	96.8	93.5

[a] 3×10^5 spores at 0 time

[b] Mean of 6 replicates

TABLE 8: PERCENT MICROBIAL SURVIVAL AFTER EXPOSURE TO HELIUM PLASMA [a]

RF POWER, WATTS	HELIUM FLOW, CC/MIN	PLASMA EXPOSURE, MINUTES	CHAMBER PRESSURE, MM HG								
			0.2			0.5			1.0		
			POS.1	POS.2	POS.3	POS.1	POS.2	POS.3	POS.1	POS.2	POS.3
50	10	5	0.04 [b]	28.57	38.10	11.43	66.67	80.95	35.71	47.62	54.76
		10	0.02	13.33	22.14	4.52	42.86	35.71	23.33	35.71	47.62
		15	0.03	19.29	23.57	0.24	26.19	26.19	11.67	26.19	33.33
	20	5	1.24	40.49	47.62	9.05	52.38	47.62	19.52	28.57	26.19
		10	0.08	28.57	54.76	1.24	28.57	35.71	14.52	26.19	26.19
		15	0.03	22.62	45.24	0.88	22.86	19.05	10.71	22.14	21.90
150	10	5	0.01	0.17	10.00	0.02	10.95	13.81	2.86	40.48	38.10
		10	0.00	0.02	2.86	0.00	3.81	12.14	0.64	33.33	40.48
		15	0.00	0.01	4.52	0.00	4.29	11.67	0.09	28.57	38.10
	20	5	0.04	0.31	33.33	0.48	73.81	97.62	1.00	35.71	33.33
		10	0.02	0.06	15.71	0.04	61.90	95.24	0.07	28.57	33.33
		15	0.01	0.03	9.05	0.04	30.95	71.43	0.04	23.81	35.71
300	10	5	0.03	0.05	11.43	0.01	6.90	15.00	0.03	8.81	16.43
		10	0.01	0.01	0.07	0.00	5.00	11.43	0.01	13.81	13.81
		15	0.00	0.01	0.08	0.00	2.21	10.71	0.01	8.81	16.90
	20	5	0.03	0.12	0.36	0.03	7.38	76.19	0.03	6.19	9.52
		10	0.01	0.02	0.12	0.01	0.76	73.81	0.02	7.14	7.86
		15	0.00	0.01	0.06	0.02	0.33	59.52	0.01	5.71	10.48

[a] 4×10^5 spores at 0 time

[b] Mean of 6 replicates

TABLE 9: TEMPERATURE OF STAINLESS STEEL PLANCHETS IMMEDIATELY AFTER 15 MINUTES EXPOSURE TO HELIUM PLASMA - ^{o}Centrigrade

RF POWER, WATTS	HELIUM FLOW, CC/MIN	CHAMBER PRESSURE, MM HG											
		0.2				0.5				1.0			
		POSITION				POSITION				POSITION			
		1	2	3	A [a]	1	2	3	A	1	2	3	A
50	10	27	23	22	21	29	23	22	21	27	23	23	22
	20	27	23	22	21	27	22	22	19	26	23	23	22
150	10	34	24	22	21	38	23	22	22	36	23	23	22
	20	32	23	21	20	33	19	19	19	34	23	23	22
300	10	44	31	26	22	43	27	23	21	50	24	22	22
	20	41	31	27	22	41	27	26	22	47	24	23	22

[a] Probe outside chamber - ambient

4.2 TASK 2 - PLASMA PHYSICS

Measurements of the plasma properties have been made, and experiments relating plasma phenomena and spore kill have been carried out. In this section, the plasma characteristics are described; some of the relevant plasma phenomena are explained; and the results of experiments to determine the mechanism of kill of plasmas are described.

4.2.1 Plasma Characteristics

The properties of the plasma have been studied by Langmuir probe techniques. The first probe results revealed that the plasma has several unusual features which demand care in interpreting measurements.

Most rf generated flowing plasmas are characterized by low electron and ion temperatures and rapid volume recombination downstream from the ionization region (between the rf plates). The visible light from these "flowing afterglows" is dominated by the recombination spectrum, and the uv light by a continuum at energies well below the resonance line. None of the ions and electrons in such discharges have sufficient energy for impact damage to any surface.

The rf generated flowing plasma used in these experiments; however, is quite different. While the ions are still cold (meaning perhaps $1000^{o}K$), the electrons are fairly hot, having a temperature of approximately $80{,}000^{o}K$ in the helium plasma, for example.

High electron temperatures have several important effects on the behavior of the plasma. First, the recombination rate is lower, and, consequently, the plasma can flow further. Second, insulating walls and other objects drawing zero net current from the plasma are charged to a negative potential, called the floating potential.

$$V_f \simeq - \frac{KT_e}{e} \tfrac{1}{2} \ln (m_+/m_-), \qquad (1)$$

Where T_e is the electron temperature, K is Boltzmann's constants, m_+ is the ion mass, and e and m_- are the charge and mass of the electron. (The term

"temperature" is used merely to denote the average electron energy, and does not necessarily imply a Boltzmann distribution, although Eq. (1) is most accurate for a Boltzmann distribution.)

All floating (insulators and any other surface collecting zero net current) surfaces are bombarded by ions attracted by the negative potential. In nitrogen, for example, the observations indicate that ions with energies up to 42 electron volts are bombarding the flowing surfaces.

The floating potential given by Eq. (1) is not measured with respect to ground potential but instead with respect to the potential of the nearby plasma, called "space potential" or "plasma potential." In most plasmas, space potential is close to ground potential, and floating potential, when measured with respect to ground, is given by Eq. (1).

In this plasma, however, space potential is high, being about 75 volts above ground, and floating potential, although properly negative with respect to space potential (Eq. (1), is positive with respect to ground. Space potential is usually very close to the potential of the most positive electrode exposed to the plasma. In this system there is no electrode in contact with the plasma.

The high positive space potential (75-100 v) results from the lack of a good reference electrode, and is easily modified by any apparatus which tends to supply such a reference. Consequently, plasma experiments must be conducted and interpreted carefully.

The unusually high electron temperature is due to rf fields which leak from the excitation area. These fields are measured at 30-50v/cm, which is not sufficient to cause breakdown, but is enough to heat the plasma.

The potential drop between the plasma and a "floating" object (a spore, for example) occurs over a distance, called the Debye length, which is characteristic of electrostatic effects in plasmas. The number of ions which will bombard the surface with the full energy given by the floating potential depends on whether or not they can travel one Debye length without colliding with a

neutral gas atom. In helium the mean-free-path of an ion is

$$\lambda_c \simeq 1/72_p \qquad (2)$$

where p is the pressure in torr. The Debye length is:

$$\lambda_D \simeq \sqrt{T_e/\eta} \qquad (3)$$

where η is the electron density (electrons/cm^3) and T_e is in degrees Kelvin. The ratio of Debye length to mean free path is:

$$\lambda_D/\lambda_c \simeq 1.5\ p/(10^{-10}\ \eta),^{\frac{1}{2}} \qquad (4)$$

for the electron temperatures observed in helium. Then most ions bombarding a floating object will have the maximum kinetic energy, eV_f, if

$$\eta \gtrsim 2 \times 10^{10}\ p^2 \qquad (5)$$

The conditions in the experiments conducted satisfy Eq. (5) at the lower pressures.

The flux of ions bombarding a floating surface is relatively independent of the pressure, and is proportional to the ion density in the nearby plasma. The total flux of accelerated heavy particles, however, increases with pressure because of charge transfer collisions--an ion being accelerated toward the surface may pick up an electron from a passing neutral, and continue (now neutral itself) with no further acceleration, while the passing neutral (now an ion) is accelerated the rest of the way to the surface.

The Debye length is relevant to another important physical process that must be considered for future investigations--penetration of holes and cracks. The one λ_D thick region where the potential drops from space potential to floating potential is called a Langmuir sheath, a space-charge sheath, or just a sheath. The electric potential in the sheath accelerates ions, and repels electrons, letting just enough electrons through to balance the ion current.

Now imagine a hole in a surface exposed to plasma. If the hole is less than a Debye length across, then the sheath will close across the hole, and prevent most electrons from passing through the hole. The ions which go through are then stopped, one Debye length beyond the hole, by another sheath set up by their own positive space charge. This phenomenon must be considered with respect to a practical application of plasma penetration and may prove to be the limiting case.

4.2.2 Langmuir Probe Characteristics

Figure 6 shows a Langmuir probe curve recorded in nitrogen plasma using a planchet as the probe. This has the usual feature of plasma probe curves, and we use it to illustrate both the standard interpretation and the dangers. At the lowest voltages there is a nearly constant positive current, called the ion saturation current, labeled (1) on the plot. Knowing the probe area, and assuming an ion temperature of 10^{3o}K, which is a good order of magnitude estimate for most plasmas, we calculate, from the ion saturation current, that the plasma density is $n_+ \simeq 3 \times 10^{11} cm^{-3}$.

At (2) on the probe curve the positive current starts to decrease as a few of the most energetic electrons get through to the probe surface. The zero current point (3), is a floating potential, here at 70 v above ground. The discontinuity in the curve just above floating potential is due to a change of instrumentation.

At (4) on the curve, the electron current is rising rapidly as the probe approaches space potential and more electrons can overcome the repulsive potential barrier. At space potential (5), all electrons can reach the probe, and the curve flattens somewhat, the continuing increase being due to the slow growth of the region from which the probe attracts electrons. At (7) the probe voltage is so high that the probe is causing breakdown, and the current increases rapidly again.

Knowing space potential and floating potential, we can obtain T_e from Eq. (1). The current at space potential then gives the electron density as $n_e \simeq 6 \times 10^{9} cm^{-3}$, or only one-fiftieth of ion density. Since the plasma must be

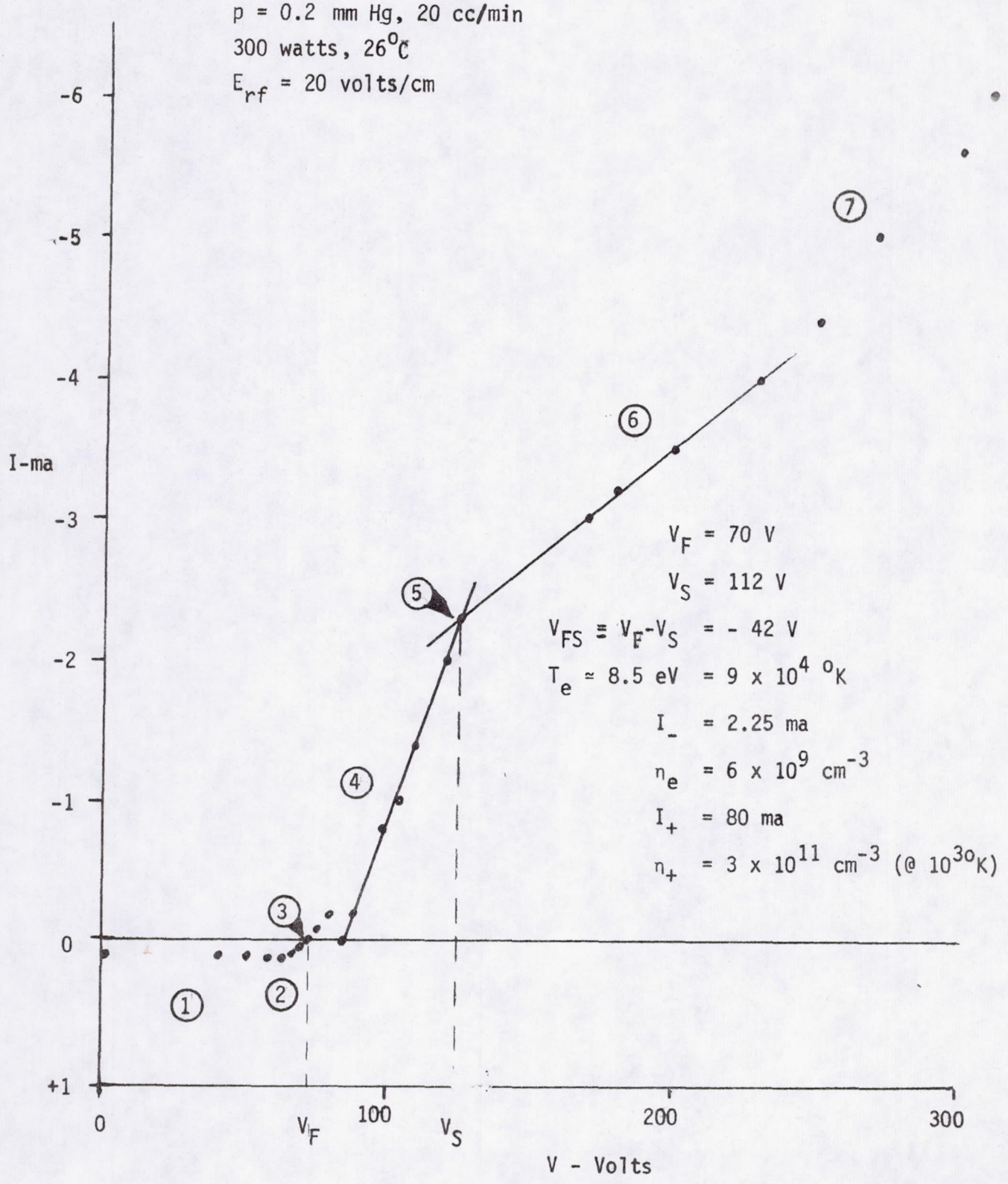

FIGURE 6: PROBE CURVE

neutral overall, one normally expected to find

$$n_+ = n_e \qquad (6)$$

and this is used as a check on the validity of the probe curves. In this case, the measurement of n_+ is sound, but somewhat uncertain because we had to guess the ion temperature. There are several explanations for the large ratio of n_+/n_- observed in nitrogen:

(a) It's real--space charge neutrality is provided by a large number of negative ions.

(b) The ions are extremely hot. This is most unlikely. The ions would have to be considerably hotter than the electrons, but they are cooled by very frequent collisions with the room temperature neutral gas.

(c) The saturation point on the curve is false. Distorted space potential data is obtained when the plasma cannot supply the probe current, or when the probe voltage generates extra plasma. This clearly occurred in the helium plasma. (Section 4.2.3.2 and Figure 7)

The deficient electron density is probably real. Nitrogen tends to form negative ions.

For the nitrogen plasma we could conclude that the ion density is $\approx 3 \times 10^{11} cm^{-3}$, that the electron density is $\approx 6 \times 10^{9}$, that the electron temperature is approximately $90{,}000^{o}K$, and that about 80 ma of ion current are bombarding each planchet (when floating) with energies of up to 42 eV per ion.

The low effectiveness of nitrogen is partly explained by the Langmuir probe results. As pointed out earlier, the preponderance of negative ions, which is the most likely explanation of the difference between n_+ and n_-, leads

to a low uv radiation flux. Furthermore, nitrogen should tend (there is no data) to be a relatively poor low energy sputterer because the molecular ion, colliding with a wall, tends to give its momentum to more than one atom of the wall material.

4.2.3 Plasma Kill Mechanisms

Data were obtained to elucidate the mechanism responsible for killing microorganisms when exposed to plasmas.

4.2.3.1 Ultraviolet Irradiation

Table 10 contains the data obtained from a screening test to detect the presence of ultraviolet in helium plasma. Spores that were protected from uv survived. Spores that were covered with a sapphire window, and saw wavelengths in the ultraviolet region (140 to 300 nanometers), did not survive.

The data may be interpreted that uv, or rather something shorter than 350 nanometers, was present in the helium plasma, and that it was lethal to the spores. The data may also suggest that exposure to the "lethal agent" is not dependent on having the helium plasma constituents in direct contact with the spores. Thus, it appears that sputtering is not the dominant kill mechanism in helium plasma.

4.2.3.2 Sputtering

Figure 7 depicts a Langmuir probe curve for helium. At points A, B, C, and D, planchet samples of spores were exposed to helium plasma. The number of spores surviving at these "potentials" are recorded in Table 11.

The experimental points, A and B, ground and floating potential, yielded data that show no apparent relationship to ion energy as would be expected if sputtering were a dominant kill mechanism. The other two points, C and D, were intended to be just below and just above space potential respectively. Unfortunately, it was impossible to reach the latter two conditions, because planchet voltage near space potential seriously disturbed the plasma, caused more ionization, and actually increased the kill rate.

Further tests showed that even very small probes disturbed the plasma when set near space potential. It is probably not possible, even with refined techniques, to carry out the experiment at points C and D in a helium plasma.

TABLE 10: PERCENT SURVIVAL OF BACILLUS SUBTILIS SPORES FOLLOWING 15 MINUTES EXPOSURE TO HELIUM PLASMA [a]

SAMPLE TREATMENT	CHAMBER POSITION		
	1	2	3
Glass Covered (No UV)	67.50[b]	50.00	57.50
Sapphire Covered (UV)	0.02	0.01	6.25
Uncovered	0.00	0.00	0.01

[a] 0.2 mm Hg, 300 watts rf

[b] Mean of 3 replicates, 4×10^5 spores at 0 time.

HELIUM, PLANCHET #13
POSITION 2

50 watts, 0.2 mm Hg, rf 3.7 volts at Pos. 2

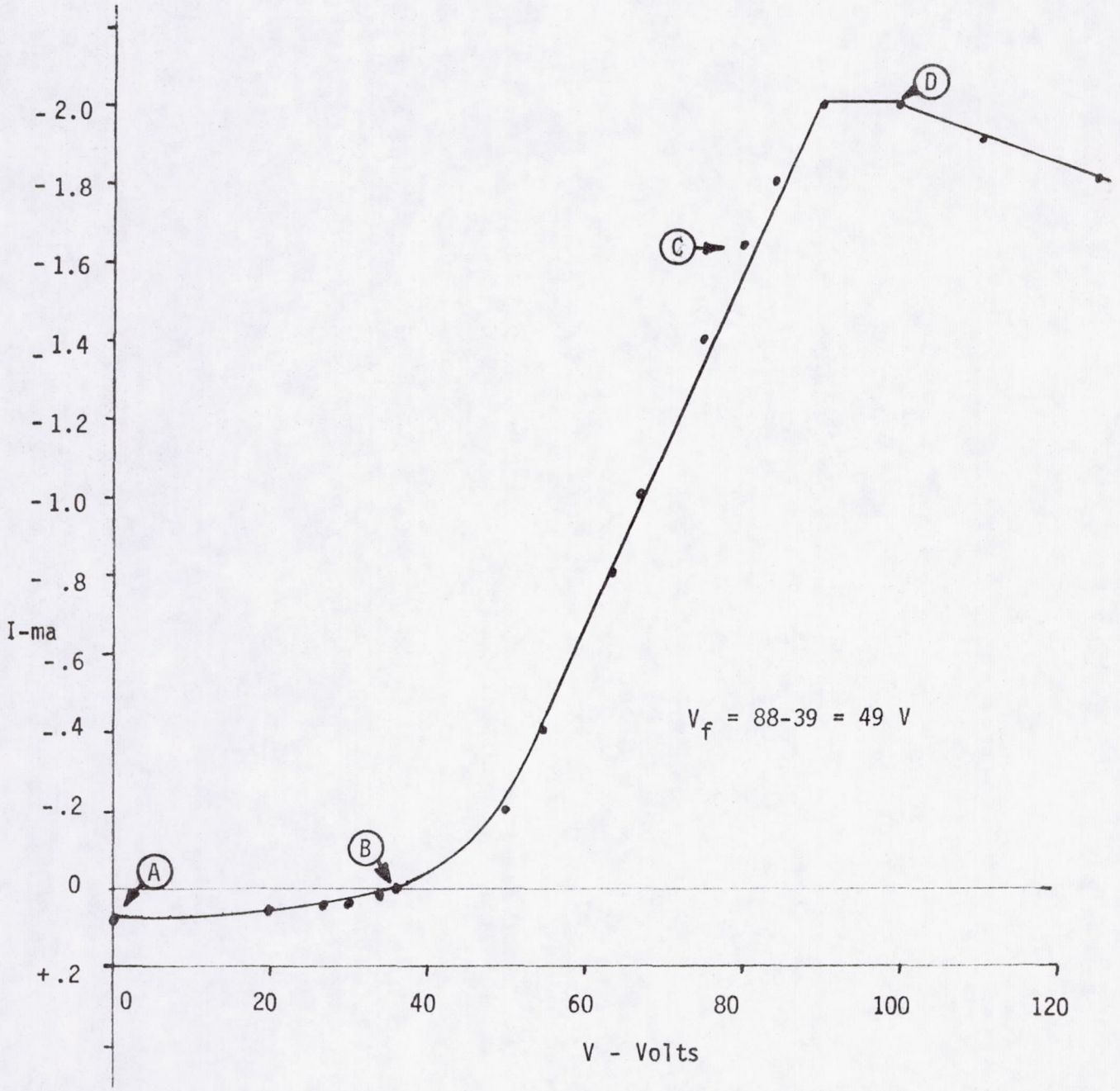

FIGURE 7: PROBE CURVE FOR HELIUM PLASMA

TABLE 11: NUMBER OF BACILLUS SUBTILIS SPORES SURVIVING A 15 MINUTE HELIUM PLASMA EXPOSURE (a)

SAMPLE PLANCHET	NUMBER SURVIVORS
A. Ground	1.9×10^4 (b)
B. Floating Potential	2.0×10^4
C. 80 Volts	7.3×10^3
D. 100 Volts	1.2×10^3

(a) 50 watts rf, 0.2 mm Hg, Position 2

(b) 4×10^5 spores at 0 time

5.0 SUMMARY

The data of the results of plasma experiments completed during Phase I indicate that the combination of a low chamber pressure (0.2 mm Hg), an ionization power input of 300 watts (rf), and the single gas helium are most efficient for killing B. subtilis spores.

In addition, the data indicate that sterilization, with helium plasma, is only weakly dependent on those factors which would strongly affect high sputtering rates. These results, although preliminary, suggest that ultraviolet irradiation is the dominant kill mechanism in plasma.

6.0 APPENDIX

The data for Phase I are presented in Tables 12 through 16.

TABLE 12

NUMBER OF BACILLUS SUBTILIS SPORES SURVIVING ARGON PLASMA EXPOSURE[a]

RF POWER, WATTS	ARGON FLOW, CC/MIN.	PLASMA EXPOSURE MIN.	CHAMBER PRESSURE, MM HG								
			0.2			0.5			1.0		
			POSITION 1	POSITION 2	POSITION 3	POSITION 1	POSITION 2	POSITION 3	POSITION 1	POSITION 2	POSITION 3
50	10	5	(b) 7.3×10^1	2.5×10^4	4.4×10^4	1.9×10^4	4.4×10^4	3.6×10^4	5.2×10^4	5.1×10^4	4.9×10^4
		10	1.2×10^2	3.1×10^4	5.0×10^4	1.4×10^4	3.7×10^4	4.4×10^4	4.7×10^4	5.1×10^4	5.4×10^4
		15	8.8×10^1	6.7×10^3	3.9×10^4	3.2×10^3	4.8×10^4	4.7×10^4	4.5×10^4	4.5×10^4	5.4×10^4
	20	5	4.2×10^1	1.3×10^4	4.7×10^4	1.5×10^4	5.2×10^4	5.2×10^4	4.9×10^4	5.4×10^4	5.4×10^4
		10	1.9×10^2	1.2×10^4	3.9×10^4	8.1×10^2	4.7×10^4	4.8×10^4	4.0×10^4	5.0×10^4	5.2×10^4
		15	1.6×10^2	1.9×10^3	3.9×10^4	1.3×10^2	3.7×10^4	4.3×10^4	4.2×10^4	5.6×10^4	5.3×10^4
150	10	5	8.6×10^1	2.2×10^2	1.0×10^4	1.4×10^2	3.3×10^4	4.5×10^4	2.5×10^4	4.4×10^4	4.9×10^4
		10	3.6×10^1	9.3×10^1	1.8×10^3	1.1×10^2	2.9×10^4	3.2×10^4	3.7×10^3	4.6×10^4	5.0×10^4
		15	2.3×10^1	1.4×10^2	2.3×10^3	1.5×10^1	6.7×10^3	3.6×10^4	1.1×10^2	4.1×10^4	4.4×10^4
	20	5	9.5×10^1	8.4×10^1	2.0×10^3	1.4×10^2	4.1×10^3	4.6×10^4	5.6×10^2	4.0×10^4	4.2×10^4
		10	6.7×10^1	5.9×10^1	1.2×10^2	1.1×10^2	1.1×10^2	3.2×10^4	8.6×10^1	3.0×10^4	4.2×10^4
		15	4.2×10^1	2.4×10^1	1.5×10^2	2.8×10^1	1.3×10^2	3.1×10^4	8.7×10^1	4.1×10^4	3.7×10^4
300	10	5	7.2×10^1	5.7×10^3	2.7×10^4	1.0×10^4	4.4×10^4	4.9×10^4	3.9×10^4	4.4×10^4	4.6×10^4
		10	2.5×10^1	6.0×10^3	3.0×10^4	1.3×10^3	4.5×10^4	4.8×10^4	3.8×10^4	4.1×10^4	4.0×10^4
		15	2.4×10^1	5.1×10^3	3.8×10^4	1.5×10^2	4.1×10^4	4.3×10^4	1.5×10^4	2.3×10^4	1.9×10^4
	10	5	3.6×10^1	6.2×10^2	3.5×10^4	1.6×10^3	4.0×10^4	4.6×10^4	3.7×10^4	4.2×10^4	4.3×10^4
		10	5.9×10^1	1.7×10^2	3.9×10^4	1.2×10^2	3.7×10^4	4.0×10^4	2.7×10^4	2.6×10^4	3.9×10^4
		15	1.2×10^1	5.5×10^0	3.2×10^4	5.6×10^1	3.3×10^4	4.3×10^4	2.4×10^4	4.8×10^4	4.2×10^4

(a) 4.9×10^4 spores at 0 time

(b) Mean of 6 replicates

TABLE 13: NUMBER OF BACILLUS SUBTILIS SPORES THAT SURVIVED A 15 MINUTE EXPOSURE TO NITROGEN PLASMA[a]

RF POWER, WATTS	CHAMBER PRESSURE, MM HG								
	0.2			0.5			1.0		
	POSITION 1	POSITION 2	POSITION 3	POSITION 1	POSITION 2	POSITION 3	POSITION 1	POSITION 2	POSITION 3
50	[b] 4.0×10^4	4.0×10^4	3.9×10^4	4.6×10^4	4.4×10^4	4.8×10^4	4.5×10^4	3.6×10^4	4.6×10^4
150	3.1×10^3	3.4×10^4	4.0×10^4	3.7×10^4	4.2×10^4	4.4×10^4	3.3×10^4	3.6×10^4	4.1×10^4
300	2.2×10^0	2.9×10^4	3.7×10^4	2.7×10^4	4.2×10^4	4.5×10^4	3.4×10^4	3.6×10^4	3.7×10^4

[a] 4.5×10^4 spores at 0 time.

[b] Mean of 6 replicates.

TABLE 14: NUMBER OF BACILLUS SUBTILIS SPORES THAT SURVIVED A 15 MINUTE EXPOSURE TO OXYGEN PLASMA [a]

RF POWER, WATTS	CHAMBER PRESSURE, MM HG								
	0.2			0.5			1.0		
	POSITION 1	POSITION 2	POSITION 3	POSITION 1	POSITION 2	POSITION 3	POSITION 1	POSITION 2	POSITION 3
50	[b] 1.1×10^5	2.3×10^5	2.2×10^5	2.0×10^5	2.5×10^5	2.6×10^5	TEST NOT APPLICABLE		
150	0	2.3×10^5	2.3×10^5	1.1×10^5	2.4×10^5	2.6×10^5	3.1×10^5	3.1×10^5	3.1×10^5
300	0	3.1×10^4	2.0×10^5	1.4×10^2	2.2×10^5	2.1×10^5	2.4×10^5	3.0×10^5	2.9×10^5

[a] 3.1×10^5 spores at 0 time.

[b] Mean of 6 replicates

TABLE 15

NUMBER OF BACILLUS SUBTILIS SPORES SURVIVING HELIUM PLASMA EXPOSURE (a)

RF POWER, WATTS	HELIUM FLOW, CC/MIN.	PLASMA EXPOSURE, MINUTES	CHAMBER PRESSURE, MM HG								
			0.2			0.5			1.0		
			POSITION 1	POSITION 2	POSITION 3	POSITION 1	POSITION 2	POSITION 3	POSITION 1	POSITION 2	POSITION 3
50	10	5	(b) 1.5×10^2	1.2×10^5	1.6×10^5	4.8×10^4	2.8×10^5	3.4×10^5	1.5×10^5	2.0×10^5	2.3×10^5
		10	9.6×10^1	5.6×10^4	9.3×10^4	1.9×10^4	1.8×10^5	1.5×10^5	9.8×10^4	1.5×10^5	2.0×10^5
		15	1.4×10^2	8.1×10^4	9.9×10^4	1.0×10^3	1.1×10^5	1.1×10^5	4.9×10^4	1.1×10^5	1.4×10^5
	20	5	5.2×10^3	1.7×10^5	2.0×10^5	3.8×10^4	2.2×10^5	2.0×10^5	8.2×10^4	1.2×10^5	1.1×10^5
		10	3.3×10^2	1.2×10^5	2.3×10^5	5.2×10^3	1.2×10^5	1.5×10^5	6.1×10^4	1.1×10^5	1.1×10^5
		15	1.3×10^2	9.5×10^4	1.9×10^5	3.7×10^3	9.6×10^4	8.0×10^4	4.5×10^4	9.3×10^4	9.2×10^4
150	10	5	2.9×10^1	7.0×10^2	4.2×10^4	6.7×10^1	4.6×10^4	5.8×10^4	1.2×10^4	1.7×10^5	1.6×10^5
		10	8.9×10^0	7.7×10^1	1.2×10^4	1.3×10^1	1.6×10^4	5.1×10^4	2.7×10^3	1.4×10^5	1.7×10^5
		15	6.7×10^0	4.7×10^1	1.9×10^4	1.7×10^1	1.8×10^4	4.9×10^4	3.6×10^2	1.2×10^5	1.6×10^5
	20	5	1.7×10^2	1.3×10^3	1.4×10^5	2.0×10^3	3.1×10^5	4.1×10^5	4.2×10^3	1.5×10^5	1.4×10^5
		10	1.0×10^2	2.7×10^2	6.6×10^4	1.5×10^2	2.6×10^5	4.0×10^5	2.8×10^2	1.2×10^5	1.4×10^5
		15	3.0×10^1	1.3×10^2	3.8×10^4	1.8×10^2	1.3×10^5	3.0×10^5	1.8×10^2	1.0×10^5	1.5×10^5
300	10	5	1.6×10^2	1.9×10^2	4.8×10^4	5.4×10^1	2.9×10^4	6.3×10^4	1.3×10^2	3.7×10^4	6.9×10^4
		10	4.2×10^1	5.8×10^1	3.0×10^2	1.6×10^1	2.1×10^4	4.8×10^4	5.4×10^1	5.8×10^4	5.8×10^4
		15	9.4×10^0	4.7×10^1	3.5×10^2	6.1×10^0	9.3×10^3	4.5×10^4	2.2×10^1	3.7×10^4	7.1×10^4
	20	5	1.1×10^2	5.1×10^2	1.5×10^3	1.4×10^2	3.1×10^4	3.2×10^5	1.2×10^2	2.6×10^4	4.0×10^4
		10	3.1×10^1	9.7×10^1	4.9×10^2	5.2×10^1	3.2×10^3	3.1×10^5	6.8×10^1	3.0×10^4	3.3×10^4
		15	1.9×10^1	5.1×10^1	2.6×10^2	6.7×10^1	1.4×10^3	2.5×10^5	3.1×10^1	2.4×10^4	4.4×10^4

(a) 4.2×10^5 spores at 0 time

(b) Mean of 6 replicates

TABLE 16:

NUMBER OF BACILLUS SUBTILIS SPORES SURVIVING

15 MINUTE EXPOSURE TO HELIUM PLASMA [a]

SPORES	CHAMBER POSITION		
	1	2	3
	[b]		
Glass Covered (no uv)	2.7×10^5	2.0×10^5	2.3×10^5
Uncovered	3.0×10^0	1.0×10^1	5.3×10^2
Sapphire Covered (uv)	6.0×10^1	5.6×10^1	2.5×10^4
Uncovered	3.0×10^0	4.3×10^1	4.3×10^1

[a] 0.2 mm Hg, 300 watts rf

[b] 4×10^5 spores at 0 time, mean of 3 replicates

SECTION III

PHASE II

PLASMA GAS CHARACTERISTICS

PHASE II

TABLE OF CONTENTS

PHASE II

1.0 PURPOSE

This phase of the program was concerned with utilizing the data obtained during Phase I to expand the range of biological testing. Measurements for diagnosing the lethal constituents of a plasma environment were developed. In addition, plasmas of mixed gases were studied.

2.0 INTRODUCTION

Experiments completed during Phase I indicated that the combination of a low chamber pressure (0.2 mm Hg), an ionization power input of 300 watts rf, and the gas helium were the most efficient for killing B. subtilis spores. These parameters were the operating conditions for most plasma tests in Phase II. Also, theoretical studies of the plasma properties pointed to two likely kill mechanisms: ultraviolet irradiation or ion sputtering.

3.0 PROCEDURE

The approach of Phase II was to obtain additional information on the biological range of effectiveness of helium plasma, develop plasma environmental diagnostics, and to modify the operating parameters to obtain the optimum conditions for sterilization.

The design of experiments for Phase II was based on data obtained during Phase I. The primary gas for plasma production was helium. Operational conditions, unless otherwise noted, were 0.2 mm Hg chamber pressure with 20 cc/minute gas glow and 300 watts rf power.

3.1 TASK 1 - DEATH RATES OF MICROORGANISMS

The lethal effect of plasma gas on a variety of organisms was investigated. Test organisms were selected to represent a typical spacecraft population upon which the range and effectiveness of the plasma process would be tested (Table 1). Spore stocks of JPL-1, JPL-2, JPL-16 and B. subtilis var.

Table 1. Test Organisms

Organism	Selection Rationale
JPL-1	Spore, spacecraft isolate
JPL-2	Spore, spacecraft isolate
JPL-16	Spore, spacecraft isolate
Bacillus subtilis var. *niger*, WCR-8	Spore, comparative control for sporeformers
JPL-5	Nonsporeformer, spacecraft isolate
Staphylococcus epidermidis ATCC 17917	Nonsporeformer, comparative control for JPL-5
Aspergillus niger	Fungus (spores)

niger (WCR-8), suspensions in ethanol, were obtained from the Jet Propulsion Laboratory. Test planchets were inoculated with these stock suspensions.. The non-sporeformers, JPL-5 and Staphylococcus epidermidis, were grown as bacterial lawns on TSA, harvested, washed three times, and resuspended in sterile deionized water. An aqueous suspension of these two organisms was used to inoculate test planchets.

Fungal spores were separated from fungal mycelium by filtering a culture through sterile gauze. A washed, aqueous suspension of fungal spores was employed to seed the test planchets.

The plasma environment for testing consisted of helium gas, ionized at 0.2 mm Hg with 300 watts rf. Inoculated test planchets were exposed to the plasma for 5, 10, 15 and 30 minutes.

The test configuration is pictured in Figure 1. Sample planchets, clipped on a glass ring, were placed at three positions within the chamber. At each chamber position were six test samples and two sterile controls. A time exposure consisted of 18 test samples, 6 replicates at each position, and 6 sterile controls, 2 located at each position.

Appropriate ambient die-off and procedural test controls were conducted for each test. Analyses of the exposed samples and controls were performed per standardized microbial recovery procedures. These procedures were adapted from NASA Standard Procedures for the Microbial Examination of Space Hardware, NHB 5340.1A, and included sample inoculation and drying in a Class 100 clean bench, microbial removal by sonication, and enumeration with TSA pour plates.

3.1.1 Plasma Sensitivity of Two Bacillus subtilis var. niger Spores

The influence of the spore suspending medium upon the subsequent plasma susceptibility of the microorganism was investigated. B. subtilis var. niger, WCR-8 spores (JPL) and B. subtilis var. niger spores ATCC 9372 (Boeing) were the test organisms compared. The JPL spore, prepared at JPL, was originally suspended in ethyl alcohol. It was observed in

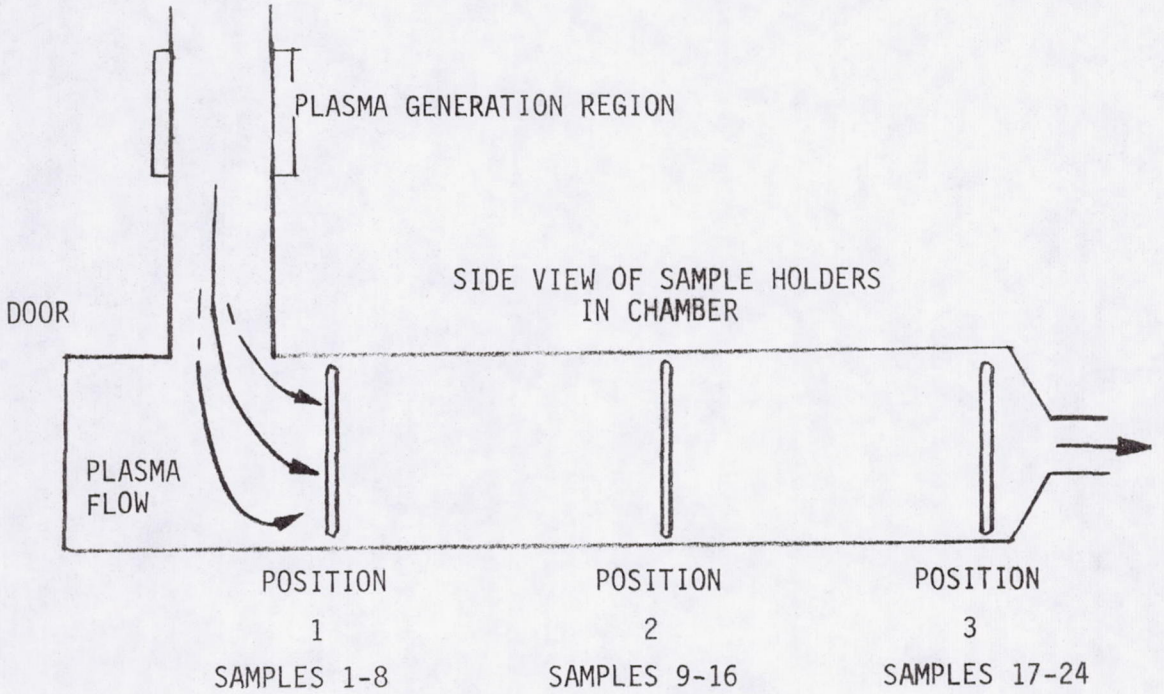

HEAD ON VIEW OF
CIRCULAR SAMPLE HOLDER

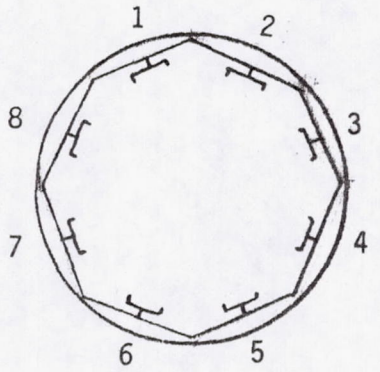

SAMPLE NUMBER

FIGURE 1. TEST CONFIGURATION

Task 1 that the JPL B. subtilis spore was killed at a significantly slower rate than the Boeing B. subtilis spore. Since the suspending medium in the latter case was water, the type of suspending medium was suspect. Aliquots of both spore types were suspended in water and alcohol, and test samples prepared. Test parameters were the same as Task 1.

3.1.2 Influence of Chamber Position on Sterility

The test rationale of Phase I was to avoid sterility so that statistical comparisons of surviving numbers would be possible. Therefore, all test samples were located in a region of moderate plasma density. However, information subsequently was required to demonstrate the sterilizing property of plasma.

Test samples inoculated with spores were positioned close to the excitation region where plasma density would be greater (Figure 2). Plasma exposure was 15 and 30 minutes. Analysis for survivors followed standardized procedures. Operating parameters of the test equipment were the same as Task 1.

3.2 TASK 2 - PLASMA GAS KILL MECHANISMS

The two most likely microbial kill mechanisms in plasmas are ultraviolet irradiation from the recombining plasma, and sputtering of the cell wall by ion bombardment. Experiments were performed to obtain data on these two possible mechanisms.

3.2.1 Ultraviolet Irradiation

The ultraviolet (uv) properties of plasma with respect to spore lethality were investigated.

The uv spectra of plasmas was separated with filters such that wavelengths below 140, 220, and 360 nanometers were not transmitted. Spores of B. subtilis var. niger were exposed to the various spectral fractions of argon, helium and oxygen plasmas by covering the samples with filters. The test matrix is shown in Table 2. Plasma exposure of the test samples, all located at Chamber Position 2, was for 15 minutes.

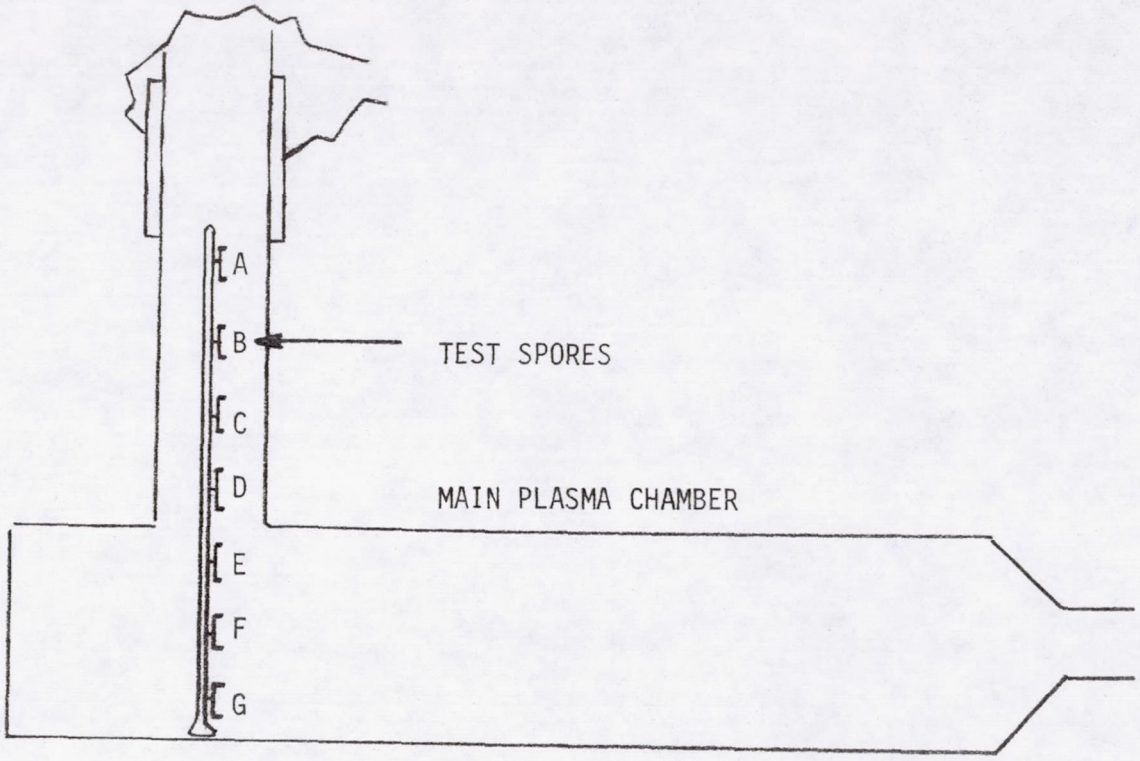

FIGURE 3. TEST SAMPLE ARRANGEMENT

Table 2. Test Matrix

Filter	Beginning Spectral Transmission, Nanometers	Plasma [a]		
		Argon	Helium	Oxygen
Glass	340	9 [b]	9	9
Corning 9-54	220	9	9	9
Sapphire Window	140	9	9	9
No Filter	-	9	9	9

[a] 150 watts rf, 0.2 mm Hg, 20 cc/min. flow

[b] Number of replicates, 6 for biological analysis, 3 for electron scan.

3.2.2 Electron Scanning Microscope

Electron scanning photomicrographs of spores exposed to plasma were performed. Spores, exposed to the different uv fractions of argon, helium, and oxygen plasmas, were examined for physical change. Untreated spore samples were used as comparative controls.

3.3 TASK 3 - PLASMAS OF MIXED GASES

The sterilizing efficiency of mixed gases for plasma production was evaluated. Argon, helium and oxygen, combined in different predetermined ratios to a total flow rate of 20 cc per minute, were ionized with 300 watts rf at 0.2 mm Hg pressure. The resulting plasmas were compared for spore lethality. B. subtilis var. niger spores were exposed to the plasmas for 15 minutes at Chamber Position 1. Analysis for survivors proceeded per standardized methods.

3.4 TASK 4 - PLASMA GAS DIAGNOSTICS

The likely mechanisms for plasma sterilization--ultraviolet irradiation and possibly sputtering--depend directly on the properties of the plasma. The readily controlled parameters, such as rf power and gas flow rates, will also control the kill rate, but only indirectly, and the relationship is confused by any irregular behavior of the plasma generator arising from surface contaminants and other factors which are difficult to monitor and analyze.

Of the variables which should directly affect rates for the kill processes, the most important are the gas pressure and species and the plasma density. The ultraviolet radiation flux from recombination is proportional to the square of the plasma density, and the uv flux from neutral gas excitation by the plasma electrons is directly proportional to the plasma density. The uv spectrum is determined by the species and the gas pressure, with a transition from a line spectrum to a less energetic continuum occurring at a pressure on the order of several torr. Electron temperature and gas pressure both influence the recombination and excitation rates strongly.

Sputtering rates should be directly proportional to the plasma density, and are extremely sensitive to the energy of the bombarding ions which is in turn proportional to the effective electron temperature. Consequently, systematic sterilization experiments require monitoring of the those important fundamental variables, specifically plasma density and electron temperature, which are not susceptible to direct control. The objective of this task was to develop the relevant plasma properties and phenomena, a description of various probe experiments conducted in the test chamber, and a tabulation of results.

3.5 TASK 5 - ELECTRODE MATERIAL AND PLACEMENT

The objective of this task was to produce a more dense plasma. Two approaches to accomplish the objective were evaluated. The first approach was to use a different material for the electrodes. The electrodes used for plasma production during Phase I were made of solid copper (Figure 3, Electrode I). Data obtained during a previous Boeing study showed that more efficient rf energy coupling might be possible with a change in electrode material plus a slight overall increase in electrode dimensions. New electrodes (Figure 3, Electrodes II) were constructed from expanded steel. Plasmas of helium and argon were produced with Electrodes II for 50 and 150 watts rf. Spores were exposed and analysis for survivors conducted. Langmuir probe measurements of the plasma densities were compared with spore survival data.

The second approach to increase plasma density was to evaluate the placement of electrodes on the exterior of the chamber. Electrodes IIa (Figure 3) were located at the middle of the chamber above Chamber Position 2. In this position, less rf energy was required to ionize the gas (10 and 50 rf). Spore survival and Langmuir probe data were obtained for comparison at these test conditions.

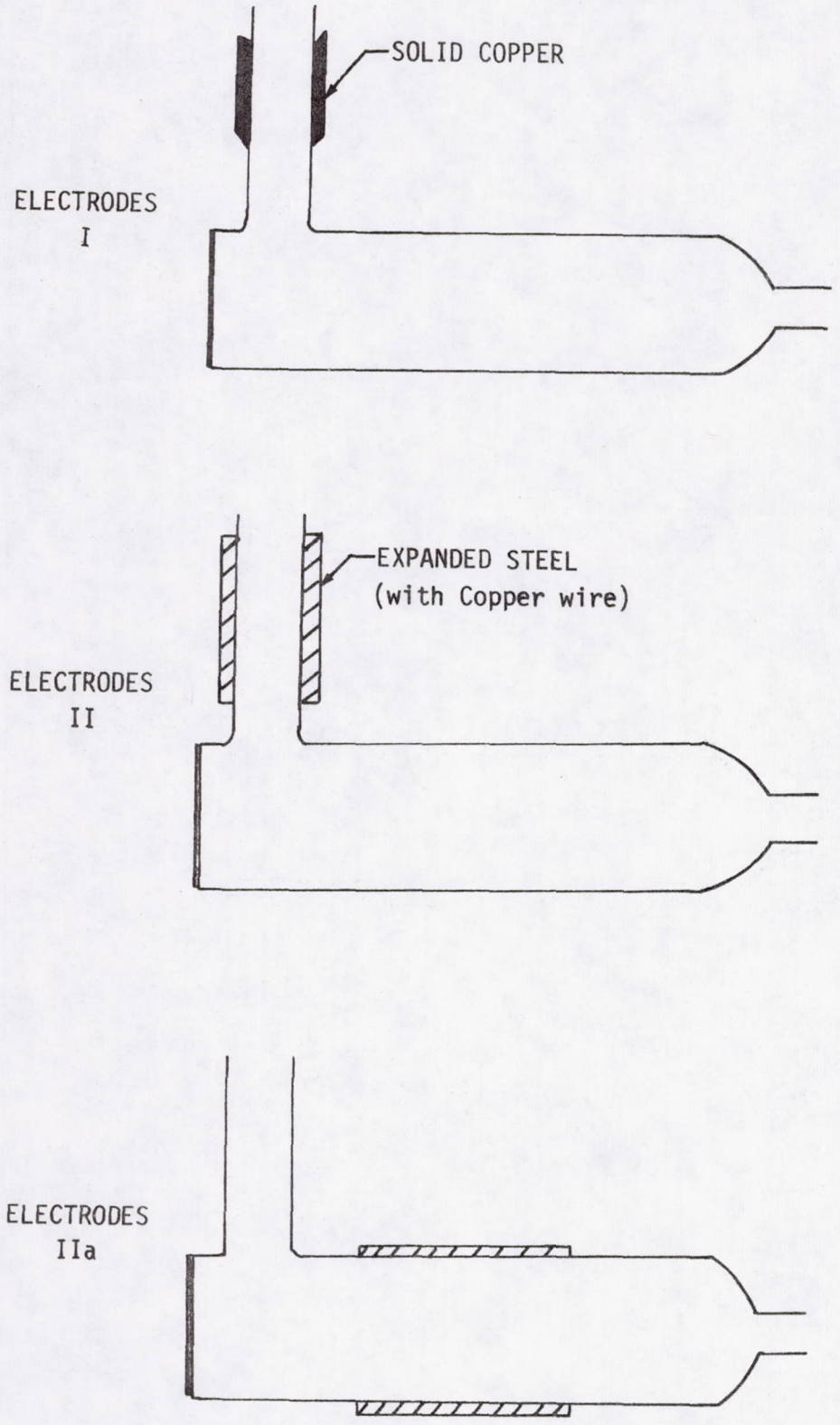

FIGURE 3: ELECTRODE MATERIAL AND PLACEMENT

4.0 RESULTS AND DISCUSSION

4.1 TASK 1 - DEATH RATES OF MICROORGANISMS

Seven different types of microorganisms were exposed to helium plasma. Analysis for survivors was performed. Percent survival calculations were conducted for these data and are shown in Table 3. The figures for B. subtilis var. niger, ATCC 9372, has been included for comparison with Phase I.

It was noted that: (1) microorganisms are killed by plasma gas, (2) the percent survival due to plasma gas exposure varies between types of organisms, (3) percent survival differed between the two strains of B. subtilis var. niger spores with respect to plasma susceptibility, and (4) the three spacecraft sporeforming isolates (JPL 1, JPL-2, JPL-16) were overall more resistant to plasma than B. subtilis.

4.1.1 Plasma Sensitivity of Two Bacillus subtilis var. niger Spores

Comparison of the plasma susceptibility of B. subtilis var. niger WCR-8 spores (JPL) and ATCC 9372 spores (Boeing) was made. Also, a comparison of water versus alcohol as spore suspending media was conducted.

Calculations for percent survival of spores surviving helium plasma exposure are shown in Table 4. The data show that the B. subtilis spores prepared by JPL are more resistant to plasma effects than Boeing prepared spores. Also, spores suspended in alcohol prior to test sample preparation are more resistant to plasma than spores suspended in water.

Communications with C. Hagen, JPL, revealed that JPL utilized a modified sporulation medium that was purposely designed to produce an especially thick spore coat not only for B. subtilis, but also the spacecraft isolates, JPL-1, JPL-2 and JPL-16. Evaluation of the biological variation due to the cultural conditions will be needed in future investigations.

Table 3. Mean Percent Survival of Microorganisms After Exposure to Helium Plasma

TEST ORGANISM	CHAMBER POSITION	HELIUM PLASMA EXPOSURE, MINUTES			
		5	10	15	30
Bacillus subtilis var. niger, ATCC 9372, Spore, Boeing[a]	1	0.03 [b]	0.01	0.00	
	2	0.12	0.02	0.01	[c]
	3	0.36	0.12	0.06	
Bacillus subtilis var. niger, WCR-8, Spore, JPL	1	0.61	0.28	0.39	0.11
	2	1.70	0.59	0.48	0.48
	3	4.35	1.83	1.11	0.54
JPL-1, Spore	1	24.62	13.85	4.46	0.97
	2	30.77	20.00	6.92	2.62
	3	35.38	33.85	15.08	2.15
JPL-2, Spore	1	2.50	1.83	1.83	0.88
	2	3.67	2.50	2.50	1.13
	3	6.83	6.33	4.00	2.17
JPL-16, Spore	1	1.00	1.50	0.75	0.38
	2	8.50	2.35	0.95	0.65
	3	7.50	3.25	3.00	1.85
JPL-5, Nonsporeformer	1	0.12	0.03	0.02	0.00
	2	0.38	0.09	0.08	0.00
	3	2.45	0.30	0.11	0.02
Staphylococcus epidermidis, Nonsporeformer	1	0.00	0.00	0.00	0.00
	2	0.00	0.00	0.00	0.00
	3	0.00	0.00	0.00	0.00
Aspergillus niger, Fungal Spore	1	0.56	0.24	0.06	0.03
	2	2.48	0.37	0.21	0.06
	3	7.04	1.70	0.67	0.16

[a] Phase I [b] Mean of 6 replicates [c] Not in Phase I test matrix.

Table 4. Mean Percent Survival of Spores to Helium Plasma

ORGANISM	SPORE SUSPENDING MEDIUM	HELIUM PLASMA EXPOSURE, MINUTES			
		5	15	30	60
Bacillus subtilis var. *niger*, WCR-8, JPL	Alcohol	3.39[a]	0.64	0.43	0.04
	Water	0.26	0.06	0.01	0.00
Bacillus subtilis var. *niger*, ATCC 9372, Boeing	Alcohol	0.01	0.01	0.02	0.00
	Water	0.00	0.00	0.00	0.00

a. Mean of 6 replicates

4.1.2 Influence of Chamber Position on Sterility

Organisms were exposed to helium plasma near the ionization region. Analysis for sterility of the samples was conducted and the results are shown in Table 5. Samples A through E were sterilized during the thirty minute plasma exposure. Temperatures in the region of E-F-G samples remained under 50°C during plasma production.

4.2 TASK 2 - PLASMA GAS KILL MECHANISMS

4.2.1 Ultraviolet Irradiation

Experimentation on the ultraviolet properties of argon, helium, and oxygen plasmas, with respect to spore survival was performed. Percent survival calculations are given in Table 6.

The spores that experienced the total plasma environment, i.e., no filter, also exhibited the least percent survival. The results indicates that the 21.2 eV resonance line photon was very effective at killing spores.

4.2.2 Electron Scanning Microscope

Helium, argon, and oxygen plasma treated spores of B. subtilis were examined with an electron scanning microscope. Photomicrographs were obtained and are reproduced in Figures 4 through 9. Visual comparison of the nontreated versus plasma treated spores suggest physical damage. However, the spores protected from the various spectral fractions of the plasmas with filters do not appear to show such damage. Although physical change in these spores is not apparent, the data presented in Table 6 showed that spore death at these conditions did occur.

4.3 TASK 3 - PLASMAS OF MIXED GASES

Table 7 presents spore survival percentages obtained from exposing spores to plasmas of mixed gases. Using Position 3 as a reference point (furthest from plasma generation area), the argon and helium combination resulted in less spore survival than the plasmas of argon combined with oxygen or oxygen combined with helium.

Table 5. Total Number of Bacillus subtilis var. niger Spores Surviving Helium Plasma Exposure [a,b]

CHAMBER POSITION	PLASMA EXPOSURE, MINUTES	
	15	30
A	0[c]	0
B	2	0
C	0	0
D	0	0
E	0	0
F	0	0
G	21	15

a. 1.1×10^5 at 0 time.

b. 300 watts, 0.2 mm Hg pressure, 20 cc/min. gas flow.

c. Total of 3 replicates.

Table 6. Percent Survival of Bacillus subtilis var. niger Spores Protected from Plasma Environment with Filters

FILTER	SPECTRAL TRANSMISSION, NANOMETERS	ARGON PLASMA	HELIUM PLASMA	OXYGEN PLASMA
Glass	340	60.00	85.00	81.82
Corning 9-54	220	1.70	0.37	43.18
Sapphire Window	140	0.19	0.08	45.45
No Filter	-	0.02	0.01	0.00

NO PLASMA

ARGON PLASMA

BACILLUS SUBTILIS VAR. NIGER SPORES EXPOSED TO ARGON PLASMA, 9000X

FIGURE 4

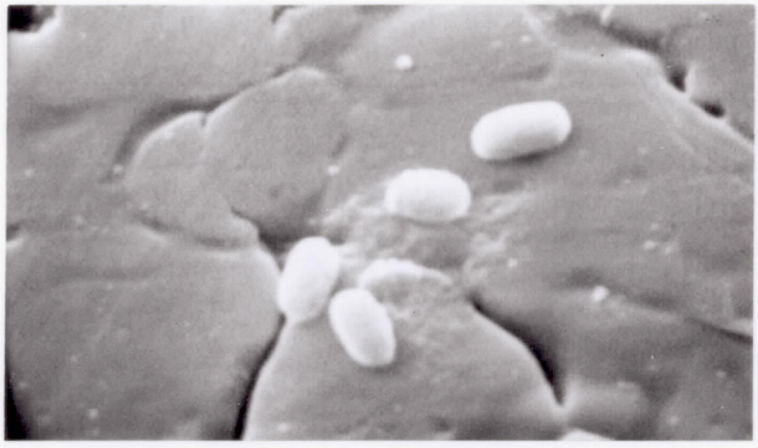

GLASS FILTER, 340 NANOMETERS

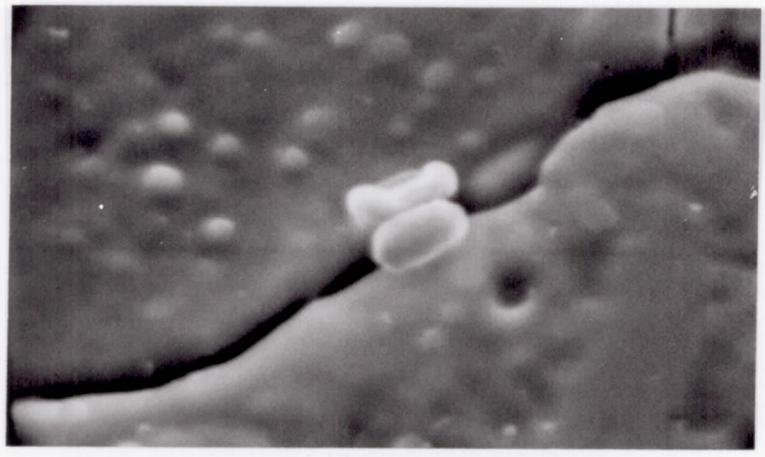

CORNING #9-54 FILTER, 220 NANOMETERS

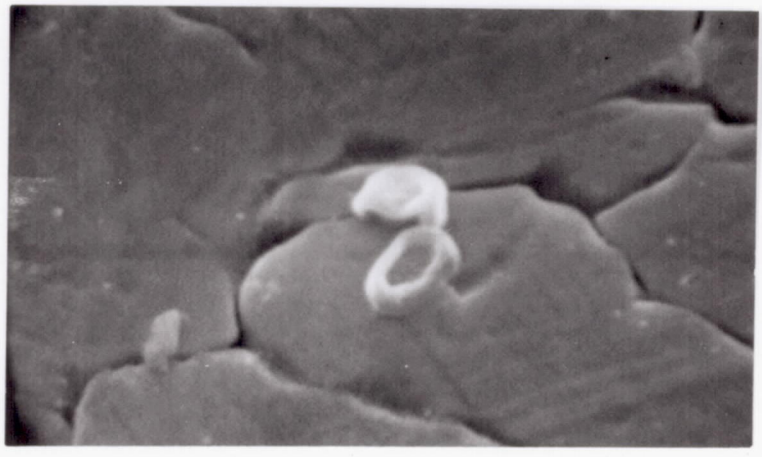

SAPPHIRE WINDOW, 140 NANOMETERS

BACILLUS SUBTILIS VAR. NIGER SPORES EXPOSED TO ARGON PLASMA, 9000X

FIGURE 5

NO PLASMA

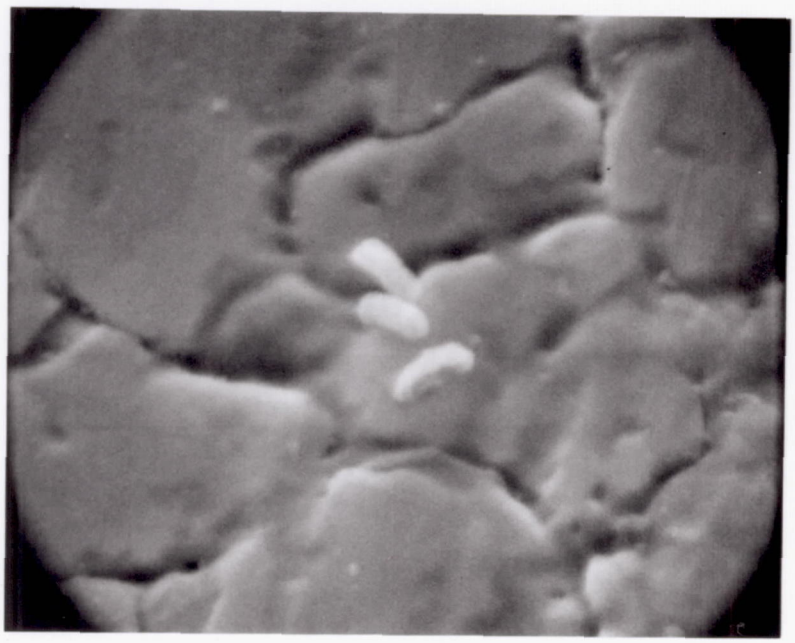

OXYGEN PLASMA

BACILLUS SUBTILIS VAR. NIGER SPORES, 10,000X

FIGURE 6

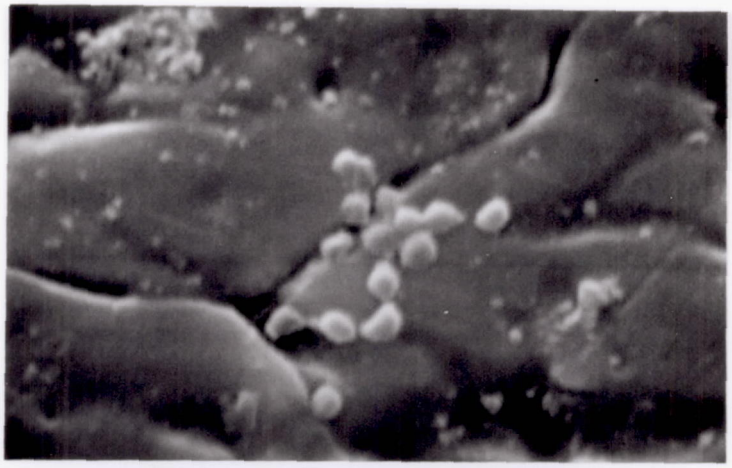

GLASS FILTER, 340 NANOMETERS

CORNING #9-54 FILTER, 220 NANOMETERS

SAPPHIRE WINDOW, 140 NANOMETERS

BACILLUS SUBTILIS VAR. NIGER SPORES EXPOSED TO OXYGEN PLASMA, 10,000X

FIGURE 7

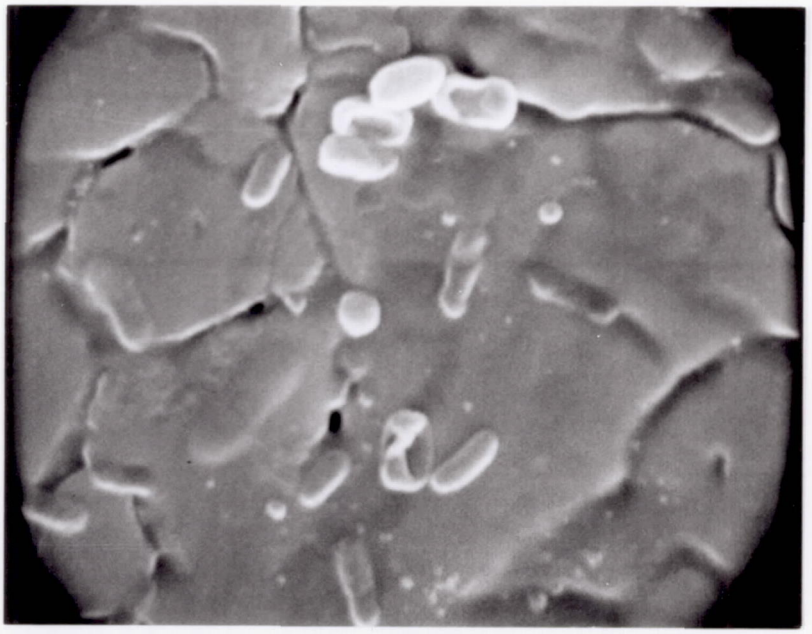

NO PLASMA

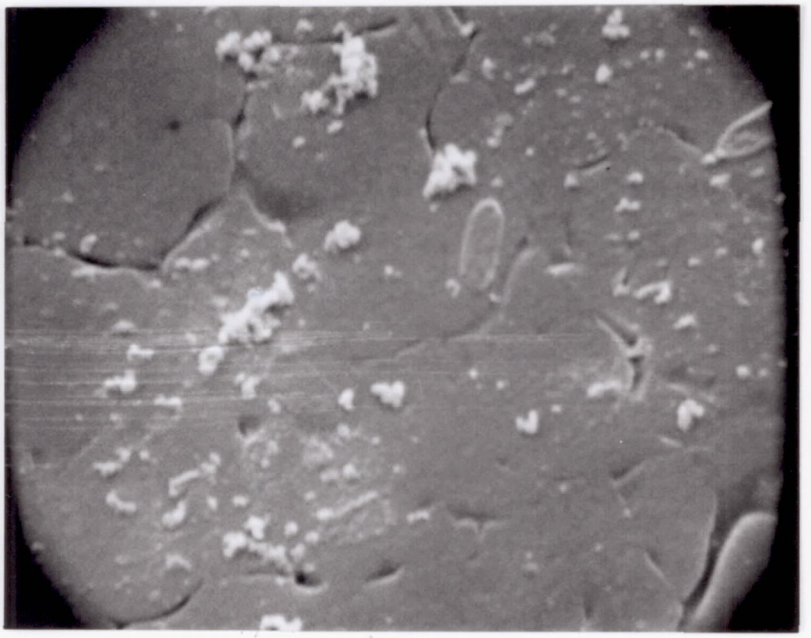

HELIUM PLASMA

BACILLUS SUBTILIS VAR. NIGER SPORES, 8000X

FIGURE 8

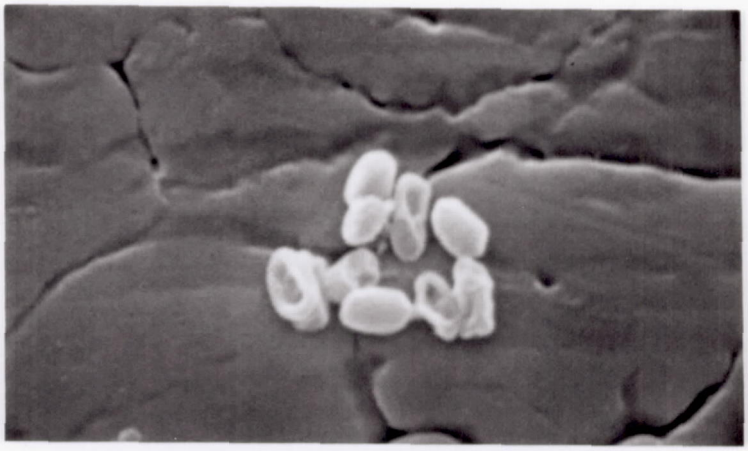

GLASS FILTER, 340 NANOMETERS

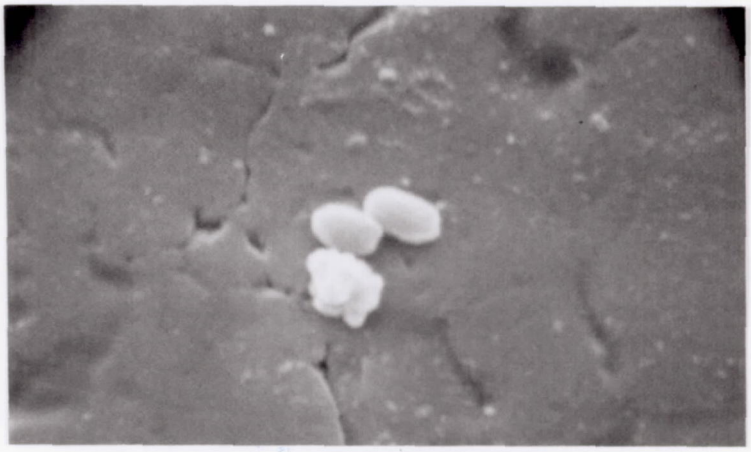

CORNING #9-54 FILTER, 220 NANOMETERS

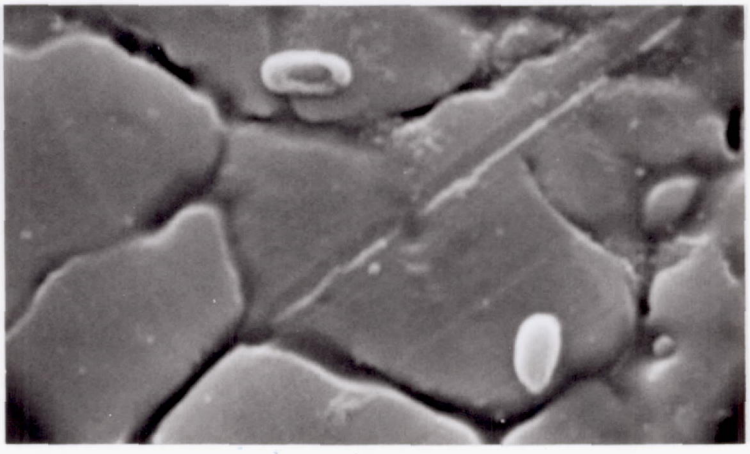

SAPPHIRE WINDOW, 140 NANOMETERS

BACILLUS SUBTILIS VAR. NIGER SPORES EXPOSED TO HELIUM PLASMA, 8000X

FIGURE 9

Table 7. Mean Percent Survival *Bacillus subtilis* var. *niger* Spores Exposed to Mixed Gas Plasmas [a]

GAS - CC/MINUTE	CHAMBER POSITION		
	1	2	3
Helium - 20	0.00	0.01	0.06
Argon - 20	0.08	0.01	65.31
Oxygen - 20	0.00	9.70	64.50
Argon - 18 + Oxygen 2	0.00	0.80	70.59
Argon - 10 + Oxygen 10	0.00	4.63	84.21
Argon - 18 + Helium 2	0.01	0.03	**10.59**
Argon - 10 + Helium 10	0.00	0.01	0.05
Oxygen - 18 + Helium 2	0.00	0.64	81.82
Oxygen - 10 + Helium 10	0.00	1.35	76.47
Oxygen - 10 + Argon 10	0.00	5.18	94.12

a. 300 watts, 0.2 mm Hg pressure, 15 minutes.

4.4 TASK 4 - PLASMA GAS DIAGNOSTICS

This section introduces the fundamental aspects of plasma behavior which pertain to plasma sterilization and diagnostics. The plasma used in the experiments is, nominally, a "flowing rf generated afterglow plasma." Gas is admitted at one end of the system and pumped out the other end by a vacuum pump. Pressure is controlled by the flow rate. A pair of electrodes, near the gas inlet, is used to apply a strong rf electric field which causes rf breakdown in the gas, creating a plasma by ionizing about one part in a million of the flowing gas. The plasma is carried through the system by the gas flow, decaying by recombination as it goes.

This Boeing developed rf plasma system, however, has a special feature in that rf current is allowed to leak out of the electrode region, and tends to follow the flowing plasma. This guided rf current will heat the electrons in the "flowing afterglow" plasma, and if it maintains an electron temperature of more than one or two electron volts, will cause further ionization, thus maintaining a denser plasma farther from the source.

RF heating is the dominant electron heating mechanism, and the electrons are cooled primarily by inelastic collisions with the cold neutral gas. These processes occur much more rapidly than the gradual changes as the plasma flows through the system. Consequently, the electron gas is in local equilibrium, with its temperature determined by the balance between heating and cooling. The heating rate is:

$$P_{in} = \frac{ne^2E^2}{m} \frac{\nu}{\omega^2+\nu^2} \qquad (1)$$

Where: n is the plasma density (number of electrons per cubic meter), e is the charge on the electron in coulombs; E is the magnitude of the rf electric field associated with the rf current, in volts per meters; m is the mass of the electron, in kilograms; ν is the frequency with which a typical electron collides with neutral gas molecules, in seconds^{-1}; and ω is the angular frequency of the rf field, $\omega = 2\pi \times 13.7$ Mhz $= 8.6 \times 10^7$ sec^{-1}, which is constant in these experiments.

The cooling rate is:

$$P_{out} = \nu n e \left[T_e \left(\frac{m}{M} \right) + \mathcal{E}_I \left(\frac{\sigma_I}{\sigma_o} \right) e^{-\mathcal{E}_I / T_e} \right] \qquad (2)$$

where: T_e is the electron temperature, in electron volts; M is the mass of the neutral atom, in kilograms; $\mathcal{E}_I$ is the mean energy lost in inelastic collisions with neutral gas molecules, in electron volts; σ_o is the cross-section for momentum exchanging collisions between electrons and neutrals; and σ_I is the mean cross-section for inelastic collisions. In the conditions found in the sterilization plasma, the first term, representing cooling by elastic collisions, is small compared to the cooling by inelastic collisions. This latter term represents a significant fraction of the power supplied to the system. The electron-neutral collision frequency is conveniently expressed as:

$$\nu = 6 \times 10^7 \; P_c \; p T_e^{1/2} \quad , \qquad (3)$$

where p is the gas pressure, in torr, and P_c is the collision probability[1]. Balancing the power flowing into the electron gas with the cooling rate, assuming that $\nu >> \omega$, expressing the rf electric field in kilovolts per meter, and using eq. (3) for ν, gives a transcendental equation for the electron temperature.

$$T_e = E_I / \ln (A * B) \quad , \qquad (4)$$

where

$$A = 3.6 \times 10^{15} \, m E_I P_c^2 \, p^2 \, T_e / e E^2 \quad , \qquad (5)$$

and

$$B = \sigma_I / \sigma_o \quad .$$

The constants are:

$$m = 9 \times 10^{-31} \text{ kg}$$

$$e = 1.6 \times 10^{-19} \text{ coul},$$

and $$P_c \simeq 10 \text{ (He)}$$

Most measurements have been done at p = 0.2 mm, and E is observed to be on the order of 3 kilovolts/meter. For helium the metastable level is at E_m = 19.80 eV, the resonance line is at 21.21 eV, and the ionization potential is 24.58 eV, so that

$$E_I \simeq 20 \text{ eV}. \tag{6}$$

The cross-sections in He are

$$\sigma_I \simeq 10^{-16} \text{ cm}^2$$

and

$$\sigma_o \simeq 2.8 \times 10^{-16} \text{ cm}^2 \quad .$$

Using these numbers and solving eq. (4) either graphically or by iteration determines T_e,

$$T_e \simeq 31 \text{ eV} \tag{7}$$

Electron temperatures on the order of tens of electron volts are sufficient to increase the ionization, so that plasma decay will be deferred. Anticipating later results, the plasma density is on the order of 10^{15} m^{-3}, i.e.

$$n \simeq 10^{15} \text{ m}^{-3}. \tag{8}$$

With the density, temperature, and pressure known, most of the important characteristic parameters of the plasma can be estimated. From eq. (3), the collision frequency in helium is

$$\nu \simeq 2 \times 10^{8} \text{ sec}^{-1} \quad , \tag{9}$$

verifying the assumption in eq. (4) that $\nu \gg \omega$.

The other important characteristic frequency is the plasma frequency

$$\omega_p = 2\pi \times 10 \times n^{1/2} = 2 \times 10^9 \text{ sec}^{-1} \quad , \tag{10}$$

so that the characteristic frequencies form a sequence,

$$\omega_p \gg \nu \gg \omega \quad . \tag{11}$$

For the conditions expressed in eq. (11), the skin-depth for rf current in the plasma is

$$\delta \simeq \frac{c}{\omega_p} \simeq 15 \text{ cm} \quad , \tag{12}$$

where c is the speed of light in vacuum.

Then the skin depth is comparable to the diameter of the plasma so that the rf heating current will be distributed throughout the plasma.

Another important length is the Debye length

$$\lambda_D = 7 \times 10^5 \, (T_e / n)^{1/2} \quad , \tag{13}$$

which is the characteristic length for electrostatic space-charge effects in the plasma. For T_e = 30 eV, n = 10^{15} m^{-3}, we have λ_D = 0.12 cm, which is about .050". The Debye length is important for plasma penetration; normally plasma will not penetrate holes much smaller than one λ_D. In order to penetrate holes smaller than about 20 thousandths of an inch, it may be necessary to ground out the rf heating current with a grounded ring electrode around the plasma. The downstream plasma should then become a true afterglow with a typical temperature of about 0.1 eV, and a Debye length of as little as .002 inch.

One other important length is the electron mean-free-path between momentum randomizing collisions with the neutral gas molecules,

$$\lambda_c = \frac{1}{n_o \sigma_o'} = \frac{1}{P_{cP}} \simeq 0.5\,\text{cm} \quad , \tag{14}$$

where n_o is the density of the neutral gas in atoms per cubic meter.

The plasma density and electron temperature are determined by Langmuir probe techniques.[2] This method involves several difficulties because of the unusual characteristics of this plasma. But alternative techniques--microwave cavities; low current, high voltage electron beam probes; laser interferometry; resonance probes; thermionic emission probes; double probes; and spectroscopy--would encounter similar or greater problems.

A Langmuir probe is a small metallic collector inserted into the plasma and connected to an adjustable d.c. power supply. The current from the plasma to the probe is measured as a function of the voltage applied to the probe. For stable, d.c. plasmas with low background gas pressure (long mean-free-path), the theory and practice of Langmuir probes has been worked out in great detail.[2,3,4,5] There are even apparatus which will automatically record probe data and reduce it to a plot of the kinetic energy distribution of the electrons.

The rf field and high electron temperature in this plasma prevent such a detailed interpretation. But the main features of probe analysis are still present and can be used to determine the electron temperature. The d.c. electric field applied to the plasma by the probe is on the order of

$$E_p \simeq T_e / \lambda_D \simeq 240\,\text{V/cm} \tag{15}$$

for the example of the plasma characteristics given above. Since this is about seven times greater than the typical rf field, the rf field is a relatively small perturbation on the electron orbits near the probe.

The characteristic time during which electrons are affected by the probe is the plasma period, $2\pi/\omega_p$. Eq. (11) shows that this time is short compared to the period by the rf field, which is $2\pi/\omega$.

Consequently, the rf field does not affect an electron orbit during the time the electron is being influenced by the probe. The resulting probe curves are the same as would be obtained in the same plasma without any rf field, except for being smoothed over a range.

$$\Delta V \simeq E\lambda_D \simeq 1 \text{ volt} . \tag{16}$$

The characteristic voltage for significant changes in the probe curve is the electron temperature, $T_e \simeq 30$ volts, so that the "rf smoothing" has relatively little effect on the probe curve.

Insulating walls and other objects drawing zero net current from the plasma are charged to a negative potential, called the <u>floating potential</u>.

$$V_f \simeq -\frac{KT_e}{e} \tfrac{1}{2} \ln(m_+/m_-) , \tag{17}$$

where T_e is the electron temperature, K is Boltzmann's constants, m_+ is the ion mass, and e and m_- are the charge and mass of the electron. (The term "temperature" is used merely to denote the average electron energy, and does not necessarily imply a Boltzmann distribution, although eq. (17) is most accurate for a Boltzmann distribution.)

The floating potential given by eq. (17) is not measured with respect to ground potential but instead with respect to the potential of the nearby plasma, called "<u>space potential</u>" or "<u>plasma potential</u>." In most plasmas, space potential is close to ground potential, and floating potential, when measured with respect to ground, is given by eq. (17).

In this plasma, however, space potential is high, and floating potential, although properly negative with respect to space potential, is positive with respect to ground.

Space potential is usually very close to the potential of the most positive electrode exposed to the plasma. The high positive space potential results from the lack of a good reference electrode, and is easily modified by any apparatus which tends to supply such a reference. Consequently, plasma experiments must be conducted and interpreted carefully.

Figure 10 shows one of our first Langmuir probe curves, recorded in nitrogen plasma using a planchet as the probe. This has the usual feature of plasma probe curves, and we use it to illustrate both the standard interpretation and some of the dangers. At the lowest voltages there is a nearly constant positive current, called the ion saturation current, labeled (1) on the plot.

At (2) on the probe curve the positive current starts to decrease as a few of the most energetic electrons get through to the probe surface. The zero current point (3), is floating potential, here at 70 v above ground. The discontinuity in the curve just above floating potential is due to a change of instrument scale.

At (4) on the curve, the electron current is rising rapidly as the probe approaches space potential and more electrons can overcome the repulsive potential barrier. At space potential (5), all electrons can reach the probe, and the curve flattens somewhat, the continuing increase being due to the slow growth of the region from which the probe attracts electrons. At (7) the probe voltage is so high that the probe is causing breakdown, and the current increases rapidly again.

Knowing space potential and floating potential, we can obtain T_e from eq. (17). The current at space potential then gives the electron density as $n_e \simeq 6 \times 10^9$ cm^{-3}.

But these results from Figure 10 can only be correct if there is a high density of negative ions ($\simeq 2.4 \times 10^{10}$ cm^{-3}) in the nitrogen plasma. The ratio of ion saturation current to electron saturation current should just

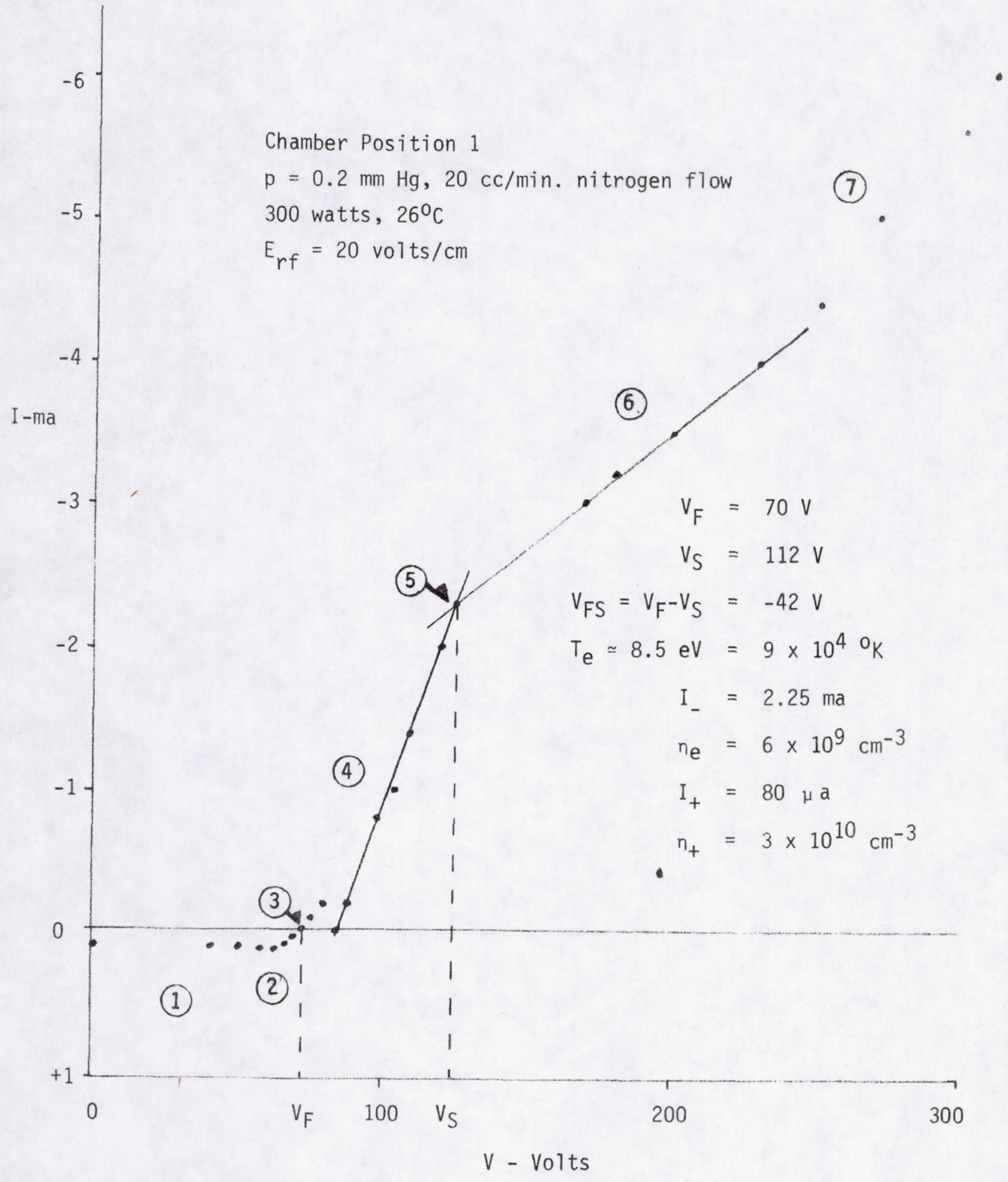

FIGURE 10. NITROGEN PLASMA PROBE CURVE

be $(m_-/m_+)^{\frac{1}{2}}$, Ref.(3). The ion current in Figure 10 is much larger than would be expected from the electron saturation current. Either there is actually a large difference between the electron density and the ion density, with space charge balanced by negative ions (which is possible in nitrogen), or else the data in Figure 10 is distorted.

One common form of distortion is using too large a probe, which draws so much current that the plasma is depleted. Figure 11 shows another early probe curve, in helium, which is a clear example of this artificial saturation. Again, the ratio of ion saturation current to electron saturation current is surprisingly large. As in several other probe curves using planchets for probes, the electron saturation is extremely flat, even decreasing somewhat. What is really happening was learned by monitoring the floating potential on another, nearby, probe while recording this data. Variations in floating potential simply follow equal variations in the space potential. Correcting the voltages in Figure 11 for these space potential variations shows that, at the higher probe voltages, the plasma potential is following the probe potential, and the voltage difference between the plasma and the probe changes very little when the probe voltage changes. This implies that the probe must be the best reference electrode available to the plasma. Consequently, probe curves like Figure 10 may be misleading, and those like Figure 11 are definitely wrong.

To obtain useful information from Figure 11 we use the fact, mentioned above, that electron and ion saturation currents to a probe differ by the square root of the mass ratio. This is based on a subtle phenomenon observed by D. Bohm, and known as the "Bohm criterion."[3] The result of the Bohm criterion is that ion current to a probe is given by the plasma density times the ion thermal speed calculated at the electron temperature (not the ion temperature, which is probably only on the order of 10^3 ^oK). Thus the electron current at the knee should be

$$I_- = (m_+/m_-)^{\frac{1}{2}} I_+ \qquad (18)$$

In helium, with $(m_+/m_-)^{\frac{1}{2}} = 86$, the knee of Figure 11 should be at $I_- \simeq 6.9$ ma, which is off the graph.

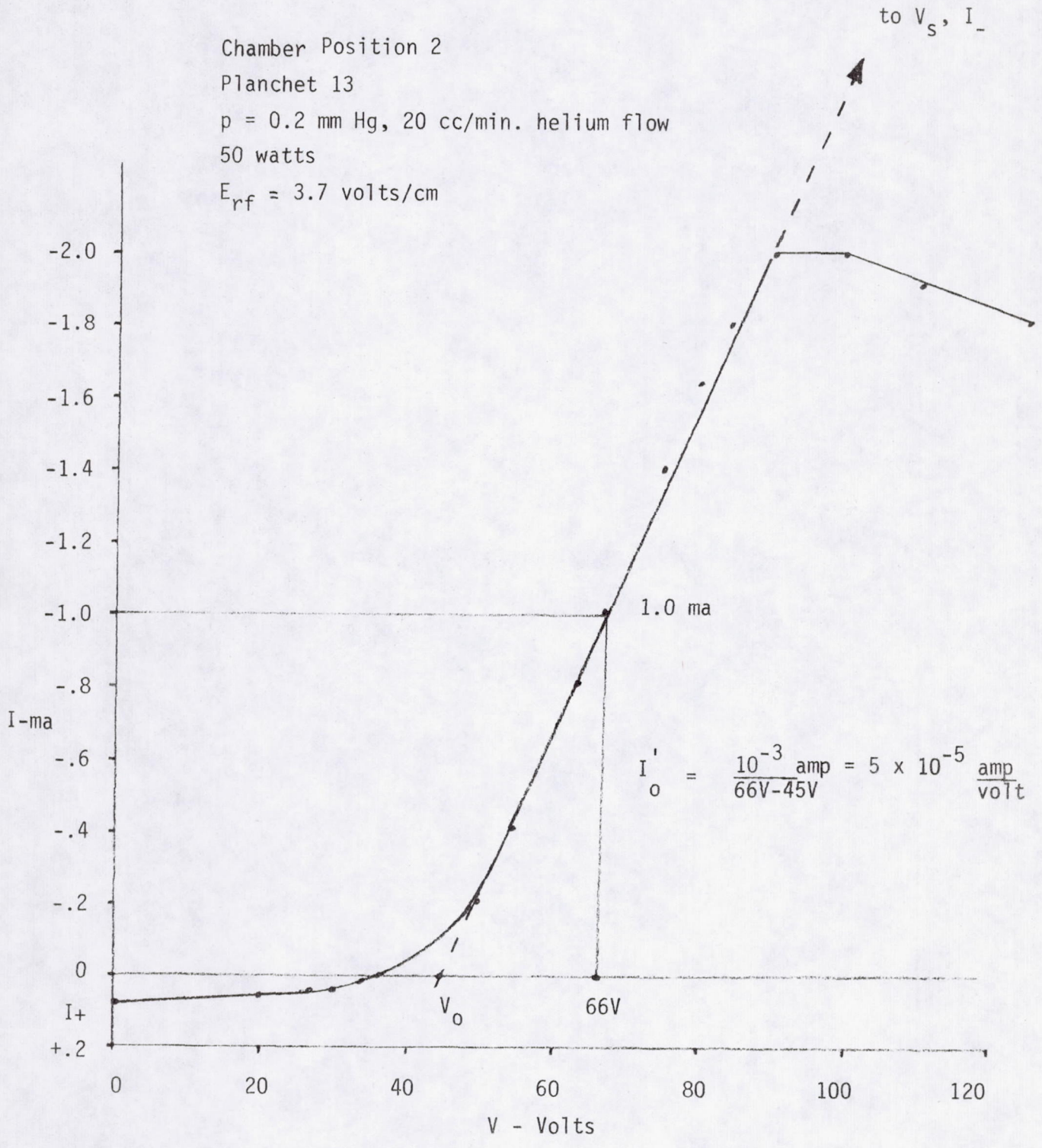

FIGURE 11. HELIUM PLASMA PROBE CURVE

The lower, linearly rising, part of the probe curve in Figure 11 is not distorted and can be used to extrapolate to the correct space potential. Let I_o' be the slope of that part of the curve, and let V_o be the intercept of the continued straight line with the zero current axis (see Figure 11). The electron saturation current is

$$I_- = I_o' * (V_s - V_o), \tag{19}$$

Using eq's (18) and (19) the true knee is at a space potential of

$$V_s = V_o + \left(\frac{m_+}{m_-}\right)^{\frac{1}{2}} I_+/I_o' . \tag{20}$$

From probe theory (Ref. 3), floating potential differs from space potential by

$$V_s - V_f = = \ln (m_+/m_-)\ kT_- , \tag{21}$$

which determines the electron temperature,

$$kT_- = (V_s - V_f)/\tfrac{1}{2} \ln (m_+/m_-). \tag{22}$$

With the electron temperature and either the electron or the ion saturation current we can determine the plasma density

$$n = 6 \times 10^{18}\ I_-/A_p\ v_-\ cm^{-3} \tag{23}$$

where A_p is the probe area and

$$v_- = 6 \times 10^7\ (kT_-)^{\frac{1}{2}}\ cm/sec, \tag{24}$$

where kT_- is in electron volts.

Carrying through this procedure for Figure 11, we find

$$T_e = 22\ eV,$$
$$n = 2 \times 10^7\ cm^{-3} . \tag{25}$$

These results are obtained from parts of the probe curve which show no sign of distortion, and so far as we know, the data is reliable. The extrapolation to floating potential along a straight line, however, is not very accurate, since the correct probe curve would not be straight. The error is almost certainly less than 50%. However, due to the difficulty of selecting the correct portion of the probe curve from which to extrapolate, the choice should be made on the basis of experience with undisturbed probe curves.

The above discussion shows the problems involved using large probes in this plasma. Small probes would draw less current, and might not drive the plasma potential, thus avoiding the artificial saturation. A series of development tests and diagnostic runs have been made with small probes. The probe curves are collected in Figures 12 through 17.

The small probe revealed a new problem. Since a small probe is driven to higher voltages than a large probe without depleting the plasma, it can, and does, increase the plasma ionization. Consequently, small probe curves have no distinguishable knee, but instead show a continuous current increase right up to breakdown.

The small probe curves are reduced by the extrapolation technique given in eq.'s (19) through (24). With this technique there are no great differences between using small probes and large probes, except that the extrapolation is easier with large, flat probes such as planchets.

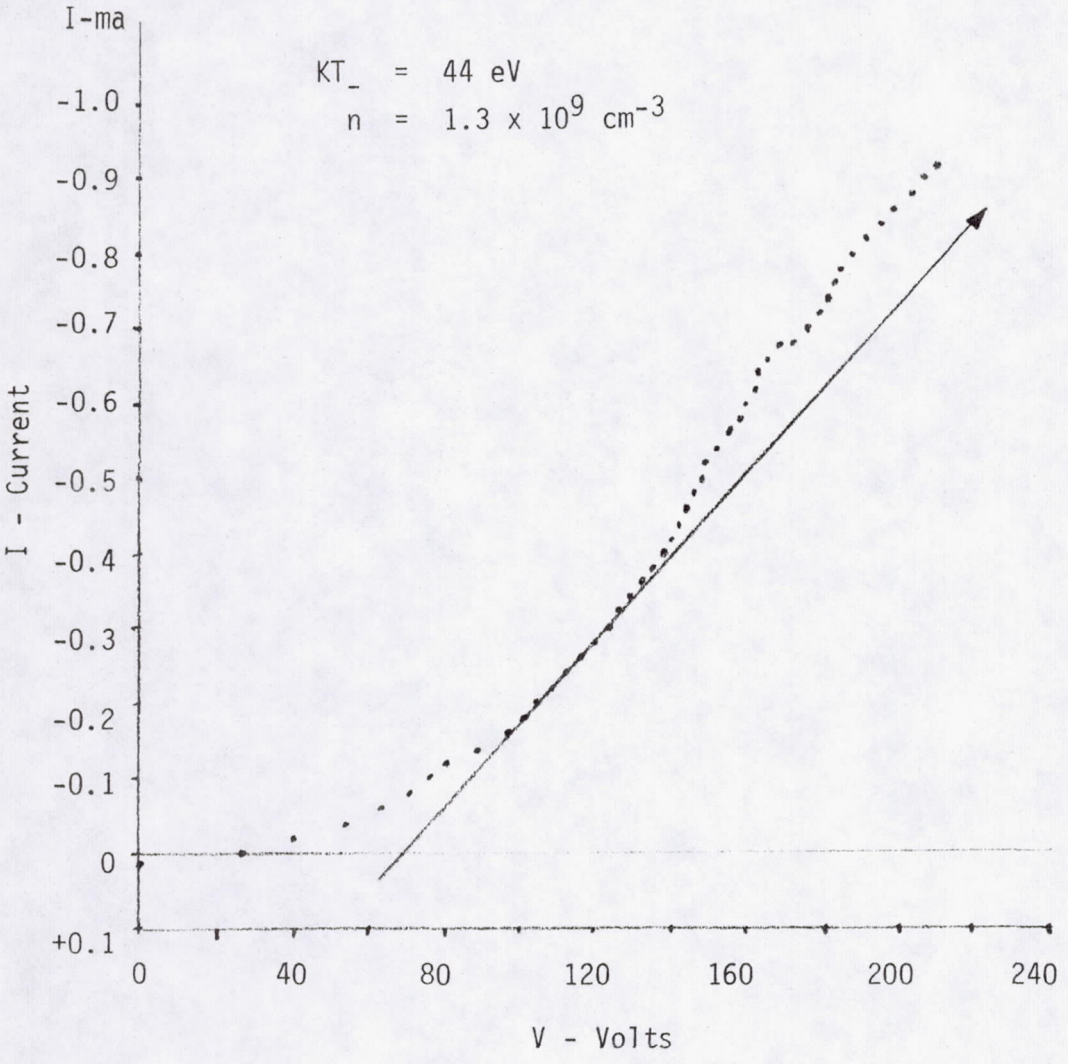

FIGURE 12. HELIUM PLASMA PROBE CURVE

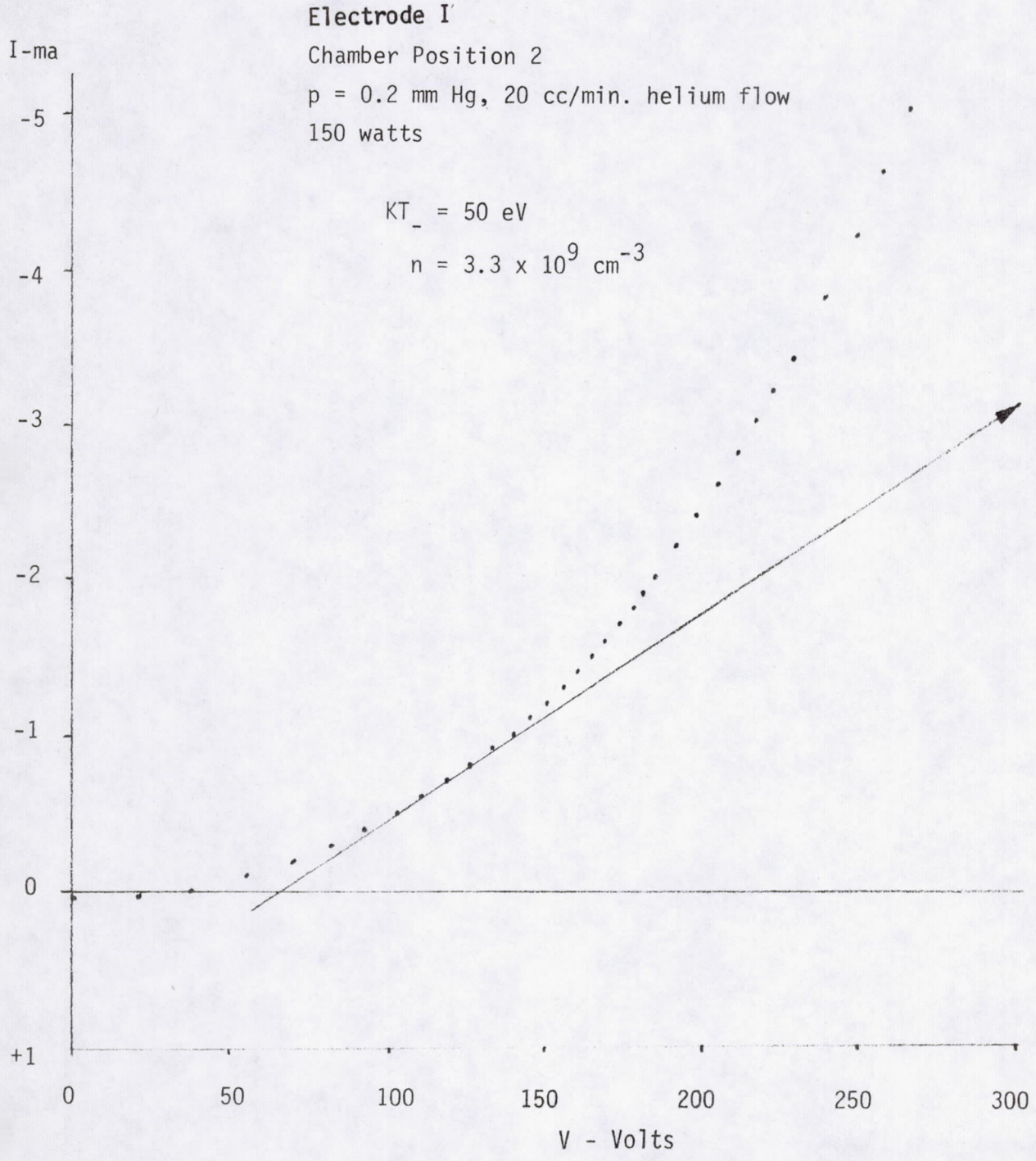

FIGURE 13. HELIUM PLASMA PROBE CURVE

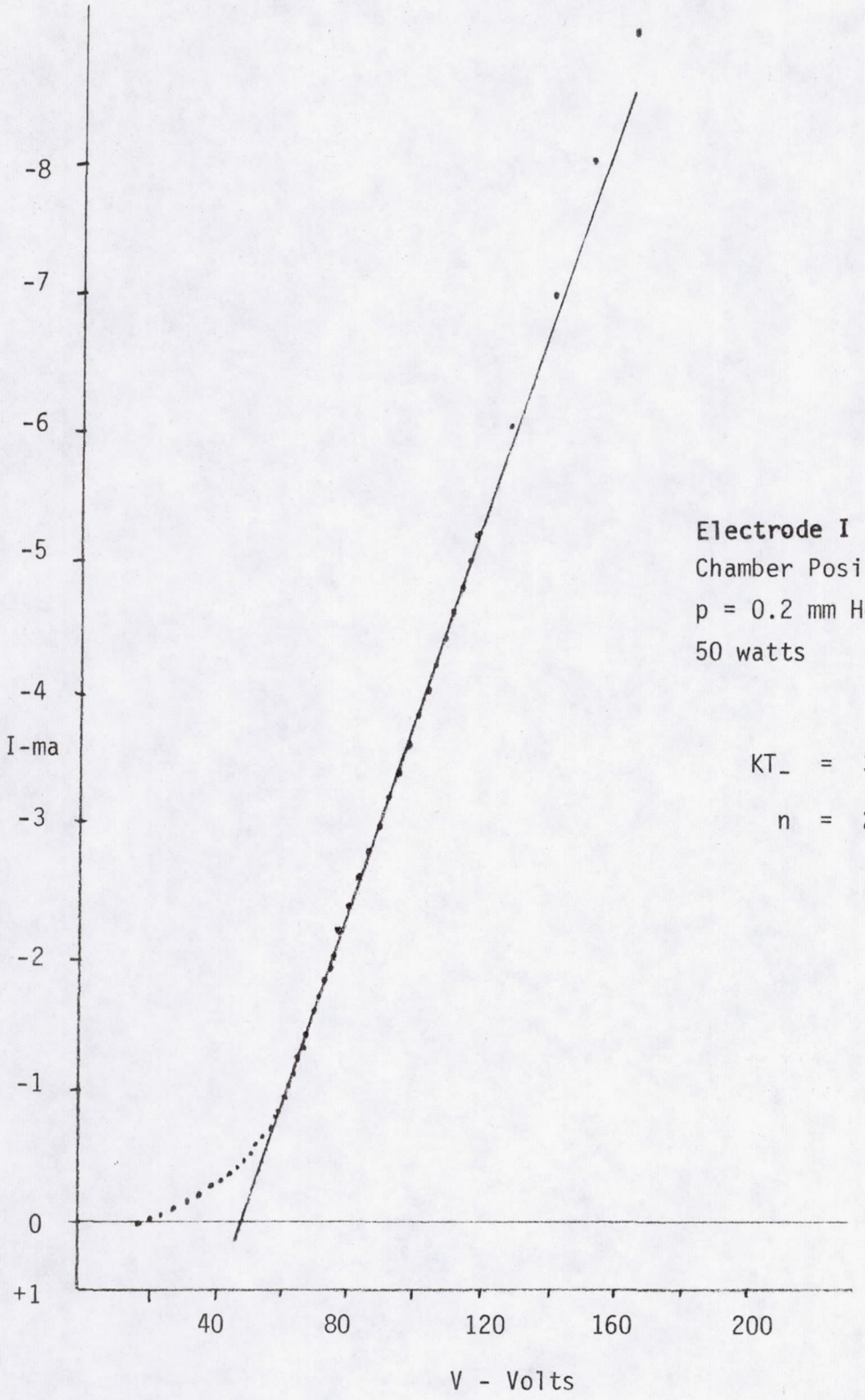

FIGURE 14. ARGON PLASMA PROBE CURVE

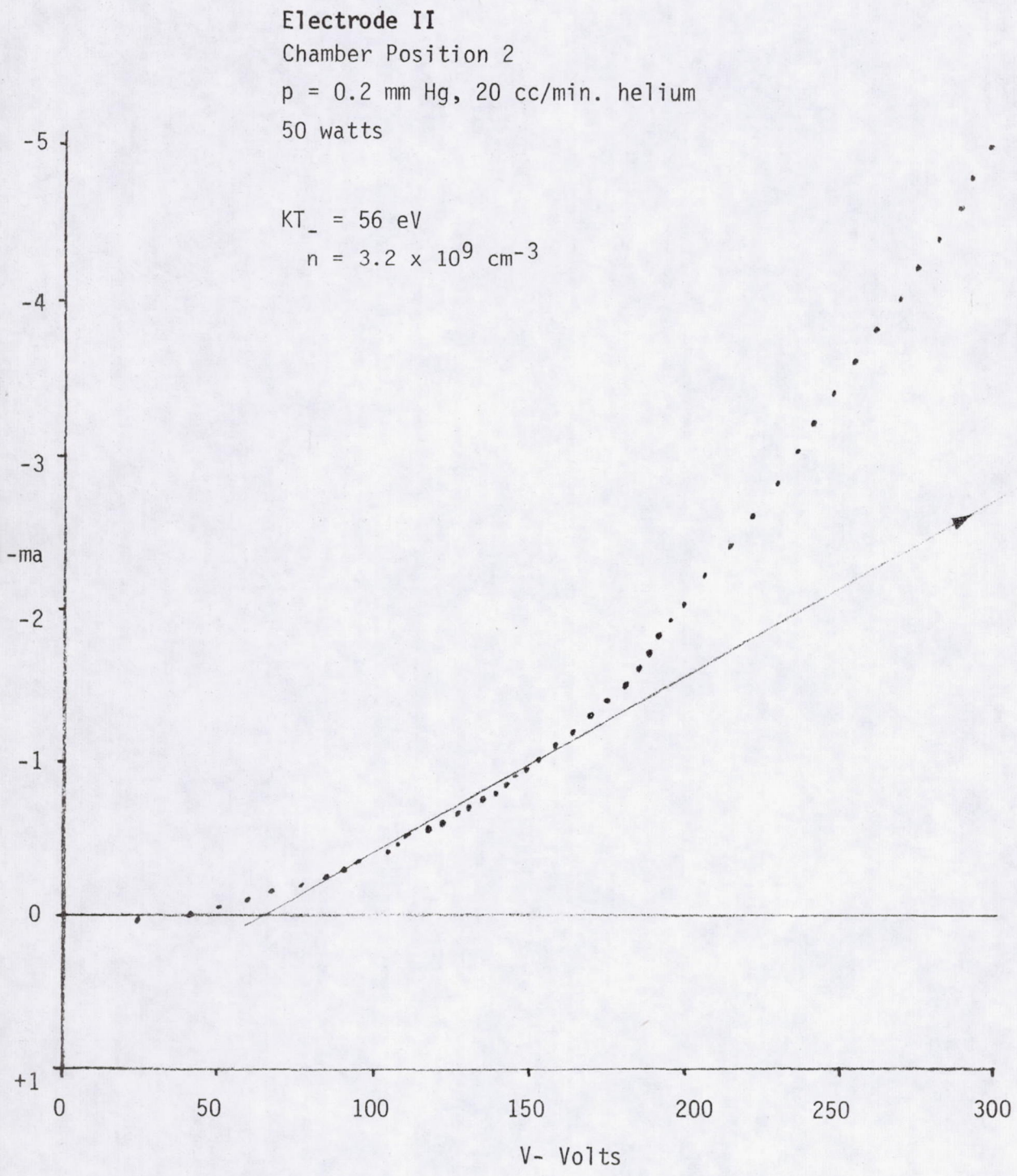

FIGURE **15.** HELIUM PLASMA PROBE CURVE

Electrode II

Chamber Position 2

p = 0.2 mm Hg, 20 cc/min. helium flow

150 watts

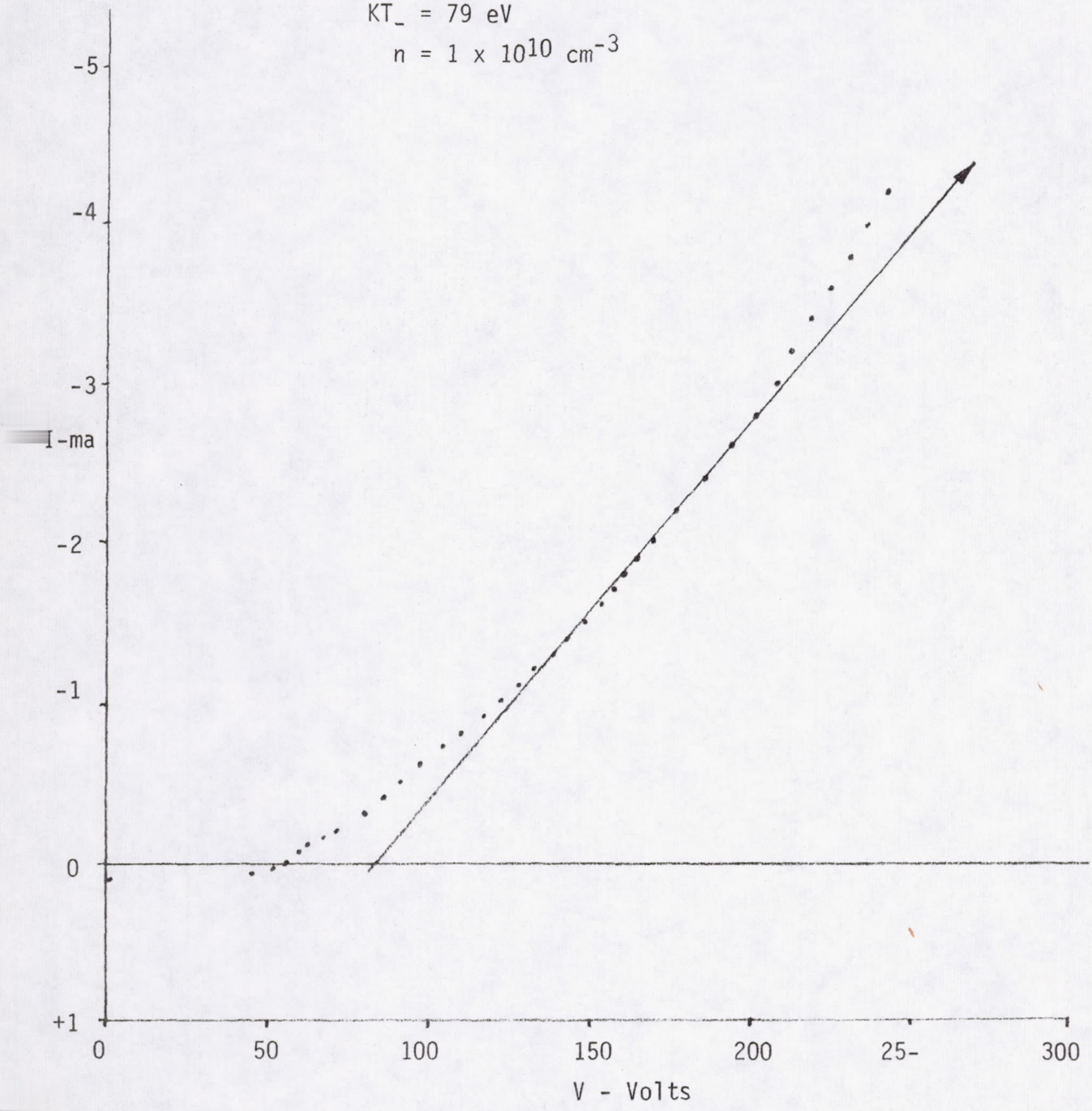

FIGURE **16.** HELIUM PLASMA PROBE CURVE

Electrode II

Chamber Position 2

p = 0.2 mm Hg, 20 cc/min. argon

50 watts

KT_{-} = 27 eV

n = 2.5×10^{10} cm^{-3}

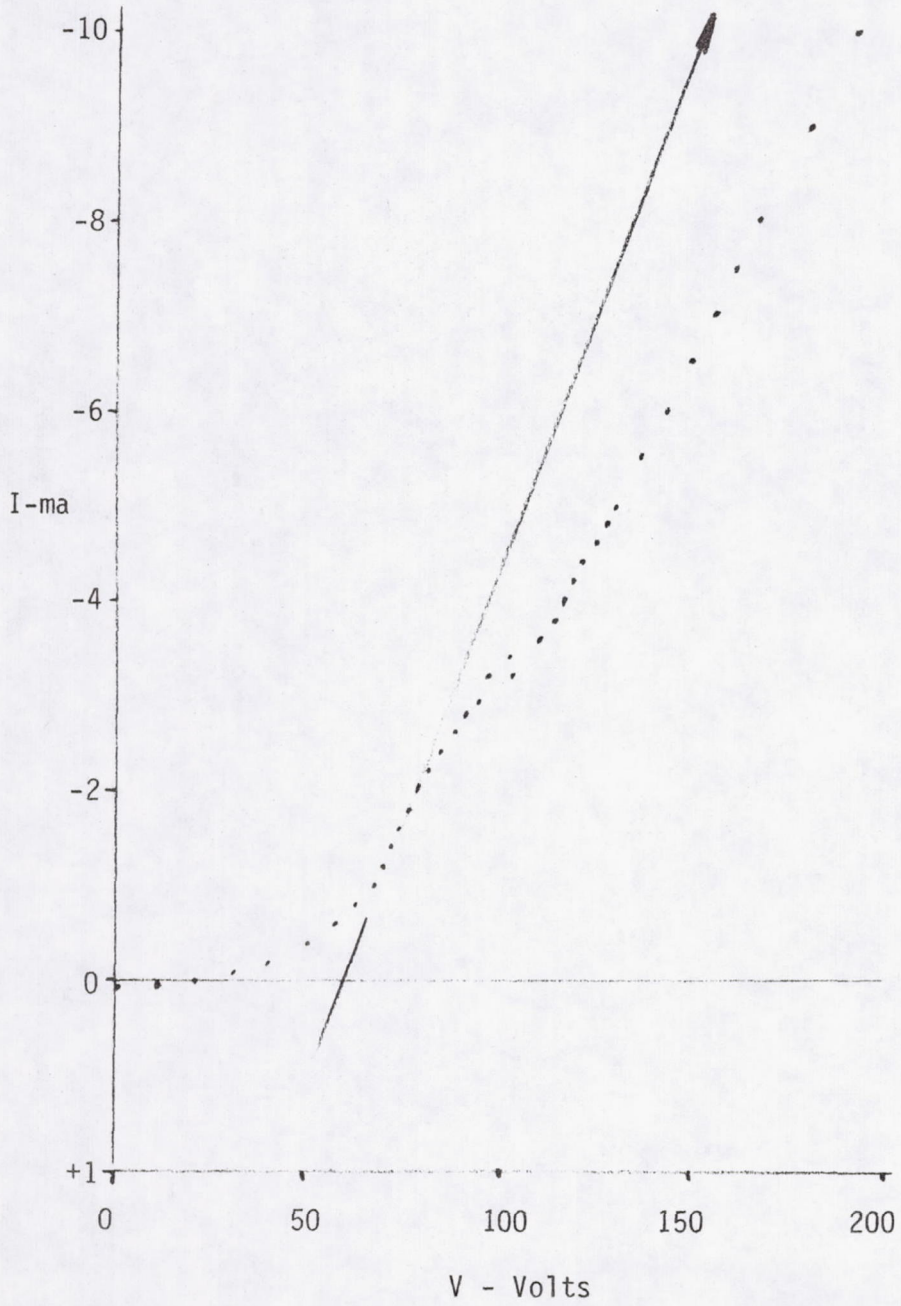

FIGURE 17. ARGON PLASMA PROBE CURVE

4.5 TASK 5 - ELECTRODE MATERIAL AND PLACEMENT

Percent survival calculations for B. subtilis spores exposed to helium and argon plasmas generated by electrodes made from expanded steel (Electrode II) are presented in Table 8. Also included in the table is data, for comparison, of the previous set of electrodes used throughout Phase I.

The most apparent improvement in plasma lethality, i.e., spore death, is seen with 50 watts for both helium and argon. The new electrodes accounted for a two log reduction in spore survival.

In addition to spore survival analyses, Langmuir probe measurements were made during each of the tests (see Figures 12, 14, 15 and 17). Calculations, obtained from these plots for electron temperature and plasma density, are compared in Table 9. In addition, spore survival percentages are included.

In the case of helium plasma, the increase in spore lethality may be explained by an increase in electron temperature of 44 eV to 56 eV. However, the same ease of interpretation is not noted for the argon data. Calculations show apparent physical similarities in the two plasmas produced by the two different electrodes, but dissimilarities in spore survival. Also, visual observation of the appearance of the two plasmas detected a readily noted difference. The color of the plasma produced with the newer electrodes was more intense and extended much further down into the chamber. The nature of this apparent difference for argon plasma is not yet understood.

Table 10 shows the percent spore survival calculations for the organisms exposed to helium plasma produced by electrodes located around the middle of the chamber. Low percentages of spore survival were noted at even the lowest rf power of 10 watts. It is difficult to compare these lethalities with data obtained during Phase I from plasmas produced with the electrodes at the original placement. The newer location or configuration may provide a means of sterilizing at lower rf power than so far envisioned.

Table 8. Mean Percent Survival of Bacillus subtilis Spores in Plasma[a]

PLASMA GAS, 20 CC/MINUTE	RF POWER, WATTS	ELECTRODE MATERIAL	
		PHASE I SOLID COPPER	PHASE II EXPANDED STEEL
Argon	50	3.877[b]	0.043
	150	0.049	0.077
Helium	50	22.143	0.160
	150	0.031	0.017

a. 15 minutes exposure, 0.2 mm Hg pressure, Position 2
b. Mean of 6 replicates.

Table 9. Comparison of Plasma Environment with Spore Survival[a]

ELECTRODE MATERIAL	RF POWER, WATTS	ARGON			HELIUM		
		MEAN % SURVIVORS	ELECTRON TEMP.	PLASMA DENSITY	MEAN % SURVIVORS	ELECTRON TEMP.	PLASMA DENSITY
Electrode I (Copper)	50	3.88 [b]	31 eV[c]	2×10^{10} [c] cm^{-3}	22.14	44 eV	1.3×10^{9} cm^{-3}
Electrode II (Expanded Steel)	50	0.04	27 eV	2.5×10^{10} cm^{-3}	0.16	56 eV	3.2×10^{9} cm^{-3}

a. 0.2 mm Hg pressure, 20 cc/min. gas flow, 15 minute exposure, Position 2.

b. Mean of 6 replicates

c. Extrapolation of Langmuir probe measurements.

Table 10. Mean Percent Survival of Bacillus subtilis Spores in Helium Plasma[a]

RF POWER, WATTS	CHAMBER POSITION		
	1	2	3
10	0.217[b]	0.314	0.134
50	0.049	0.019	0.008

a. 20 cc per minute, 0.2 mm Hg pressure, 15 minutes exposure

b. Mean of 8 replicates

5.0 SUMMARY

The following conclusions of Phase II have been reached:

(1) Microorganisms are killed by plasma gas. Death rates vary between microbial types.

(2) Energetic ultraviolet radiation (the 21.2 eV resonance line particularly) appears to be primary kill mechanism and causes disruption of the physical integrity of the cell.

(3) Helium gas, or a combination of helium and argon, yield plasmas which are the most efficient for sterilization.

(4) Plasma density and electron temperature measurements were developed that provide plasma diagnostics for comparison with microbial kill data. Increases in electron temperatures will increase the amount of microbial death.

Plasma density was increased by using electrodes made of different material and of slightly larger dimensions.

6.0 REFERENCES

1. E. W. McDaniel in "Collision Phenomena in Ionized Gases," John Wiley, 1964, p. 115.

2. I. Langmuir and H. Mott Smith, Gen. Elec. Review 27, 449, 538, 616, 762, 810 (1924).

3. D. Bohm, E.H.S. Burhop, and H.S.W. Massey, in A. Guthrie and R. K. Wakerling, Eds., "The Characteristics of Electrical Discharge in Magnetic Fields," NNES, Div. 1, Vol. 5, McGraw-Hill Book Co., Inc., 1949, p. 13.

4. J. E. Allen, R.L.F. Boyd, and P. Reynolds, Pro. Phys. London, B70, 297 (1953).

5. D. B.Bernstein and I. N. Rabinowitz, Phys. Fluids 2, 112 (1959).

7.0 APPENDIX

The data for Phase II are presented in Tables 11 through 13.

Table II. Mean Number of Microorganisms Surviving Helium Plasma Exposure [a]

TEST ORGANISM	CHAMBER POSITION	HELIUM PLASMA EXPOSURE, MINUTES				
		0	5	10	15	30
Bacillus subtilis WCR-8, Spore	1	4.6×10^5	2.8×10^3 [b]	1.3×10^3	1.8×10^3	4.9×10^2
	2		7.8×10^3	2.7×10^3	2.2×10^3	2.2×10^3
	3		2.0×10^4	8.4×10^3	5.1×10^3	2.5×10^3
JPL-1, Spore	1	6.5×10^5	1.6×10^5	9.0×10^4	2.9×10^4	6.3×10^3
	2		2.0×10^5	1.3×10^5	4.5×10^4	1.7×10^4
	3		2.3×10^5	2.2×10^5	9.8×10^4	1.4×10^4
JPL-2, Spore	1	6.0×10^5	1.5×10^4	1.1×10^4	1.1×10^4	5.3×10^3
	2		2.2×10^4	1.5×10^4	1.5×10^4	6.8×10^3
	3		4.1×10^4	3.8×10^4	2.4×10^4	1.3×10^4
JPL-16, Spore	1	2.0×10^5	2.0×10^3	2.3×10^3	1.5×10^3	7.6×10^2
	2		1.7×10^4	4.7×10^3	1.9×10^3	1.3×10^3
	3		1.5×10^4	6.5×10^3	6.0×10^3	3.7×10^3
JPL-5, Nonsporeformer	1	5.3×10^5 [c] (2.4×10^6)	6.2×10^2	1.4×10^2	1.2×10^2	3.3×10^0
	2		2.0×10^3	5.0×10^2	4.1×10^2	7.5×10^0
	3		1.3×10^4	1.6×10^3	5.9×10^2	8.8×10^1
Staphylococcus epidermidis, Nonsporeformer	1	6.5×10^4 [c] (5.0×10^5)	0	0	0	0
	2		0	0	0	0
	3		0	0	0	0
Aspergillus niger, Fungal Spore	1	2.7×10^4	1.5×10^2	6.6×10^1	1.5×10^1	9.0×10^0
	2		6.7×10^2	1.0×10^2	5.6×10^1	1.7×10^1
	3		1.9×10^3	4.6×10^2	1.8×10^2	4.3×10^1

a. 300 watts, 0.2 mm Hg pressure, 20 cc/minute gas flow

b. Mean of 6 replicates

c. Corrected for vacuum effects

Table 12. Mean Number of Spores Surviving Helium Plasma Exposure [a]

ORGANISM	SPORE SUSPENDING MEDIUM	HELIUM PLASMA EXPOSURE, MINUTES				
		0	5	15	30	60
Bacillus subtilis var. niger, WCR-8, Spore, JPL	Alcohol	5.6×10^4 [b]	1.9×10^3	3.6×10^2	2.4×10^2	2.5×10^2
	Water	6.1×10^4	1.6×10^2	3.8×10^1	8.3×10^0	2.2×10^0
Bacillus subtilis var. niger, ATCC 9372, Spore, Boeing	Alcohol	7.7×10^3	0.5×10^0	1.0×10^0	1.3×10^0	0
	Water	1.1×10^4	0	0	0	0

a. 300 watts, 0.2 mm Hg pressure, 20 cc/minute gas flow, Chamber Position 1

b. Mean of 6 replicates

Table 13. Mean Percent Survival of Bacillus Subtilis var. Niger Spores Protected from Plasma Environment with Filters

FILTER	BEGINNING SPECTRAL TRANSMISSION, NANOMETERS	ARGON PLASMA	HELIUM PLASMA	OXYGEN PLASMA
Glass	340	1.7×10^5 [c]	1.2×10^5 [c]	1.8×10^5 [d]
Corning 9-54	220	7.4×10^2	3.4×10^3	9.5×10^4
Sapphire Window	140	1.6×10^2	3.8×10^2	1.0×10^5
No Filter	-	2.3×10^1	4.4×10^1	0

a. 150 watts, 0.2 mm Hg pressure, 20 cc/min. gas flow, Position 1, 15 minutes exposure.

b. Mean of 6 replicates.

c. 2.0×10^5 at 0 time.

d. 2.2×10^5 at 0 time.

SECTION IV

PHASE III

PLASMA GAS PENETRATION

PHASE III

TABLE OF CONTENTS

PHASE III

PLASMA GAS PENETRATION

1.0 PURPOSE

The objective of this task was to determine the effectiveness of plasma gas in contacting and sterilizing surfaces of different geometric configurations.

2.0 INTRODUCTION

In the previous phases of this study, it had been demonstrated that plasma gas sterilized exposed flat surfaces. Also, an earlier contract conducted for the National Heart and Lung Institute showed that argon plasma was capable of sterilizing plastic hollow fiber, medical devices. During this latter investigation no effort had been made to determine the degree of plasma penetration nor microbial reduction; i.e., analysis was to determine if the device was sterile or unsterile.

3.0 PROCEDURE

Two geometric configurations were selected to evaluate the penetrating property of helium plasma. Tubing of varied lengths and internal diameters and protected or "mated" surfaces were chosen. Samples of metal and glass were selected because of differences in conductive electrical properties.

3.1 CAPILLARY TUBING

Capillary tubing of three different internal diameters were tested. Originally, the test plan was to use tubing of 1.0, 0.5 and 0.1 cm inside diameter (I.D.). However, test results of the 0.1 cm tubing revealed that more meaningful data would be obtained if we selected even smaller tubing for the remainder of the investigation. Tube size availability and spore recovery limited the investigation to tubing of 0.1, 0.07 and 0.05 cm I.D. The test matrix is shown in Table 1.

Table 1: Test Matrix to Determine the Effectiveness of Helium Plasma in Penetrating and Sterilizing Capillary Tubes

Dimensions, cm		Glass			Stainless Steel		
		[a] Helium Plasma, min.			Helium Plasma, min.		
I.D.	Length	0	15	60	0	15	60
0.1	4.0	[b] A 1	A 4	A 7	B 10	B 13	B 16
0.1	[c] 8.0	A 2	A 5	A 8	B 11	B 14	B 17
0.1	12.0	A 3	A 6	A 9	B 12	B 15	B 18
0.07	4.0				D 28	D 31	D 34
0.07	8.0	(TUBING NOT AVAILABLE)			D 29	D 32	D 35
0.07	12.0				D 30	D 33	D 36
0.05	4.0	E 37	E 40	E 43	F 46	F 49	F 52
0.05	8.0	E 38	E 41	E 44	F 47	F 50	F 53
0.05	12.0	E 39	E 42	E 45	F 48	F 51	F 54

[a] 150 watts rf, 0.2 mm Hg pressure, 20 cc helium flow per minute, Chamber Position 1

[b] Five replicates

[c] Lengths longer than 4 cm consisted of 4 cm sections attached end-to-end.

Lengths of glass and stainless steel tubes 4 cm long, cleaned and sterilized, were inoculated with an aqueous suspension of B. subtilis var. niger spores. This was accomplished by capillary action. The excess volume was removed by touching the tube tip to sterile filter paper. Seeded tubes were allowed to clean bench dry before testing.

Tubing lengths of 4, 8 and 12 cm long were assembled from 4 cm segments. They were attached end to end and formed a continuous length of tubing of uniform diameter. Following plasma exposure, each 4 cm segment was assayed separately to determine the extent of penetration and sterilization. Bioassay for surviving spores was conducted with techniques previously outlined. Procedural controls to determine the effectiveness of insonation for removal of all internal spores from vacuum treated tubes were conducted and the results showed that the procedure was successful.

Plasma exposures were for 15 and 60 minutes. Helium plasma was generated with 150 watts rf at 0.2 mm Hg and 20 cc per minute gas flow. Test tubing, clipped to a circular ring, was placed at Chamber Position 1 so that the tubes were oriented lengthwise in the chamber.

3.2 MATED SURFACES

Mated surfaces were investigated by using stacked discs of mated pairs. Figure 1 shows the arrangement of a mated surface test stack. A stack consisted of two sterile discs sandwiched between two inoculated discs. Test discs were inoculated on one surface with B. subtilis spores and dried overnight in the airflow of a Class 100 clean bench. On each inoculated surface, a completely sterilized disc was placed. After plasma exposure, the discs were analyzed separately. However, the data obtained were evaluated for each pair of discs. Some of the disc pairs were analyzed to determine the total number of spores that survived plasma exposure and some were overlayed with a nutrient medium for subsequent visual inspection for indication of plasma gas penetration.

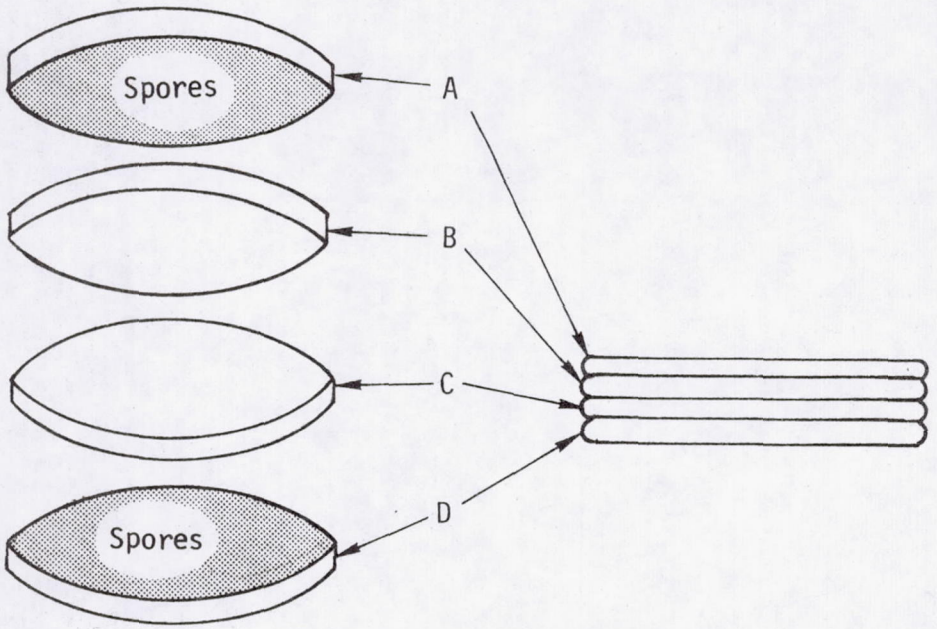

FIGURE 1: SCHEMATIC OF MATED SURFACE TEST STACK

4.0 RESULTS AND DISCUSSION

Analysis for the number of spores that survived plasma exposure was conducted.

4.1 CAPILLARY TUBING

Percentage calculations for spore survival was performed for all data. The values for glass capillaries are shown in Table 2. It was noted that no spores survived after 60 minutes plasma exposure for tubing 0.1 cm I.D. and 12 cm long. Tubing of 0.05 cm I.D. still had some viable spores after 60 minutes of plasma treatment, although the percent survival was very low.

Plasma treated stainless steel tubing did not show as low percent survival figures as the glass tubing (Table 3). However, spore reduction was noted. The middle 4 cm segment of the 12 cm long tubes showed more percent survival than either 4 cm end. Helium plasma, at the operating conditions of these experiments, was able to penetrate in both directions into a tube.

The higher spore reductions observed for glass tubing may be due to two factors. Irradiation, due to intense uv that is capable of penetrating through the glass walls, may be one explanation. The other possibility is that the dielectric properties of stainless steel may neutralize or "shield" organisms from plasma.

Although sterilization did not occur in the stainless steel tubes, spore reduction did. A series of tests were performed that kept all test conditions the same except the rf power was increased to 300 watts. Inoculated stainless steel tubing, exposed to helium plasma at the higher rf power value was analyzed for survivors. Percentage survival figures are given in Table 4. Sterility of all segments of a 12 cm long tube was noted after 60 minutes plasma treatment.

Table 2: Mean Percent Survival of Bacillus subtilis var. niger Spores in Glass Tubing After Exposure to Helium Plasma

Sample Diameter, Centimeters	Helium Plasma Exposure, Minutes [a]	Tube Length, Centimeters	Mean Percent Survival Entire Tube	Mean Percent Survival/ Tube Segments		
				4 cm	4 cm	4 cm
0.102	15	4	0.22	0.22		
		8	1.25	0.74	1.76	
		12	1.59	2.68	0.90	1.19
	60	4	0.00	0.00		
		8	0.13	0.01	0.01	
		12	0.00	0.00	0.00	0.00
0.051	15	4	1.00	1.00		
		8	2.24	2.22	2.26	
		12	0.57	0.42	1.09	0.19
	60	4	0.02	0.02		
		8	0.12	0.09	0.14	
		12	0.05	0.03	0.14	0.00

[a] 10^4 spores at 0 time

Table 3: Mean Percent Survival of Bacillus subtilis var. niger Spores in Stainless Steel Tubing After Exposure to Helium Plasma

Sample Diameter, Centimeters	Helium Plasma Exposure, Minutes	Tube Length, Centimeters	Mean Percent Survival Entire Tube	Mean Percent Survival/ Tube Segments		
				4 cm	4 cm	4 cm
0.127	15	4	87.53	87.53		
		8	71.43	72.65	70.20	
		12	78.91	75.92	100.00	60.82
	60	4	2.37	2.37		
		8	5.55	7.06	4.04	
		12	13.80	8.46	28.29	4.66
0.071	15	4	4.60	4.60		
		8	5.96	6.59	5.32	
		12	14.14	1.80	28.80	11.82
	60	4	0.52	0.52		
		8	0.04	0.03	0.06	
		12	0.80	0.00	2.35	0.02
0.053	15	4	21.89	21.89		
		8	25.40	27.17	23.64	
		12	22.30	20.50	28.89	17.50
	60	4	4.35	4.35		
		8	3.77	4.58	2.95	
		12	5.85	3.18	9.46	4.93

Table 4: Mean Percent Survival of Bacillus subtilis var. niger Spores in Stainless Steel Tubing after Exposure to Helium Plasma[a]

Sample Diameter, Centimeters	Helium Plasma Exposure, Minutes	Tube Length Centimeters	Mean Percent Survival/Tube	Mean Percent Survival/ Tube Segments		
				4 cm	4 cm	4 cm
0.071	15	4	0.00	0.00		
		8	0.00	0.00	0.00	
		12	1.04	0.11	2.39	0.63
	60	4	0.00	0.00		
		8	0.00	0.00	0.00	
		12	0.00	0.00	0.00	0.00

[a] 300 watts rf

Table 5: Percent Survival of Bacillus subtilis var. niger Spores on Mated Surfaces that Were Exposed to Helium Plasma [a]

Test Number	Percent Spores Surviving per Mated Surface		
	Mean	Mated Pair	
		A + B	C + D
1	70.18	64.46	75.90
2	49.55	40.91	58.18
3	73.49	73.77	73.21
4	73.89	61.11	86.66
5	52.01	34.03	69.99
Mean	64.25	55.57	72.93

[a] 60 minutes, 300 watts rf, 0.2 mm Hg, 20 cc/min. gas flow

4.2 MATED SURFACES

The ability of plasma to penetrate and sterilize contaminated, mated surfaces was investigated. Data obtained for the number of microorganisms surviving a plasma treatment of such surfaces show a slight reduction from those numbers originally present. Table 5 shows the percent survival of the mated surface pairs following a 60 minute helium plasma exposure. These data are from mated aluminum discs. Studies performed with mated glass surfaces showed that few, or no organisms survived. However, as noted previously it is felt that penetration along the surface did not occur, but that most of the kill was caused by ultraviolet irradiation of intense amounts penetrating through the thin glass.

5.0 SUMMARY

The results of this phase of the investigation lead to the following conclusions:

1) Helium plasma (300 watts rf) sterilized metal capillary tubes 0.07 by 12.0 cm and contaminated with 10^4 spores within 60 minutes.

2) Plasma is a surface sterilizer. If objects are exposed to plasma for sufficient time, sterilization of all surfaces will occur.

3) Helium plasma was not able to penetrate mated metal surfaces to any great extent.

6.0 APPENDIX

The data for Phase III are presented in Tables 6 through 12.

Table 6: Number of *Bacillus subtilis* var. *niger* Spores Surviving Helium Plasma Exposure of Inoculated Glass Capillary Tubing of 0.10 Centimeters I.D.

Helium Plasma Exposure, Minutes	Test Number Sample Position	Number Surviving Spores Per 4 cm Tube			Mean Number Survivors/Entire Tube	No Plasma Exposure, Mean	
		a	b	c		Per 4 cm	Per Entire Tube
15	A4 1	0				5866	5866
	2	0					
	3	3					
	4	7					
	5	53			13		
	A5 1	10	53			4460	8920
	2	3	10				
	3	20	47				
	4	10	83				
	5	123	197		111		
	A6 1	0	0	37		1968	5904
	2	7	3	0			
	3	20	3	10			
	4	57	10	20			
	5	180	78	50	71		
60	A7 1	0				5866	5866
	2	0					
	3	0					
	4	0					
	5	0			0		
	A8 1	0	0			4460	8920
	2	0	0				
	3	0	0				
	4	0	0				
	5	3	3		1		
	A9 1	0	0	0		1968	5904
	2	0	0	0			
	3	0	0	0			
	4	0	0	0			
	5	0	0	0	0		

Table 7: Number of Bacillus subtilis var. niger Spores Surviving Helium Plasma Exposure of Inoculated Glass Capillary Tubing of 0.05 Centimeters I.D.

Helium Plasma Exposure, Minutes	Test Number Sample Position	Number Surviving Spores Per 4 cm Tube			Mean Number Survivors/Entire Tube	No Plasma Exposure, Mean	
		a	b	c		Per 4 cm	Per Entire Tube
15	E40 1	23				3287	3287
	2	67					
	3	33					
	4	17					
	5	23			33		
	E41 1	10	17			2277	4554
	2	27	0				
	3	73	110				
	4	50	30				
	5	93	100		102		
	E42 1	0	0	0		2377	7131
	2	0	0	0			
	3	17	47	3			
	4	33	40	10			
	5	0	43	10	41		
60	E43 1	0				3287	3287
	2	3					
	3	0					
	4	0					
	5	0			1		
	E44 1	0	0			2277	4554
	2	0	3				
	3	0	0				
	4	7	13				
	5	3	0		5		
	E45 1	0	0	0		2377	7131
	2	0	0	0			
	3	3	13	0			
	4	0	3	0			
	5	0	0	0	4		

Table 8: Number of Bacillus subtilis var. niger Spores Surviving Helium Plasma Exposure of Inoculated Stainless Steel Capillaru Tubing of 0.127 Centimeters I.D.

Helium Plasma Exposure, Minutes	Test Number Sample Position	Number Surviving Spores Per 4 cm Tube			Mean Number Survivors/Entire Tube	No Plasma Exposure, Mean	
		a	b	c		Per 4cm	Per Entire Tube
15	B13 1	4400				6000	6000
	2	6200					
	3	5030					
	4	4230					
	5	6400			5252		
	B14 1	3900	4400			4900	9800
	2	3100	3000				
	3	3900	3100				
	4	2600	2600				
	5	4300	4100		7000		
	B15 1	2800	4100	3400		4900	14,700
	2	3600	5700	2500			
	3	4300	6500	3500			
	4	4800	6600	3000			
	5	3100	4900	2500	12,260		
60	B16 1	40				6000	6000
	2	100					
	3	170					
	4	180					
	5	220			142		
	B17 1	150	410			6434	12,868
	2	253	150				
	3	650	230				
	4	510	300				
	5	707	210		714		
	B18 1	33	913	267		6434	19,302
	2	220	1373	110			
	3	727	2000	400			
	4	713	2087	310			
	5	1030	2737	417	2664		

Table 9: Number of Bacillus subtilis var. niger Spores Surviving Helium Plasma Exposure of Inoculated Stainless Steel Capillary Tubing of 0.07 Centimeters I.D.

Helium Plasma Exposure, Minutes	Test Number Sample Position	Number Surviving Spores Per 4 cm Tube a	b	c	Mean Number Survivors/Entire Tube	No Plasma Exposure, Mean Per 4cm	Per Entire Tube
15	D31 1	120				2030	2030
	2	50					
	3	87					
	4	57					
	5	153			93		
	D32 1	110	170			2367	4734
	2	310	210				
	3	100	70				
	4	90	90				
	5	170	90		282		
	D33 1	60	920	450		2410	7230
	2	0	550	347			
	3	53	763	177			
	4	3	500	130			
	5	100	737	320	1022		
60	D34 1	10				2030	2030
	2	0					
	3	33					
	4	3					
	5	7			11		
	D35 1	0	0			2367	4734
	2	0	0				
	3	3	0				
	4	0	7				
	5	0	0		2		
	D36 1	0	3	3		2410	7230
	2	0	0	0			
	3	0	10	0			
	4	0	60	0			
	5	0	210	0	57		

Table 10: Number of Bacillus subtilis var. niger Spores Surviving Helium Plasma Exposure of Inoculated Stainless Steel Capillary Tubing of 0.05 Centimeters I.D.

Helium Plasma Exposure, Minutes	Test Sample	Number Position	Number Surviving Spores Per 4 cm Tube a	b	c	Mean Number Survivors/Entire Tube	No Plasma Exposure, Mean Per 4 cm	Per Entire Tube
15	F49	1	863				4057	4057
		2	977					
		3	770					
		4	760					
		5	1070			888		
	F50	1	907	1167			3433	6866
		2	1000	890				
		3	823	683				
		4	887	590				
		5	1047	727		1744		
	F51	1	807	1540	707		5033	15,099
		2	1130	1430	1037			
		3	1290	1740	893			
		4	793	1030	920			
		5	1140	1530	847	3367		
60	F52	1	237				4057	4057
		2	173					
		3	310					
		4	310					
		5	163			177		
	F53	1	220	153			3433	6866
		2	113	70				
		3	150	127				
		4	230	117				
		5	73	40		259		
	F54	1	160	270	210		5033	15,099
		2	280	1280	170			
		3	110	150	210			
		4	80	330	290			
		5	170	350	360	884		

Table 11: Number of Bacillus subtilis var. niger Spores Surviving Helium Plasma (300 Watts RF) Exposure of Inoculated Stainless Steel Capillary Tubing of 0.07 Centimeters I.D.

Helium Plasma Exposure, Minutes	Test Number Sample Position	Number Surviving Spores Per 4 cm Tube			Mean Number Survivors/Entire Tube	No Plasma Exposure, Mean	
		a	b	c		Per 4cm	Per Entire Tube
15	I64 1	0				2100	
	2	0					
	3	0					
	4	0					
	5	0			0		
	I65 1	0	0			2623	5246
	2	0	0				
	3	0	0				
	4	0	0				
	5	0	0		0		
	I66 1	17	107	17		5080	15,240
	2	0	73	10			
	3	3	100	63			
	4	0	93	23			
	5	7	233	47	159		
60	I67 1	0				2100	
	2	0					
	3	0					
	4	0					
	5	0			0		
	I68 1	0	0			2623	5246
	2	0	0				
	3	0	0				
	4	0	0				
	5	0	0		0		
	I69 1	0	0	0		5080	15,240
	2	0	0	0			
	3	0	0	0			
	4	0	0	0			
	5	0	0	0	0		

Table 12: *Bacillus subtilis* var. *niger* Spores Recovered from Mated Metal Surfaces that Were Exposed to Helium Plasma [a]

Helium Plasma Test	Number of Surviving Spores per Mated Surface		Control Number of Spores Per Mated Surface (No Plasma)
	a + b	c + d	
1	4280	5040	6640
2	2700	3840	6600
3	6334	6286	8586
4	4306	6106	7046
5	2486	5114	7306
Mean	4021	5277	7236

[a] 300 watts rf, 60 minutes, 0.2 mm Hg, 20 cc per minute gas flow

SECTION V

PHASE IV

EFFECT OF PLASMA GAS ON SELECTED SPACECRAFT MATERIALS

PHASE IV

TABLE OF CONTENTS

PHASE IV

EFFECT OF PLASMA GAS ON SELECTED SPACECRAFT MATERIALS

1.0 PURPOSE

The objective of this task was to determine the effect of plasma gas on candidate spacecraft materials.

2.0 INTRODUCTION

Previous preliminary Boeing data showed that plasma gas did not visibly affect a test group of different materials. The materials included aluminum, stainless steel, glass, plexiglass, Millipore membrances (cellulose acetate), rubber, polypropylene and paper. However, specific spacecraft coatings and films had not been examined. Also, analysis of material damage in the initial study was limited to gross, observable alterations.

Spacecraft materials, chosen after consultation with JPL, were subjected to a plasma environment to determine material compatibility with the process. Specific analysis per American Society Testing Materials Standards, where applicable, were conducted.

3.0 PROCEDURE

The test approach of Phase IV was to expose materials to a plasma environment for an extended time. Following plasma treatment, laboratory analyses of the exposed materials were conducted to evaluate material compatibility with the process. Compatibility was determined by comparing sample materials exposed to plasma to similar specimens that had not been exposed to plasma. Analyses were conducted by the Microbiology Laboratory and the Materials Technology Laboratories.

3.1 CANDIDATE MATERIALS

A description of the nine different spacecraft materials used in this test phase is given in Table 1. Specimens of teflon, mylar, kapton and graphite epoxy were prepared from uniform sheets of materials. Test

Table 1: Selected Spacecraft Test Materials

Material	Description	Sample Size	Source
Teflon FEP Film	Polymer, 1.0 mil, aluminized (resistivity = 1.25 ohms per square)	2 in. squares, 1 x 4 in. strips	DuPont
Mylar Film	Polymer, 0.5 mil, aluminized (resistivity = 1.25 ohms per square)	Same	Same
Kapton Film	Polymer, 1.0 mil, aluminized (resistivity = 1.25 ohms per square)	Same	Same
1R81E	Gold optical coating on fused silica	2 in. squares	Libbey-Owens-Ford
Mark 8	Antireflectance coating on fused silica	2 in. squares	Herron Optics
Polyurethane Flatblack	Chemglaze Z-306	2 in. squares	Hughson Chemicals
Anodized Aluminum	Black, per JPL FS502703, Class II	2 in squares	Hixon Metal Finishing
Aluminized Mirrors	Aluminized (99.9% pure Al) fused silica, vacuum deposited, 1000Å minimum	2 in. squares 3 in. dia. circles	Herron Optics
Graphite Epoxy	Fiberite HY-# 1334A, HM-S graphite fiber, X-934 epoxy resin, 1-2 mil	2 in squares 1/2 x 2 in. strips	Aerotronics Ford

squares were cut with a scapel and handled with lint-free dacron gloves. The remaining material types were prepared by the manufacturers in the dimensions required for testing (2 inch square, 3 inch disc).

3.2 ANALYSES

The matrix of the analyses performed on materials before and after plasma exposure is given in Table 2.

3.2.1 Reflectance

Both total and diffuse reflectance were measured with the Beckman DK-2A Spectroreflectometer in the reflectance mode using an integrating sphere. Specimen orientation was to face the film side towards the light beam source. Reflectance was calculated from the spectra using a 28 point integration at equal solar energy increments. The results were presented as an integrated value of the reflectance over the wavelength measured.

3.2.2 Transmission

The Beckman DK-2A Spectrophotometer in the transmission mode was used to measure the optical transmission. The measurement was made and recorded from 0.25 to 2.5 microns. Any changes effected by plasma exposure was noted and tabulated as to wavelength and intensity.

3.2.3 Mechanical Testing

An Instron tensile test machine, with a cell movement of 0.22 in./min., was used to determine the elongation and ultimate strength of the films (tension). Three point bend was measured, per ASTM 790, on the Instron test machine equipped with a 50 lb load cell.

3.2.4 Electrical Resistivity

Surface resistivity tests were performed on test specimens using the Heathley Model 6105 Resistivity Adaptor. A minimum of three measurements were made on each specimen before and after exposure to radiation. The test method used is described in ASTM D-257 except that no contact material such as foil or silver paint was applied to the specimens. The

Table 2: Analysis Matrix for Evaluation of Effect of Plasmas on Selected Spacecraft Materials

ANALYSIS \ MATERIALS →	Teflon Film	Mylar Film	Kapton Film	1R81E Coating	Mark 8 Coating	Polyurethane Flatblack	Anodized Aluminum	Vacuum Deposited Aluminum	Graphite Epoxy	
Reflectance	•	•	•	•	•	•	•	•		
Transmission				•	•					
Mechanical Tension	•	•	•							
Mechanical Three Point Bend									•	
Electrical Resistivity								•		
Visual Examination	•	•	•	•	•	•	•	•	•	
Scanning Electron Microscope	o	o	o	o	o	o	o	o	o	
Sterility	•	•	•	•	•	•	•	•	•	

• Analysis performed.

o Analysis performed if surface alteration visible.

method deviation resulted in some measurement uncertainty, but was used to avoid damage to the deposited surfaces of the samples. The test voltage of 20V d-c was applied through a 20 Kohm limiting resistor. The resistivity in ohms (avg. of 3 readings) = $\frac{53.4V}{I}$.

3.2.5 Visual Examination

Visual examination of test materials was performed with a Bausch and Lomb microscope (14-60X magnification range). Any visual alteration in a surface was noted, and if judged significant, further examination of the alteration was performed with a scanning electron microscope.

3.2.6 Scanning Electron Microscope

The Ultrascan, a scanning electron microscope (SEM) was used for the examination of those test samples that had detectable visible alteration after plasma exposure. Photomicrographs were made of each sample selected for SEM examination.

3.2.7 Sterility

Specimens of each test material were inoculated with approximately 10^6 Bacillus subtilis var. niger spores. Spores were suspended in water and deposited on the surface of a sample in a 0.1 ml drop. No attempt to spread the liquid was made. Evaporation of the liquid was in the airflow of a Class 100 clean bench. After drying, the area of inoculation was noted to be a spot no larger than 1 cm in diameter. Inoculated test materials were included in each plasma exposure test. The samples were analyzed, after plasma exposure, for sterility by implantation in melted Trypticase Soy Agar. The absence of microbial growth on the specimen material, after 14 days incubation at $30^{o}C$, indicated sterility.

3.3 PLASMA ENVIRONMENT

A plasma test environment, produced at 150 watts rf, was generated for helium gas and oxygen gas. Earlier study results indicated possible variations in mechanisms of kill for the two gases. Chamber pressure was maintained during oxygen or helium plasma production at 0.2 mm Hg for 20 cc per minute test gas flow.

exposure of the test materials to plasma totaled 6 hours. If plasma and material incompatibilities did exist, they should occur and be detected at these prolonged test exposures.

3.4 TEST SEQUENCE

Figure 1 diagrams the stepwise flow of the nine test materials from sample preparation through analysis. Three separate plasma tests were replicated for each material type. Different materials were never exposed together. Also, separate specimens of each test material were prepared for each required analysis. This procedure was established to prevent excessive handling of specimens. An exception was in samples analyzed for electrical resistivity. Testing on unexposed specimens was performed to obtain control data. The same specimens were then exposed to plasma and analyzed for changes in resistivity.

4.0 RESULTS AND DISCUSSION

Specimens of materials, exposed to helium and oxygen plasmas, were analyzed to detect any alterations in material properties with respect to values for reflectance, transmission, mechanical tension and three point bend, electrical resistivity, and visual appearance.

4.1 REFLECTANCE

Reflectance values (R) were calculated from spectra of test samples obtained in the total reflectance mode with a spectroreflectometer (Table 3). The test material, polyurethane flatblack, was the only material in which its R value changed after exposure to either helium or oxygen plasma. The other seven materials did not show any major changes in R after plasma exposure when compared to controls that had not been exposed to plasma.

4.2 OPTICAL TRANSMISSION

Transmission measurements (T) of plasma treated sample materials were made. The transmission spectral values were calculated. The T values are presented in Table 4. The two sample coatings, IR81E and Mark 8, did not show any change in transmission after plasma exposure.

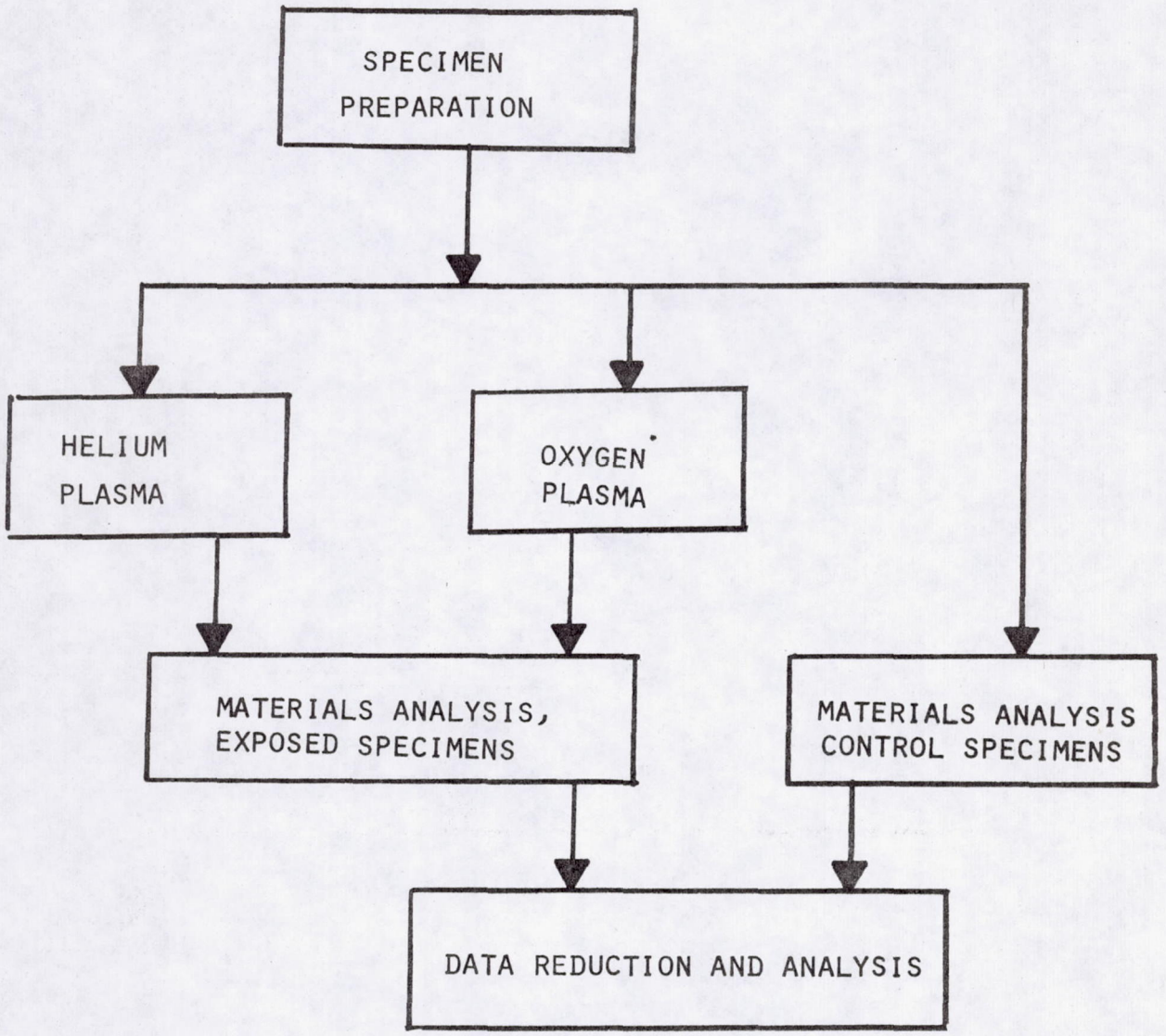

FIGURE 1: TEST SEQUENCE

Table 3: Reflectance of Materials Exposed to Helium and Oxygen Plasmas [a]

Material	Sample Number	Treatment	Reflectance (R)[a]
Teflon FEP Film	A1	No plasma	0.81
	B4	"	0.83
	C7	"	0.84
	A10	Helium plasma	0.79
	B13	" "	0.83
	C16	" "	0.80
	A19	Oxygen plasma	0.68
	B22	" "	0.79
	D25	" "	0.82
Mylar Film	A1	No plasma	0.77
	B4	"	0.77
	C7	"	0.77
	A10	Helium plasma	0.69
	B13	" "	0.76
	C16	" "	0.76
	A19	Oxygen plasma	0.75
	B22	" "	0.75
	C25	" "	0.74
Kapton Film	A1	No plasma	0.55
	A10	Helium plasma	0.55
	A19	Oxygen plasma	0.53
	B22	" "	0.53
	C25	" "	0.52
1R81E	A1	No plasma	0.21
	A10	Helium plasma	0.22
	B13	" "	0.23
	C16	" "	0.22
	A19	Oxygen plasma	0.21
	B22	" "	0.23
	C25	" "	0.23
Mark 8	A1	No plasma	0.10
	A10	Helium plasma	0.10
	B13	" "	0.10
	C16	" "	0.10
	A19	Oxygen plasma	0.09
	B22	" "	0.10
	C25	" "	0.10

Table 3: Reflectance of Materials Exposed to Helium and Oxygen Plasmas [a] (Continued)

Material	Sample Number	Treatment	Reflectance (R) [a]
Polyurethane Flatblack	A1	No plasma	0.04
	B	"	0.05
	C7	"	0.05
	A10	Helium plasma	0.02
	B13	" "	0.02
	C16	" "	0.02
	A19	Oxygen plasma	0.11
	B22	" "	0.14
	C25	" "	0.14
Anodized Aluminum	A1	No plasma	0.25
	A10	Helium plasma	0.24
	A19	Oxygen plasma	0.25
	B22	" "	0.28
	C25	" "	0.28
Vacuum Deposited Aluminum	A1	No plasma	0.90
	A10	Helium plasma	0.89
	B13	" "	0.90
	C16	" "	0.90
	A19	Oxygen plasma	0.89
	B22	" "	0.90
	C25	" "	0.90

[a] R values obtained with Beckman DK-2A Spectroreflectometer. Values calculated from spectra obtained in the total reflectance mode for the spectral range 0.25-2.5 microns. The calculations were made using a 29 point integration. A National Bureau of Standards reflectance tile was measured immediately prior to specimen measurement. It served as a standard material of known R to which all spectra were corrected. The accuracy and precision of the R determinations are $\pm$ 0.02 and $\pm$ 0.01 respectively.

Table 4: **Transmission Measurement of Materials Exposed to Helium and Oxygen Plasmas**

Material	Sample Number	Treatment	Transmission (T)
1R81E	A2	No plasma	0.62
	B5	"	0.61
	C8	"	0.61
	A11	Helium plasma	0.62
	B14	" "	0.62
	C17	" "	0.62
	A20	Oxygen plasma	0.60
	B23	" "	0.60
	C16	" "	0.60
Mark 8	A2	No plasma	0.90
	A11	Helium plasma	0.89
	B14	" "	0.89
	C17	" "	0.89
	A20	Oxygen plasma	0.89
	B23	" "	0.89
	C26	" "	0.89

4.3 MECHANICAL TESTING

Specimens of the three aluminized films, teflon, mylar and kapton, and the structural material graphite epoxy were exposed to plasmas and measured for changes in mechanical properties.

4.3.1 Mechanical Tension

Tension analysis of the three aluminized films were conducted. Measurements of ultimate load and calculations for percent elongation are shown in Table 5. Mylar film which was exposed to helium plasma was not noticeably affected with respect to its tension property. However, oxygen plasma treated mylar exhibited a marked decrease in elongation characteristics.

Teflon film also was not, with respect to tension measurements, affected by exposure to helium plasma. A moderate reduction in elongation was noted for oxygen plasma treated samples.

Kapton film was not noticeably affected by oxygen plasma. However, helium plasma exposure resulted in an increase in percent elongation of kapton film.

4.3.2 Mechanical Three Point Bend

Three point bend measurements of plasma treated graphite epoxy specimens are recorded in Table 6. Graphite epoxy, which was exposed to helium plasma, was unaffected. No measurable changes occurred following a 6 hour helium plasma treatment, whereas oxygen plasma effected a moderate reduction in load values of exposed specimens of graphite epoxy.

4.4 ELECTRICAL RESISTIVITY

Surface resistivity tests were performed on specimens of vacuum deposited aluminized mirrors. The average of three measurements for each specimen, before and after plasma exposure, is shown in Table 7. The results showed surface resistivities from 10^{11} to 10^{14} ohms and no consistent changes between before and after plasma exposure specimens.

Table 5: Mechanical Tension Properties of Materials Exposed to Helium and Oxygen Plasmas [a]

Material	Sample Number	Treatment	Ultimate Load (lbs)	Elongation (%)
Mylar	A3	No plasma	6.2	72
	B6	"	6.2	105
	C9	"	6.0	100
	A12	Helium plasma	5.3	89
	B15	"	5.0	76
	C18	"	3.9	37
	A21	Oxygen plasma	1.6	0
	B24	"	2.3	1
	C27	"	2.6	2
Teflon	A3	No plasma	2.0	150
	B6	"	4.9	280
	C9	"	3.6	240
	A12	Helium plasma	2.1	230
	B15	"	2.1	241
	C18	"	2.2	180
	A21	Oxygen plasma	1.7	76
	B24	"	1.6	68
	C27	"	2.2	87
Kapton	A3	No plasma	21.5	28
	B6	"	29.0	70
	C9	"	25.2	30
	A12	Helium plasma	32.3	80
	B15	"	32.3	70
	C18	"	34.6	87
	A21	Oxygen plasma	17.6	18
	B24	"	25.0	46
	C27	"	20.4	25

[a] Values obtained using an Instron tester with a cell movement of 0.11"/minute.

Table 6: Three Point Bend Properties of Graphite Epoxy Exposed to Helium and Oxygen Plasmas [a]

Sample Number	Treatment	Thickness (inches)	Width (inches)	Ultimate Load (lb)
A3	No plasma	0.012	0.545	17 [b]
B6	"	0.011	0.554	10.1
C9	"	0.015	0.568	13.7
A12	Helium plasma	0.011	0.521	10.1
B15	"	0.012	0.555	10.8
C18	"	0.011	0.499	8.8
A21	Oxygen plasma	0.011	0.536	9.4
B24	"	0.010	0.548	7.8
C27	"	0.010	0.534	5.0

[a] Per ASTM standard, span 1/2", head movement 0.11"/minute, 50 lb cell

[b] 500 lb/cell for this sample only.

Table 7: Electrical Resistivity of Vacuum Deposited Aluminum Mirrors

Sample Number	Plasma Treatment	Resistivity	
		Before	After
A3	No plasma	7.12×10^{13}	1.78×10^{14}
C9	No plasma	1.46×10^{13}	3.14×10^{11}
A12	Helium plasma	5.72×10^{13}	1.03×10^{14}
B15	Helium plasma	6.28×10^{12}	shorted
C18	Helium plasma	8.05×10^{11}	1.79×10^{12}
A21	Oxygen plasma	1.19×10^{13}	3.56×10^{13}
B24	Oxygen plasma	2.14×10^{12}	1.9×10^{12}
C27	Oxygen plasma	7.0×10^{12}	1.89×10^{12}

4.5 VISUAL EXAMINATION

Low power visual examination of oxygen and helium plasma treated materials was performed. No surface changes were noted in any of the specimens with the exception of the black coating, polyurethane flatblack. Slight changes were observed in this material for helium plasma treated samples, whereas oxygen plasma effected a major surface change. Erosion of the surface to the primer was noted. The polyurethane flatblack specimens were examined further with the scanning electron microscope.

4.6 SCANNING ELECTRON MICROSCOPE

Electron micrographs were made of the test material polyurethane flatblack (Section 4.5) after plasma exposure (Figure 2). Surface alteration is readily observed in both the helium and oxygen plasma treated samples.

4.7 STERILITY

Results of sterility testing of sample materials, inoculated with controlled numbers of B. subtilis spores, and exposed to plasmas are given in Table 8. Sterility of all samples was not attained. However, from initial numbers of 10^6, the number of organisms that survived totaled no more than 2 spores per three specimens of material. Visual location of the dense spot of inoculum on a specimen was not identifiable following plasma exposure.

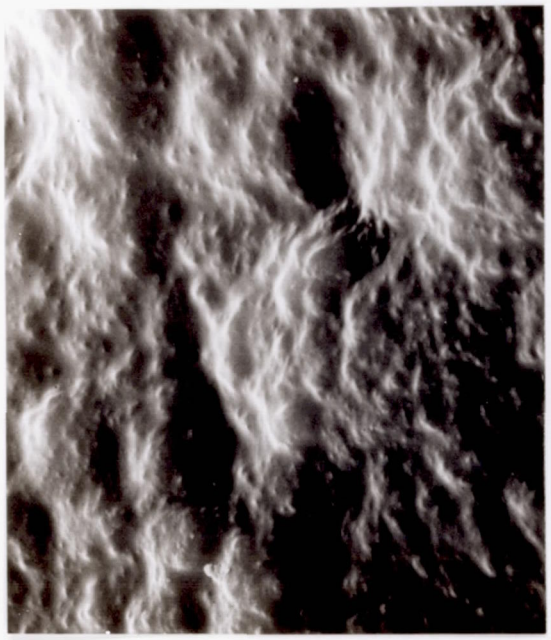

NO PLASMA

HELIUM PLASMA

OXYGEN PLASMA

FIGURE 2: POLYURETHANE FLATBLACK, 1200X

Table 8: Sterility of Materials Exposed to Plasma

Material [a]	Helium Plasma	Oxygen Plasma
Teflon	NS [b]	NS
Mylar	S [c]	S
Kapton	NS	S
Mark 8	S	S
Polyurethane Flatblack	S	S
Anodized Aluminum	NS	S
Graphite Epoxy	NS	S

[a] Three replicates of each material per plasma.

[b] Not sterile (NS); no more than 2 organisms per sample (10^6) survived.

[c] Sterile (S)

5.0 SUMMARY

Nine selected spacecraft materials were subjected to excessive exposures of helium and oxygen plasmas (6 hours). Specific material analyses were conducted to determine material compatibility with the process. The results are summarized in Table 9. The reflectance of all materials, exposed to helium plasma and oxygen plasma, with the exception of one, polyurethane flatblack, remained unaffected by the plasmas. Transmission and electrical resistivity also were unchanged.

The three aluminized films tested, teflon, mylar and kapton, did experience some modifications in mechanical properties due to plasma. The changes in measurements ranged from slight to marked, with particular observation of alterations in percent elongation due to oxygen plasma.

Complete sterility of all material specimens with thick inoculation "spots" was not observed. However, those samples that were not sterilized had no more than 2 viable spores from an original level of 10^6.

Table 9: Effect of Plasmas on Selected Spacecraft Materials

ANALYSIS \ MATERIALS →	Teflon Film		Mylar Film		Kapton Film		1R8IE Coating		Mark 8 Coating		Polyurethane Flatblack		Anodized Aluminum		Vacuum Deposited Aluminum		Graphite Epoxy	
	H	O	H	O	H	O	H	O	H	O	H	O	H	O	H	O	H	O
Reflectance	NC	NC	NC	NC	NC	NC	NC	NC	NC	NC	C	C	NC	NC	NC	NC		
Transmission							NC	NC	NC	NC								
Mechanical Tension	SC	C	SC	C	C	SC												
Mechanical Three Point Bend																	NC	C
Electrical Resistivity															NC	NC		
Visual Appearance	NC	NC	NC	NC	NC	NC	NC	NC	NC	NC	SC	C	NC	NC	NC	NC	NC	NC
Scanning Electron Microscope											C	C						

H = Helium Plasma

O = Oxygen Plasma

NC = No Change

SC = Slight Change

C = Change

SECTION VI

DESIGN OF PLASMA GAS STERILIZER

DESIGN

Detailed drawings of the plasma sterilizer used in this study are presented in Figures 1 through 11.

The electronics package that provided radio frequency power was described in Section II, Phase I, of this document.

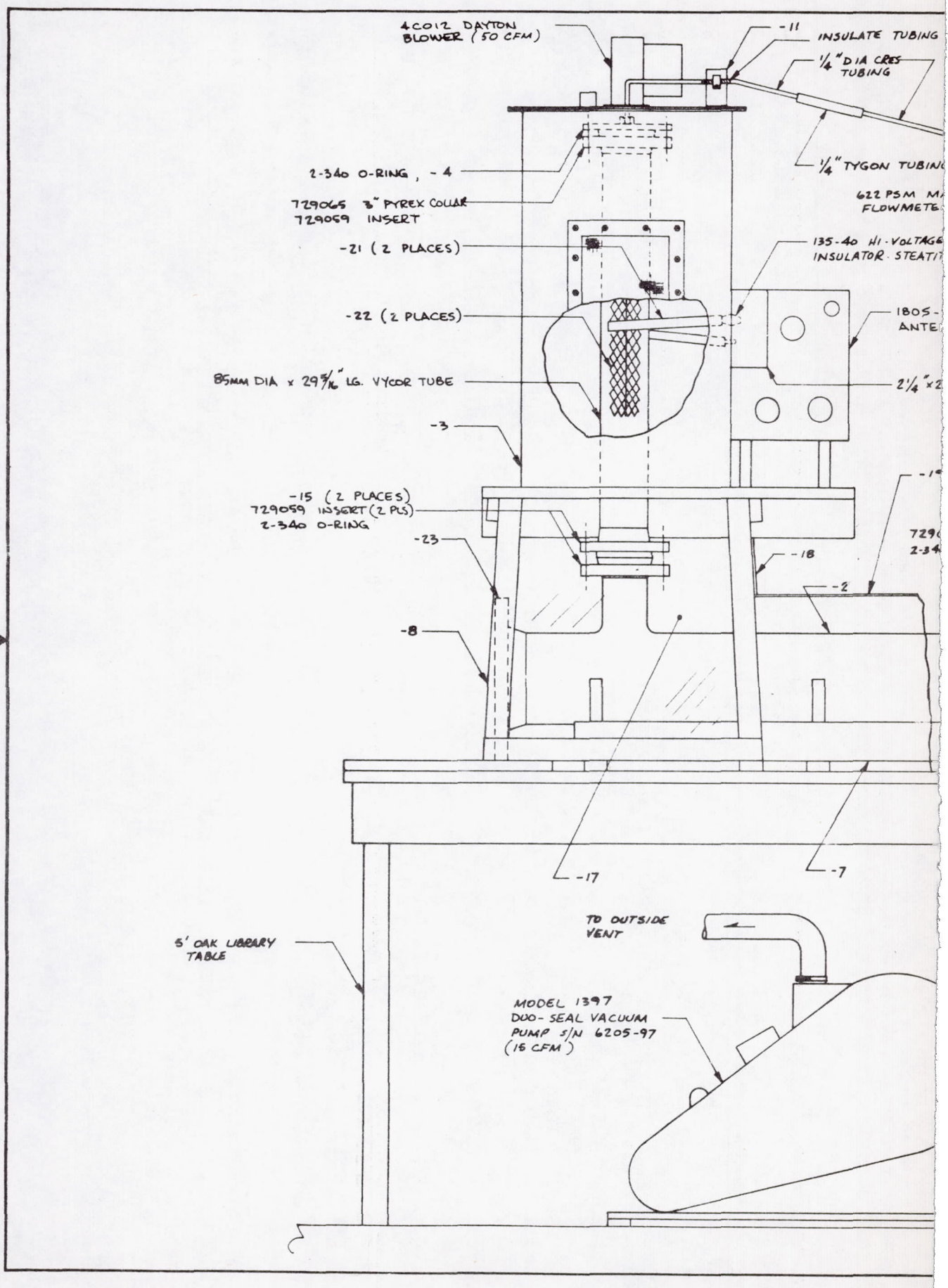
4C012 DAYTON BLOWER (50 CFM)
-11
INSULATE TUBING
1/4" DIA CRES TUBING
1/4" TYGON TUBING
2-340 O-RING, -4
729065 3" PYREX COLLAR
729059 INSERT
622 PSM MA
FLOWMETE
-21 (2 PLACES)
135-40 HI-VOLTAGE
INSULATOR STEATI
-22 (2 PLACES)
1805-
ANTE
85MM DIA x 29 5/16" LG. VYCOR TUBE
2 1/4" x 2
-3
-15 (2 PLACES)
729059 INSERT (2 PLS)
2-340 O-RING
-23
-18
-2
-8
-17
-7
TO OUTSIDE VENT
5' OAK LIBRARY TABLE
MODEL 1397
DUO-SEAL VACUUM
PUMP S/N 6205-97
(15 CFM)

FRO— WITH 1/32" x 2" WIDE TEFLON TAPE (2 TURNS)

REVISIONS			
ZONE	LTR	DESCRIPTION	DATE	APPROVED

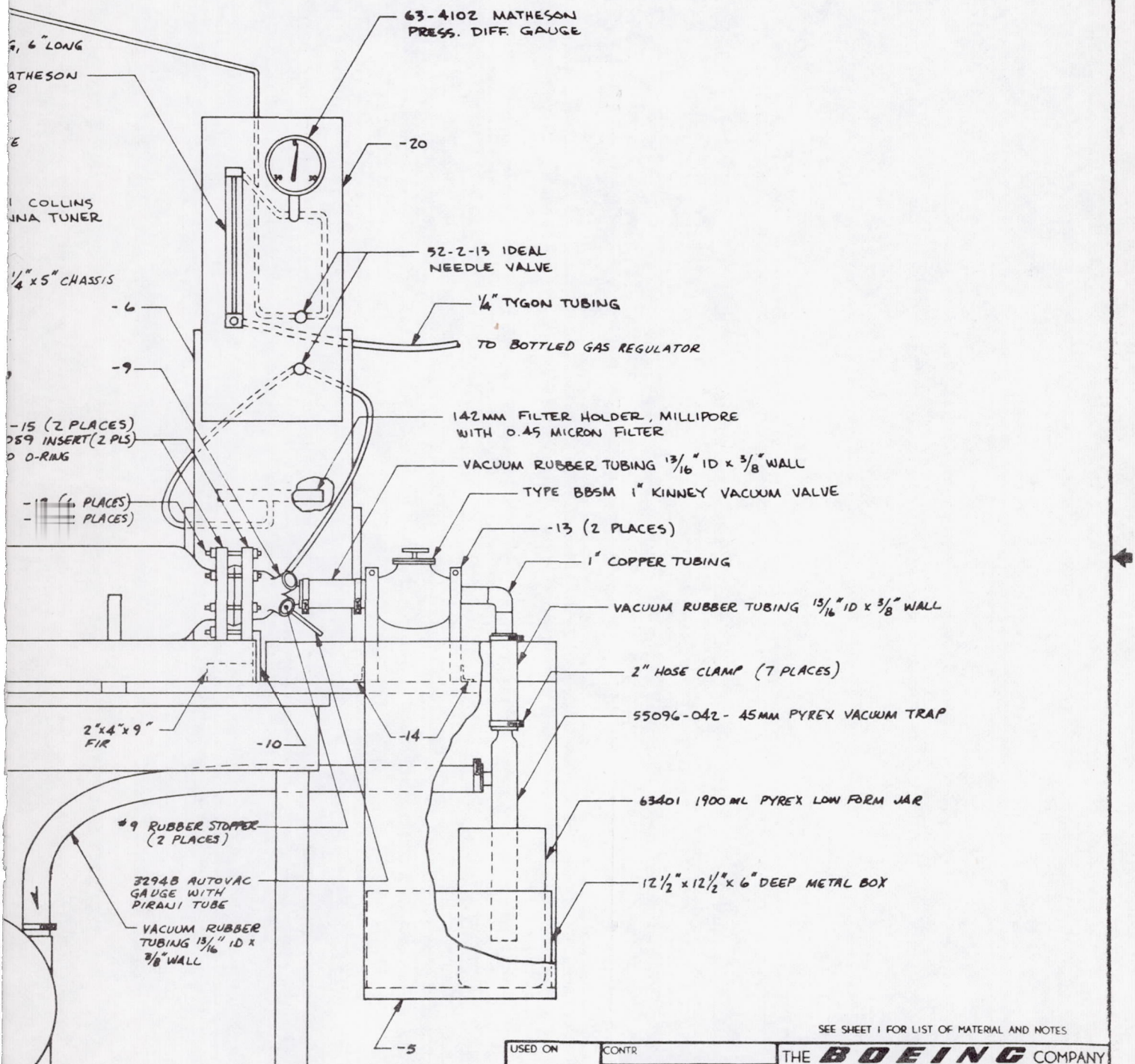

SEE SHEET 1 FOR LIST OF MATERIAL AND NOTES

USED ON	CONTR	THE BOEING COMPANY SEATTLE, WASHINGTON	
	DR BOB NELSON 8/4/75		
	CHK	GAS PLASMA STERILIZER	
SECT NO.	STRUCT		
	ENGR 8-21-75		
CHG NO.	GR PROJ RZ Olson	SIZE D	CODE IDENT NO. 81205 — 29-50548
ORIG BY (GROUP) 2-5640		SCALE 1/4	SH 1 OF 11

DRAWING RECORDS CLERK

D1 4709 1004

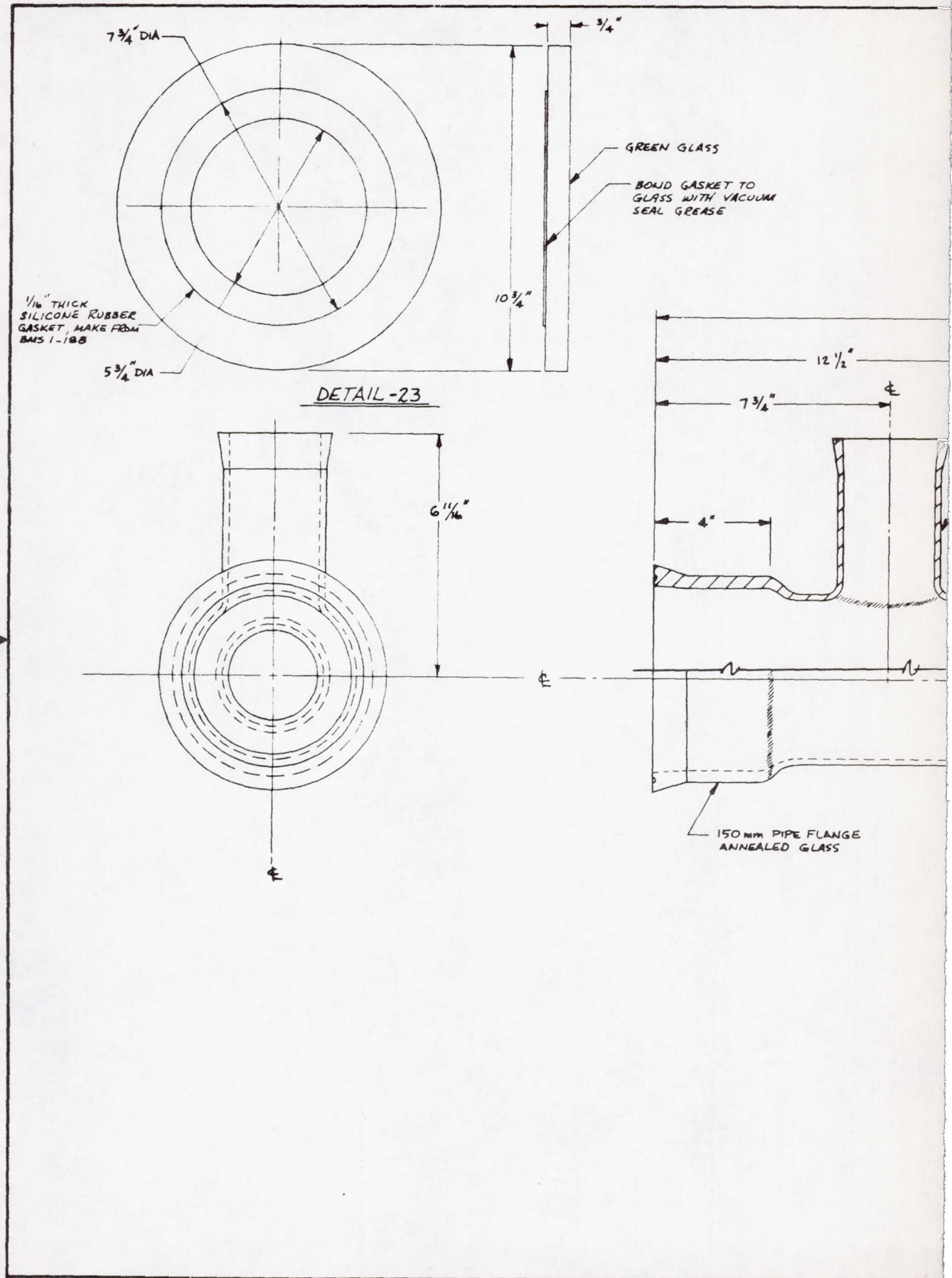
7 3/4" DIA
3/4"
GREEN GLASS
BOND GASKET TO GLASS WITH VACUUM SEAL GREASE
10 3/4"
1/16" THICK SILICONE RUBBER GASKET, MAKE FROM BMS 1-188
5 3/4" DIA
DETAIL-23
12 1/2"
7 3/4"
6 11/16"
4"
150 mm PIPE FLANGE ANNEALED GLASS

REVISIONS			
LTR	DESCRIPTION	DATE	APPROVED

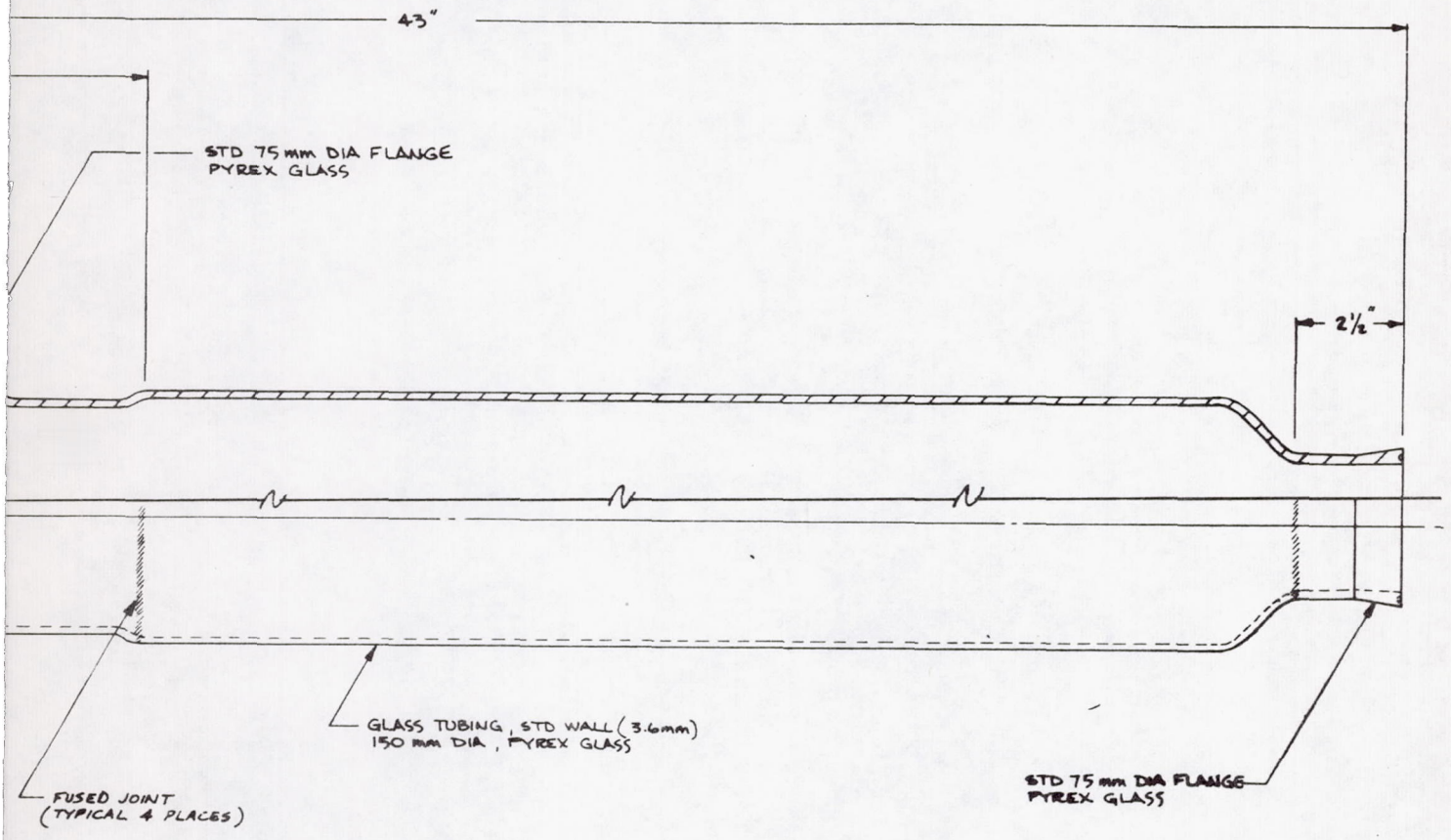

DETAIL -2

FOR PARTS LIST AND APPLICATION DATA SEE PL

DIMENSIONING & TOLERANCING PER ANSI (USAS) Y 14.5 UNLESS OTHERWISE SPECIFIED DIMENSIONS ARE IN INCHES TOLERANCES: ANGLES ± DECIMALS .XX ± DECIMALS .XXX ± RIVET & BOLT EDGE MARG ±.05 BEND RADII ±.01 ON .03 & .06 ±.03 ON .09 & GREATER SHEET METAL CORNER RADII INT 1/16 .25 EXT .00	REVIEW & APPROVAL ORIG QUAL STRUCT MATL & PROC CHANGE/ITEM NUMBER	CONTRACT NUMBER DWN BOB NELSON 8/4/75 CHK [illegible] 8/21/75 ENGR [illegible] 8/21/75 ORG PROJECT APPROVAL	THE BOEING COMPANY CORPORATE OFFICES SEATTLE, WASHINGTON 98124 GAS PLASMA STERILIZER SIZE D CODE IDENT NO. 81205 29-50548 SCALE 1/2 SH. 2

DWG ORNG BY HORGE 2.5640

29-50548

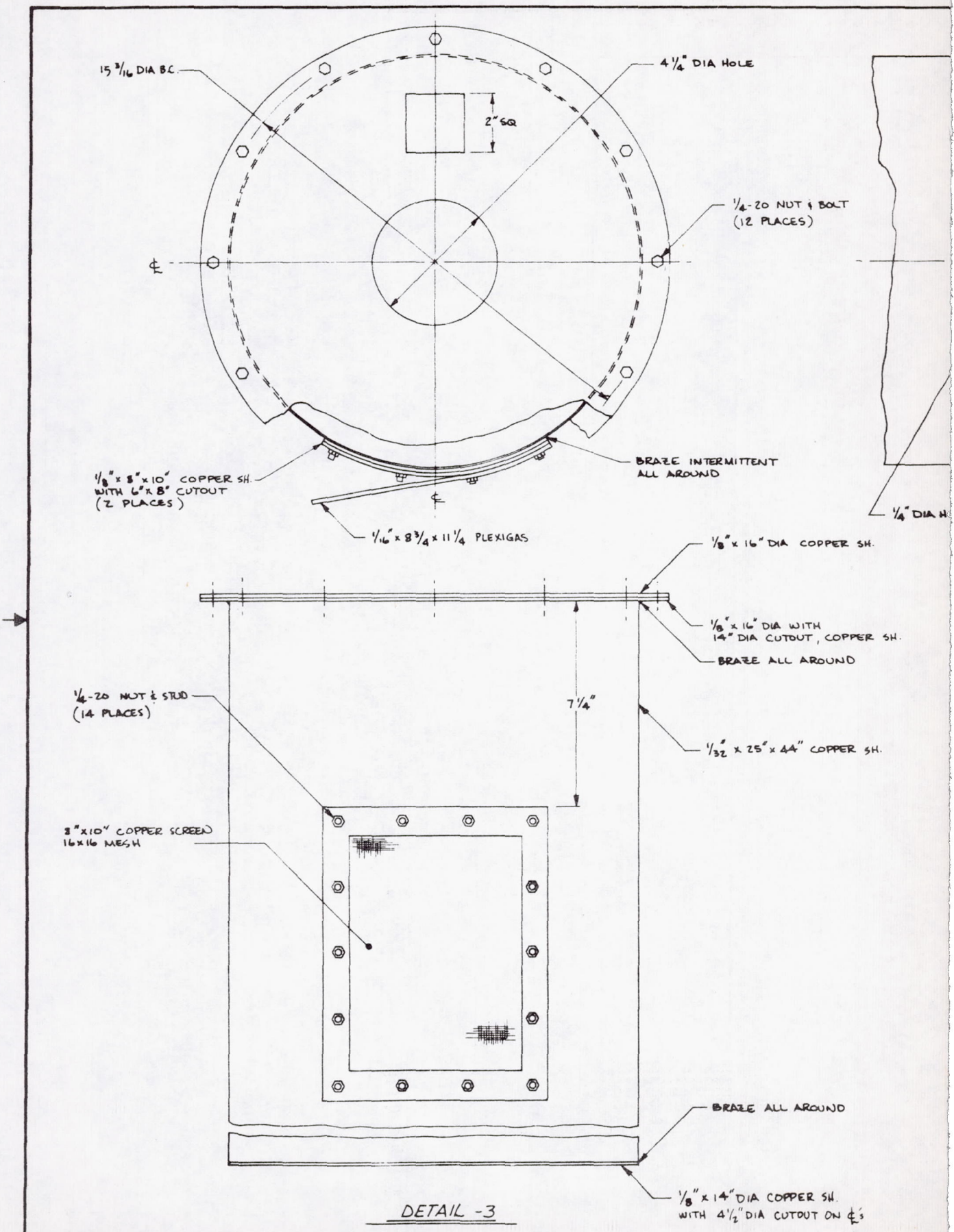
15 3/16 DIA B.C.
4 1/4" DIA HOLE
2" SQ
1/4-20 NUT & BOLT
(12 PLACES)
1/8" x 8" x 10" COPPER SH.
WITH 6" x 8" CUTOUT
(2 PLACES)
BRAZE INTERMITTENT
ALL AROUND
1/16" x 8 3/4 x 11 1/4 PLEXIGAS
1/8" x 16" DIA COPPER SH.
1/8" x 16" DIA WITH
14" DIA CUTOUT, COPPER SH.
BRAZE ALL AROUND
1/4-20 NUT & STUD
(14 PLACES)
7 1/4"
1/32" x 25" x 44" COPPER SH.
8" x 10" COPPER SCREEN
16 x 16 MESH
BRAZE ALL AROUND
1/8" x 14" DIA COPPER SH.
WITH 4 1/2" DIA CUTOUT ON ℄'s

DETAIL -3

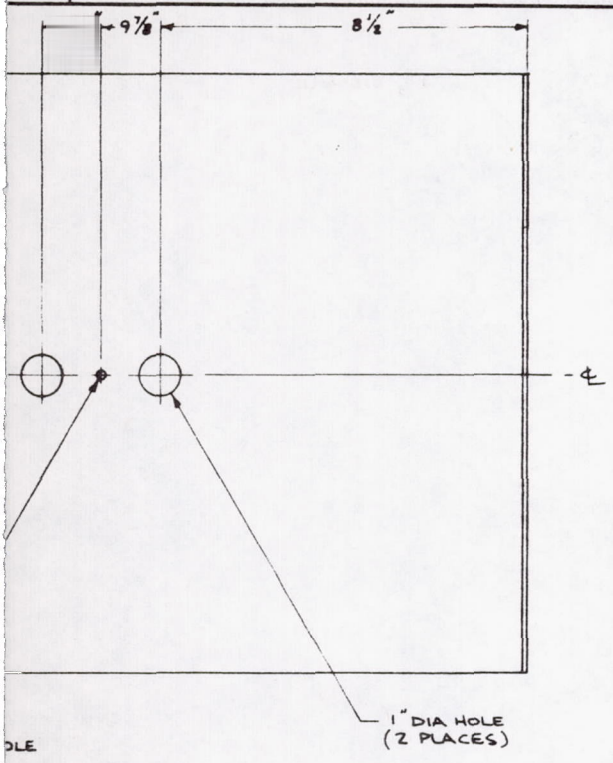

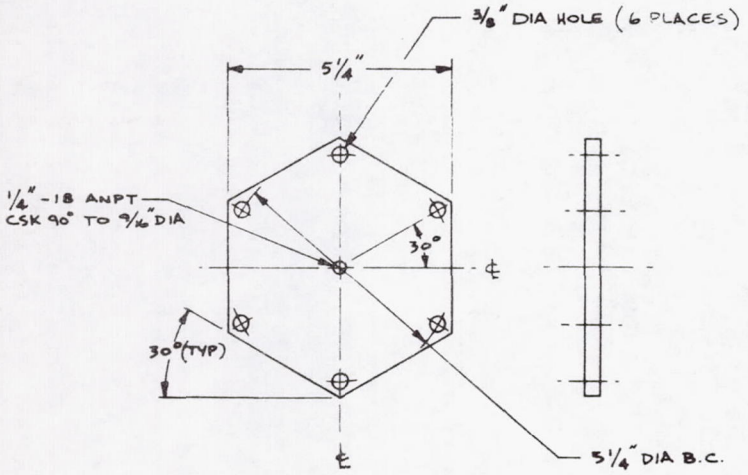

DETAIL -4

3/8" 2024-T4, ALUM.

REVISIONS

LTR	DESCRIPTION	DATE	APPROVED

FOR PARTS LIST AND APPLICATION DATA SEE PL

DIMENSIONING & TOLERANCING PER ANSI (USASI) Y14.5

UNLESS OTHERWISE SPECIFIED
DIMENSIONS ARE IN INCHES
TOLERANCES: ANGLES ±
DECIMALS .XX ±
DECIMALS .XXX ±
RIVET & BOLT EDGE MARG ± .05
BEND RADII ±.01 ON .03 & .06
±.02 ON .09 & GREATER
SHEET METAL CORNER RADII
INT .19/16 EXT .25/.00

REVIEW & APPROVAL

DWG QUAL	
STRUCT	
MATL & PROC	
CHANGE/ITEM NUMBER	

CONTRACT NUMBER

DWN	BOB NELSON	8/4/75
CHK		
ENGR		
ORG		
PROJECT APPROVAL		

THE BOEING COMPANY
CORPORATE OFFICES SEATTLE, WASHINGTON 98124

GAS PLASMA STERILIZER

SIZE	CODE IDENT NO.	
D	81205	29-50548
SCALE NONE		SH 3

REV

29-50548

DRAWING RECORDS CLERK

DWG ORIG BY (ORG) 2-5640

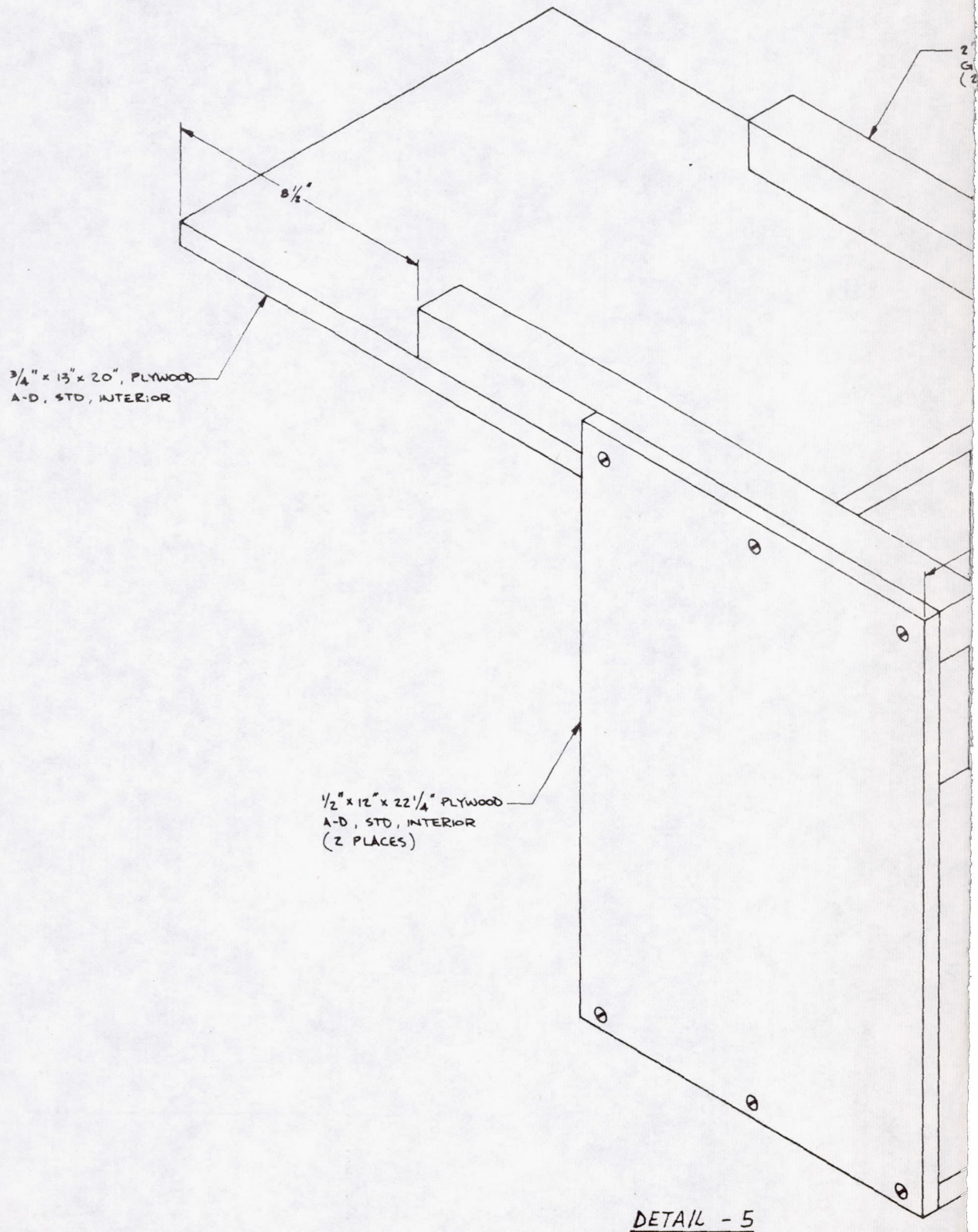
8½"
3/4" x 13" x 20", PLYWOOD
A-D, STD, INTERIOR
½" x 12" x 22¼" PLYWOOD
A-D, STD, INTERIOR
(2 PLACES)

DETAIL - 5

REVISIONS			
LTR	DESCRIPTION	DATE	APPROVED

x 2" x 18 1/4", 545, COMMERCIAL
RADE, HEMLOCK OR FIR
. PLACES)

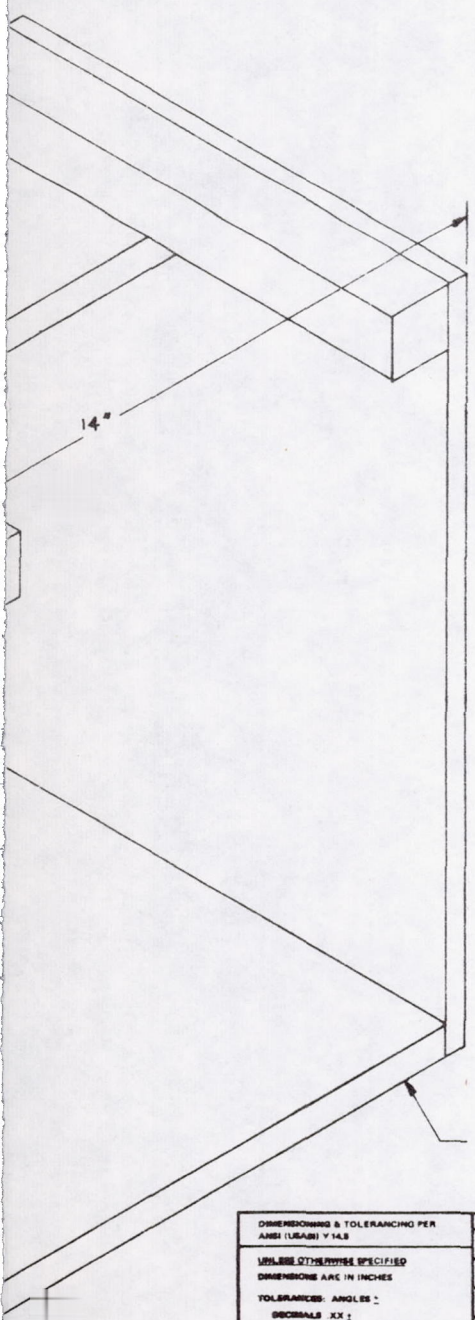

NOTE: ASSEMBLE WITH #8 FLAT HD WOOD SCREWS AS REQUIRED.

FOR PARTS LIST AND APPLICATION DATA SEE PL

DIMENSIONING & TOLERANCING PER ANSI (USASI) Y 14.5	REVIEW & APPROVAL	CONTRACT NUMBER	THE BOEING COMPANY
UNLESS OTHERWISE SPECIFIED DIMENSIONS ARE IN INCHES	DWG QUAL		CORPORATE OFFICES SEATTLE, WASHINGTON 98124
TOLERANCES: ANGLES ±	STRUCT	DWN BOB NELSON 8/4/75	GAS PLASMA STERILIZER
DECIMALS .XX ±	MATL & PROC	CHK [illegible]	
DECIMALS .XXX ±		ENGR Sheila Fraser 8-21-75	
RIVET & BOLT EDGE MARG ± .05		ORG	
BEND RADII ± .01 ON .03 & .05 ± .05 ON .09 & GREATER		PROJECT APPROVAL [illegible]	
SHEET METAL CORNER RADII INT .10 .16 EXT .35 .60	CHANGE/ITEM NUMBER		SIZE D CODE IDENT NO. 81205 29-50548 SCALE NONE SH 4

DWG ORIG BY (ORG) 2-5640

DRAWING RECORDS CLERK

DD 6000 1228 ORIG 6/73

REV

29-50548

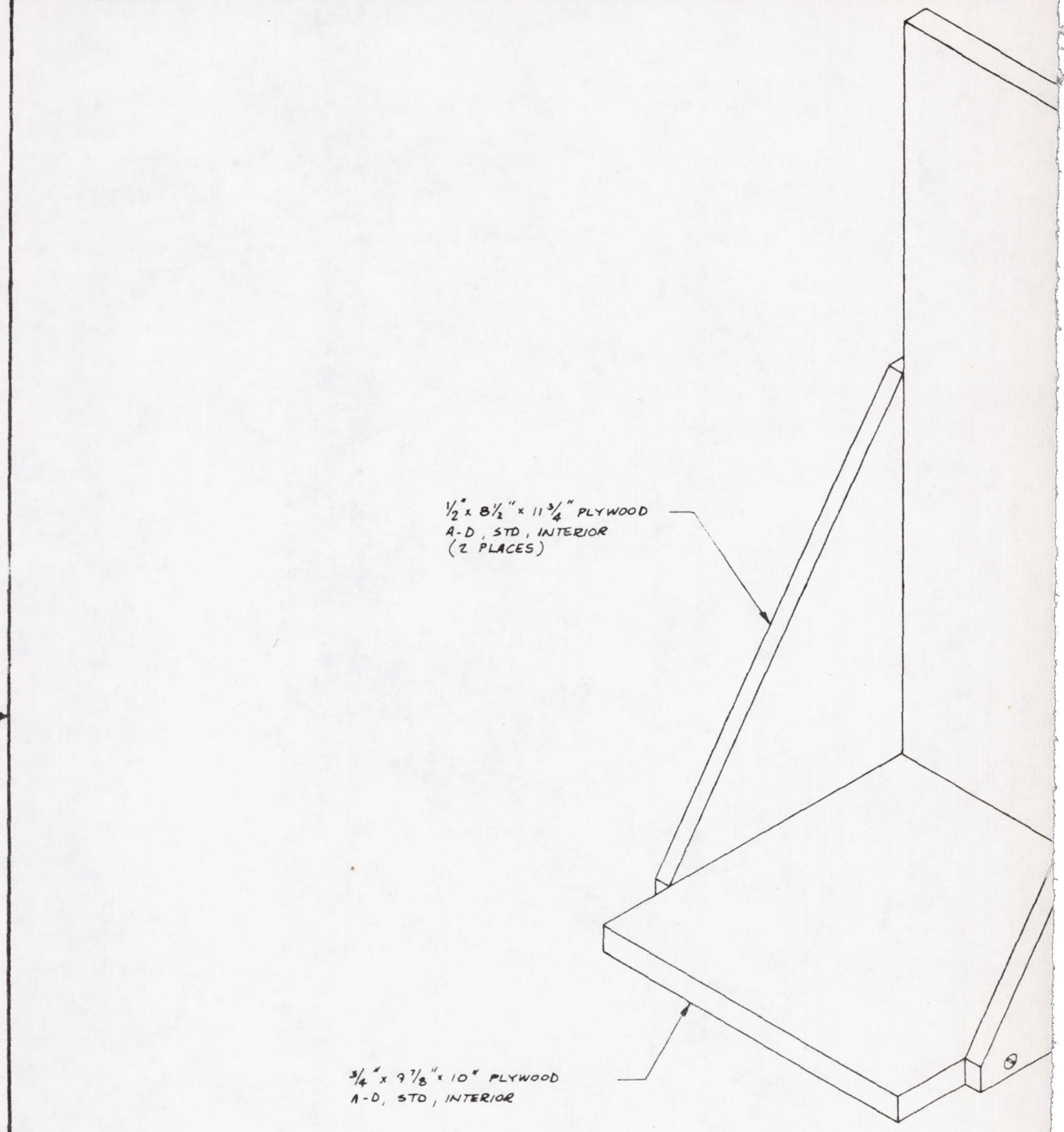
1/2" x 8 1/2" x 11 3/4" PLYWOOD
A-D, STD, INTERIOR
(2 PLACES)
3/4" x 9 7/8" x 10" PLYWOOD
A-D, STD, INTERIOR

DETAIL - 6

REVISIONS			
LTR	DESCRIPTION	DATE	APPROVED

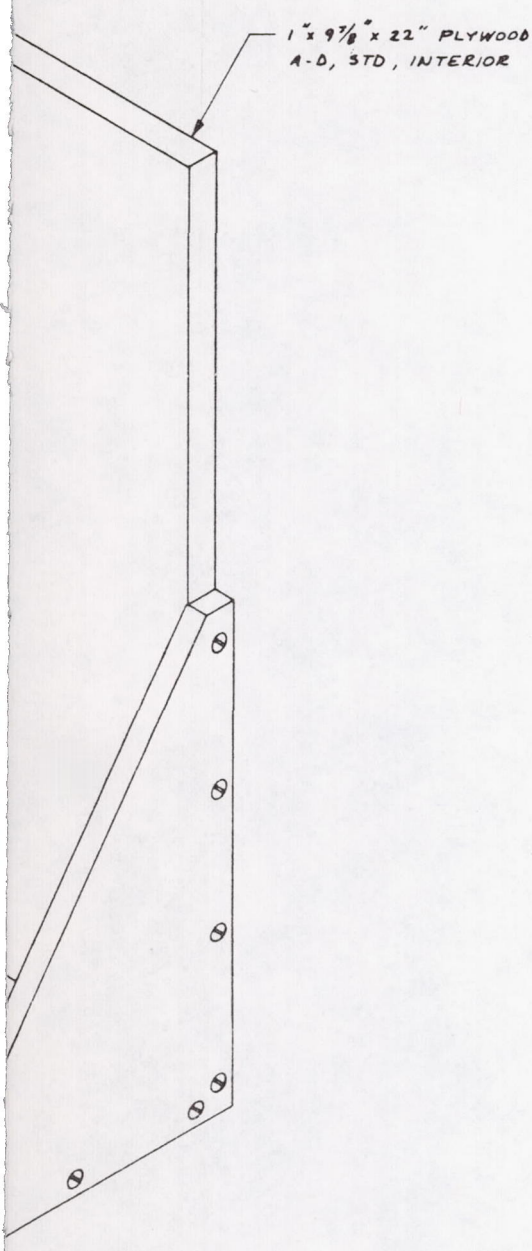

NOTE: ASSEMBLE WITH #8 FLAT HD WOOD SCREWS AS REQUIRED.

FOR PARTS LIST AND APPLICATION DATA SEE PL

DIMENSIONING & TOLERANCING PER ANSI (USASI) Y14.5 UNLESS OTHERWISE SPECIFIED DIMENSIONS ARE IN INCHES TOLERANCES: ANGLES ± DECIMALS .XX ± DECIMALS .XXX ± RIVET & BOLT EDGE MARG ±.05 BEND RADII ±.01 ON .03 & .05 ±.05 ON .08 & GREATER SHEET METAL CORNER RADII INT 1/16 EXT .25 .00	REVIEW & APPROVAL DWG QUAL STRUCT MATL & PROC CHANGE/ITEM NUMBER	CONTRACT NUMBER DWN BOB NELSON 8/4/75 CHK [illegible] ENGR [illegible] ORG PROJECT APPROVAL	THE BOEING COMPANY CORPORATE OFFICES SEATTLE, WASHINGTON 98124 GAS PLASMA STERILIZER SIZE D CODE IDENT NO. 81205 29-50548 SCALE NONE SH 5

DWG ORIG BY (ORG) 2-5640

DRAWING RECORDS CLERK

DD 8000 1228 ORIG 4/75

29-50548 REV

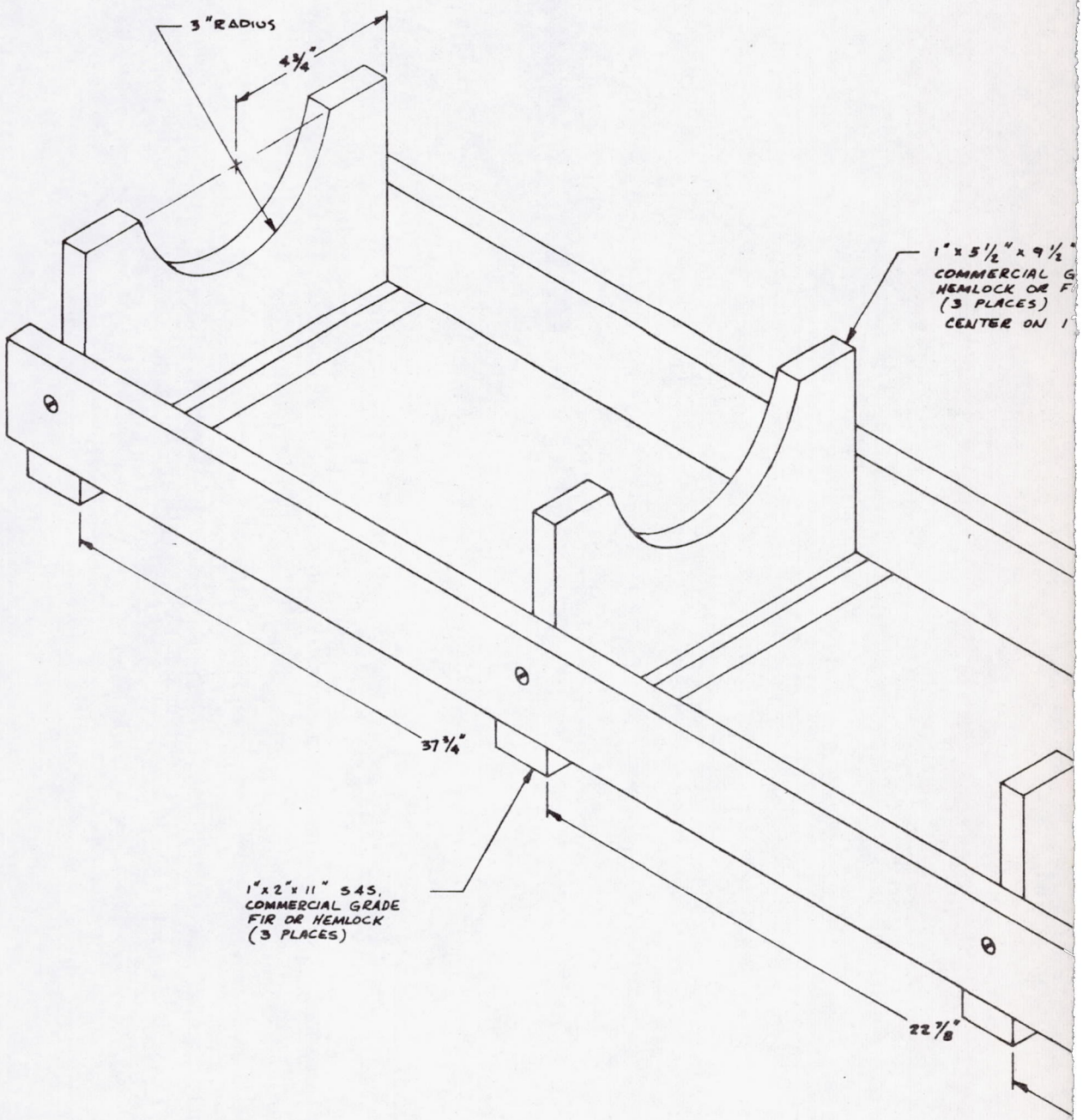
3" RADIUS
4¾"
1" x 5½" x 9½"
COMMERCIAL G
HEMLOCK OR F
(3 PLACES)
CENTER ON 1
37¾"
1" x 2" x 11" S4S,
COMMERCIAL GRADE
FIR OR HEMLOCK
(3 PLACES)
22⅞"

DETAIL - 7

REVISIONS			
LTR	DESCRIPTION	DATE	APPROVED

S4S
RADE
R

x 2"

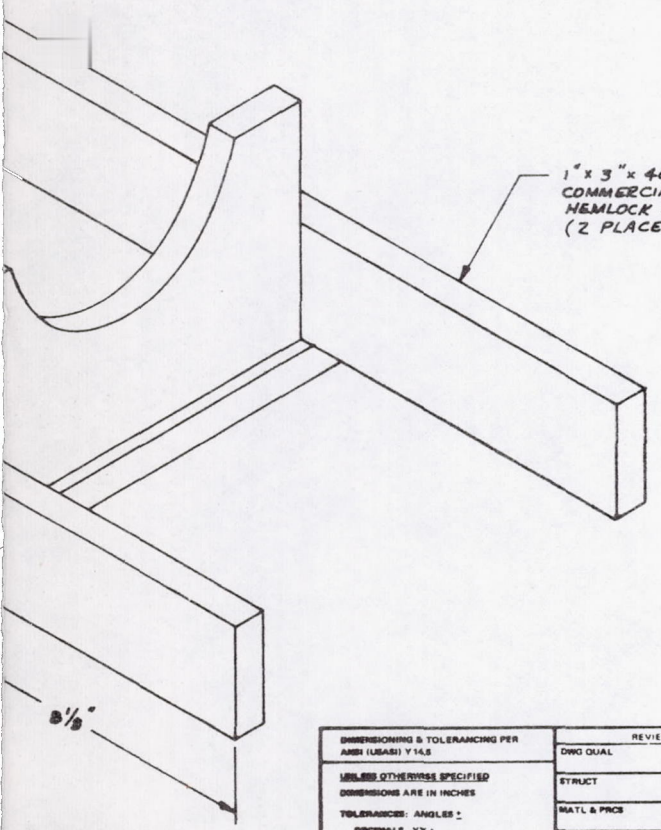

NOTE: ASSEMBLE WITH #8 FLAT HEAD WOOD SCREWS AS REQUIRED

FOR PARTS LIST AND APPLICATION DATA SEE PL

DIMENSIONING & TOLERANCING PER ANSI (USAS) Y14.5 UNLESS OTHERWISE SPECIFIED DIMENSIONS ARE IN INCHES TOLERANCES: ANGLES ± DECIMALS .XX ± DECIMALS .XXX ± RIVET & BOLT EDGE MARG ±.05 BEND RADII ±.01 ON .03 & .05 ±.02 ON .09 & GREATER SHEET METAL CORNER RADII INT .10 .16 EXT .35 .48	REVIEW & APPROVAL DWG QUAL STRUCT MATL & PRCS CHARGE/ITEM NUMBER	CONTRACT NUMBER DWN BOB NELSON 8/4/75 CHK [illegible] 8/21/75 ENGR [illegible] 8-21-75 ORG PROJECT APPROVAL [illegible] 8-21-75	THE BOEING COMPANY CORPORATE OFFICES SEATTLE, WASHINGTON 98124 GAS PLASMA STERILIZER SIZE D CODE IDENT NO. 81205 29-50548 SCALE NONE SH 6

DRIG ORIG BY (ORG) 2-5640

29-50548 REV

DRAWING RECORDS CLERK: DD 6888 1328 OR66 4/79

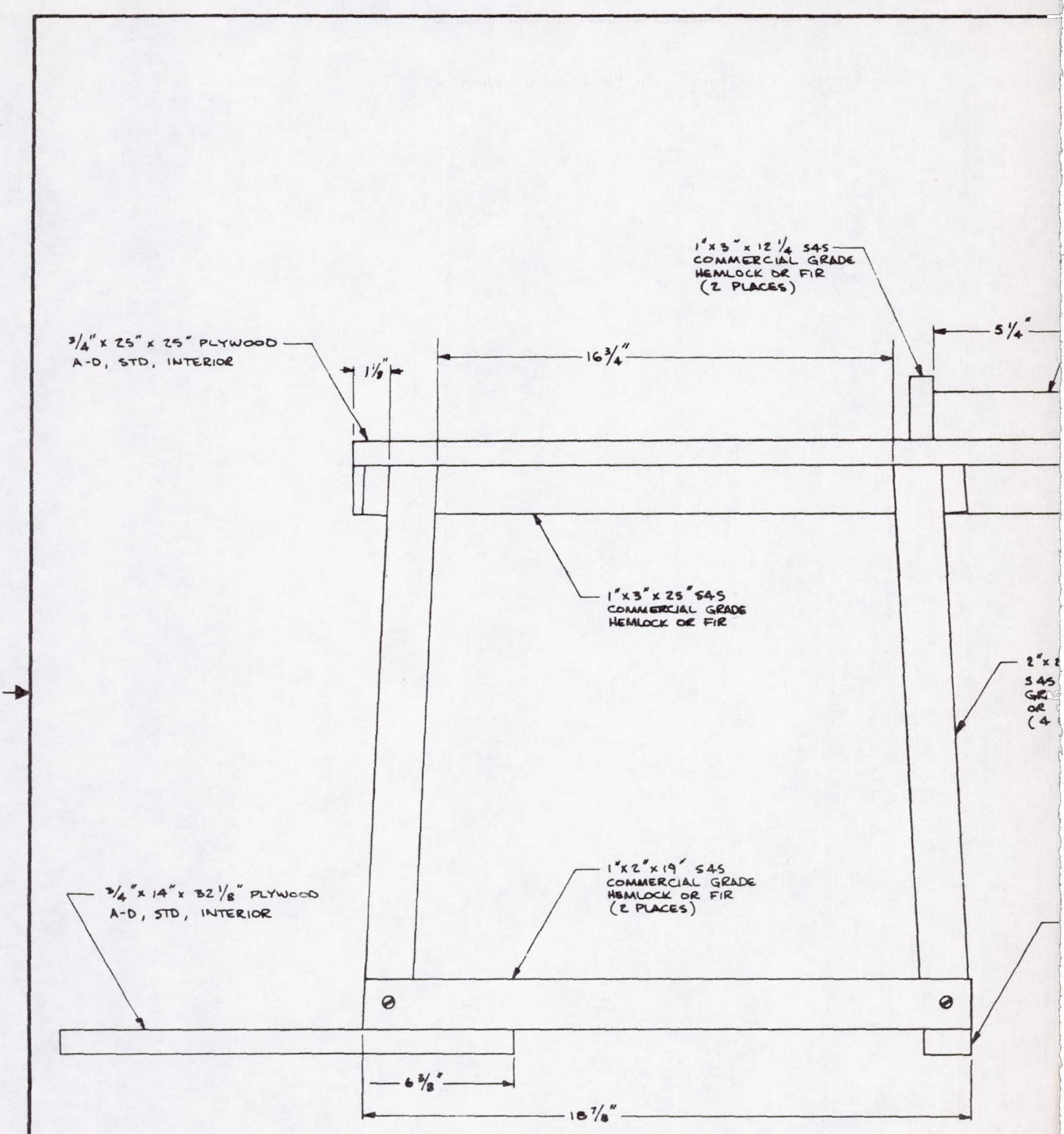

FRONT VIEW
DETAIL - 8

REVISIONS			
LTR	DESCRIPTION	DATE	APPROVED

NOTE : ASSEMBLE WITH #8 FLAT HD WOOD SCREWS AS REQUIRED.

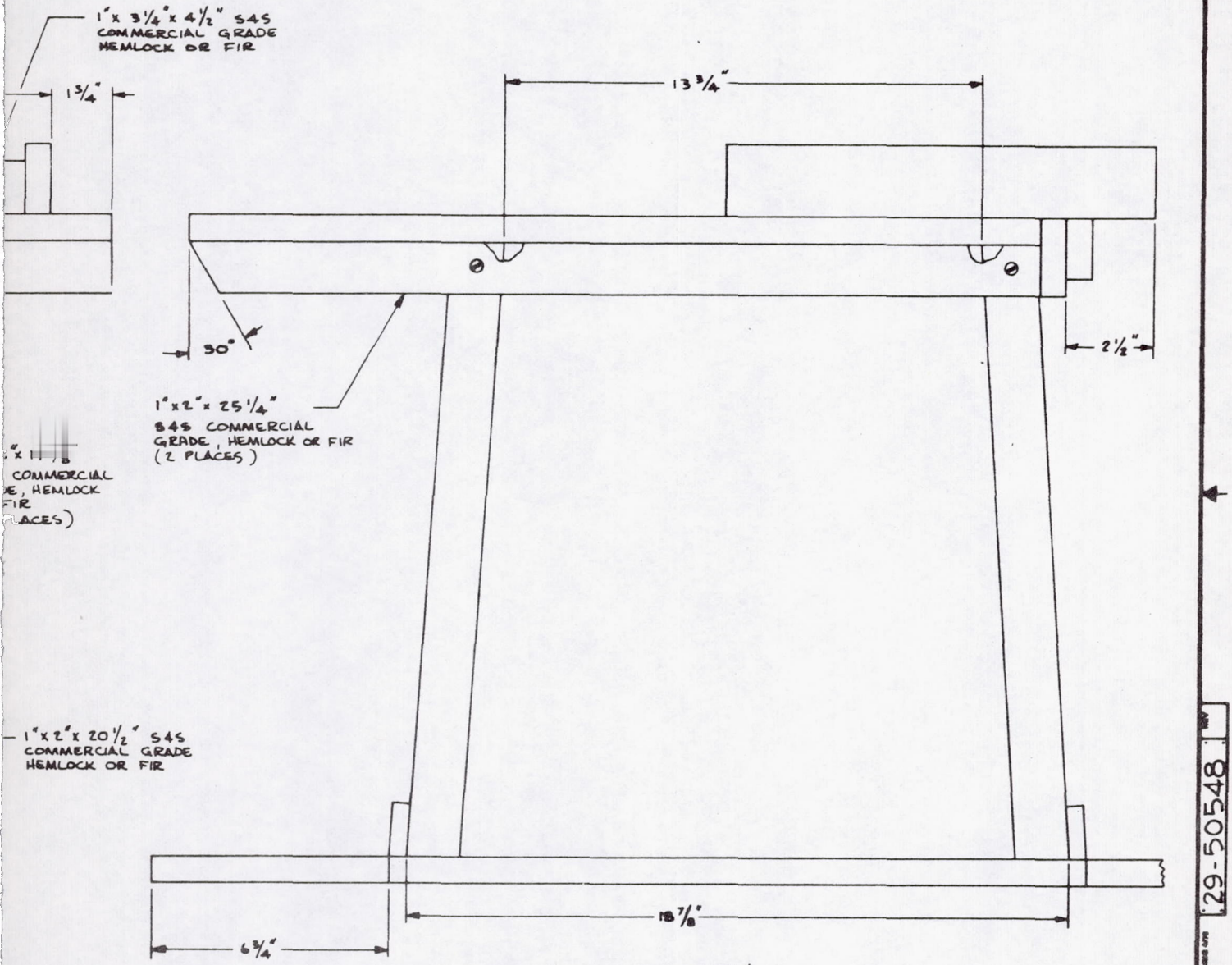

SIDE VIEW

FOR PARTS LIST AND APPLICATION DATA SEE PL

DIMENSIONING & TOLERANCING PER ANSI (USASI) Y 14.5	REVIEW & APPROVAL	CONTRACT NUMBER	THE BOEING COMPANY
UNLESS OTHERWISE SPECIFIED DIMENSIONS ARE IN INCHES	DWG QUAL		CORPORATE OFFICES SEATTLE, WASHINGTON 98124
TOLERANCES: ANGLES ±	STRUCT	DWN Bob Nelson 8/4/75	GAS PLASMA STERILIZER
DECIMALS .XX ±	MATL & PRCS	CHK [illegible] 8/14/75	
DECIMALS .XXX ±		ENGR Shirley Fraser 8-21-75	
RIVET & BOLT EDGE MARG ± .05		ORG	
BEND RADII ± .01 ON .03 & .06 ± .05 ON .09 & GREATER		PROJECT APPROVAL [illegible] 9-24-75	SIZE D CODE IDENT NO. 81205 29-50548
SHEET METAL CORNER RADII INT .10 .16 EXT .25 .00	CHANGE/ITEM NUMBER		SCALE NONE SH. 7

DWG ORIG BY (ORIG) 2-5640

DRAWING RECORDS CENTER

29-50548

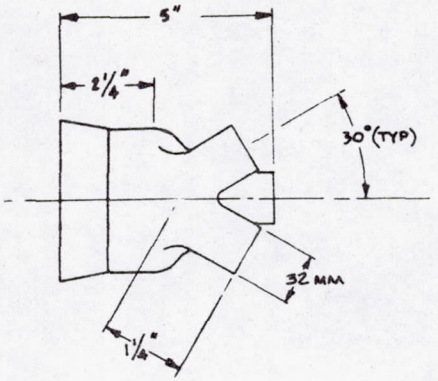

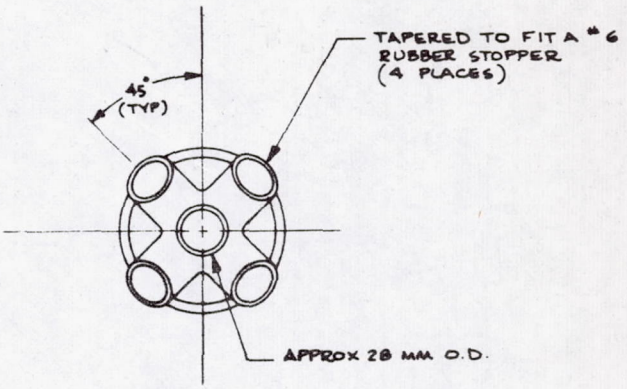

DETAIL -9

(MAKE FROM STD 75MM DIA FLANGE, PYREX GLASS)

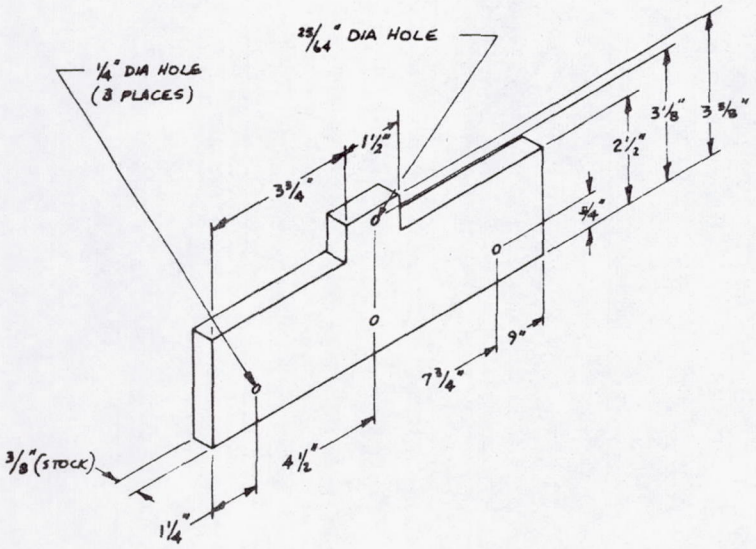

DETAIL -10

(PHENOLIC)

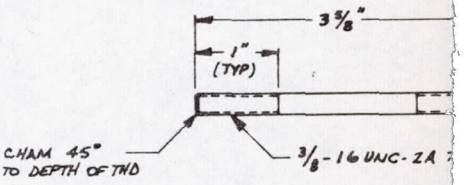

DETAIL -12

(3/8" DIA NYLON RO

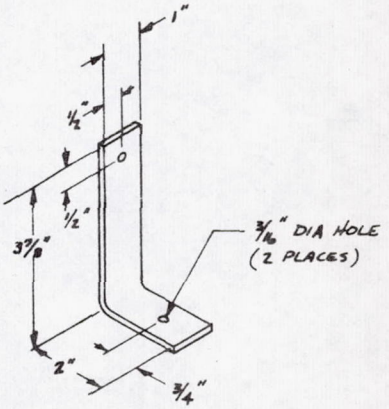

DETAIL -11

1/8" AL SH. 2024-T4 OR 6061-T0 BEND RADIUS 1/4"

REVISIONS

LTR	DESCRIPTION	DATE	APPROVED

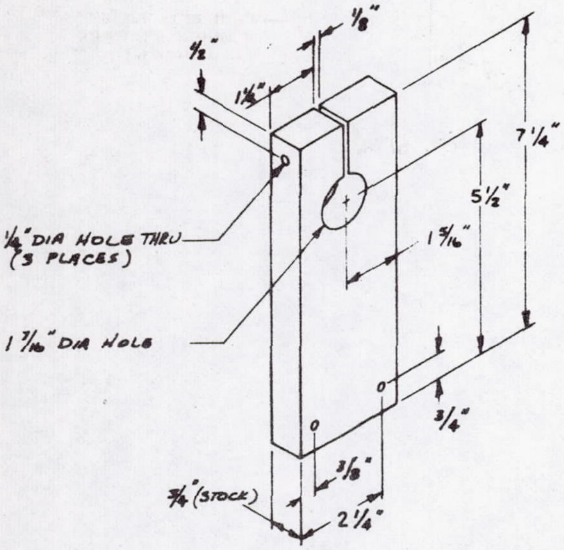

DETAIL -13
1"x 3" S4S COMMERCIAL GRADE, HEMLOCK OR FIR

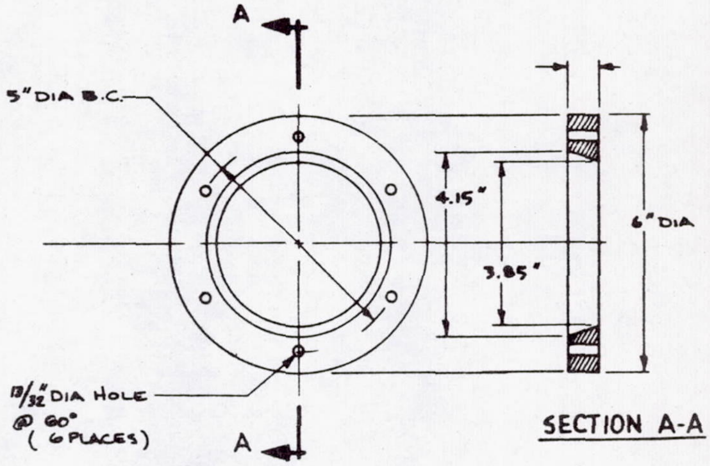

SECTION A-A

DETAIL -15
(PHENOLIC)

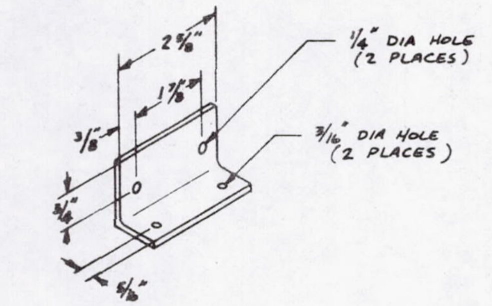

DETAIL -14
(AL ANGLE 1"x 1 1/2" x 1/8" 2024-T4 OR 6061-T6)

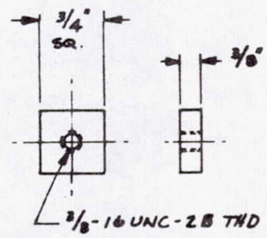

DETAIL -16
(PHENOLIC)

FOR PARTS LIST AND APPLICATION DATA SEE PL

DIMENSIONING & TOLERANCING PER ANSI (USASI) Y 14.5 UNLESS OTHERWISE SPECIFIED DIMENSIONS ARE IN INCHES TOLERANCES: ANGLES ± DECIMALS .XX ± DECIMALS .XXX ± RIVET & BOLT EDGE MARG ± .05 BEND RADII ± .01 ON .03 & .06 ± .03 ON .06 & GREATER SHEET METAL CORNER RADII INT .19 .16 EXT .38 .00	REVIEW & APPROVAL DWG QUAL STRUCT MATL & PRCS CHANGE/ITEM NUMBER	CONTRACT NUMBER DWN BOB NELSON 8/4/75 CHK [illegible] 7-[illegible]-75 ENGR Shila [illegible] 8-21-75 ORG PROJECT APPROVAL [illegible] 8-21-75	THE BOEING COMPANY CORPORATE OFFICES SEATTLE, WASHINGTON 98124 GAS PLASMA STERILIZER SIZE D CODE IDENT NO. 81205 29-50548 SCALE NONE SH. 8

29-50548 REV

DG 6000 1235 ORIG 4/72

DRAWING RECORDS (ILLEG)

DWG ORIG BY (ORG) 2-5640

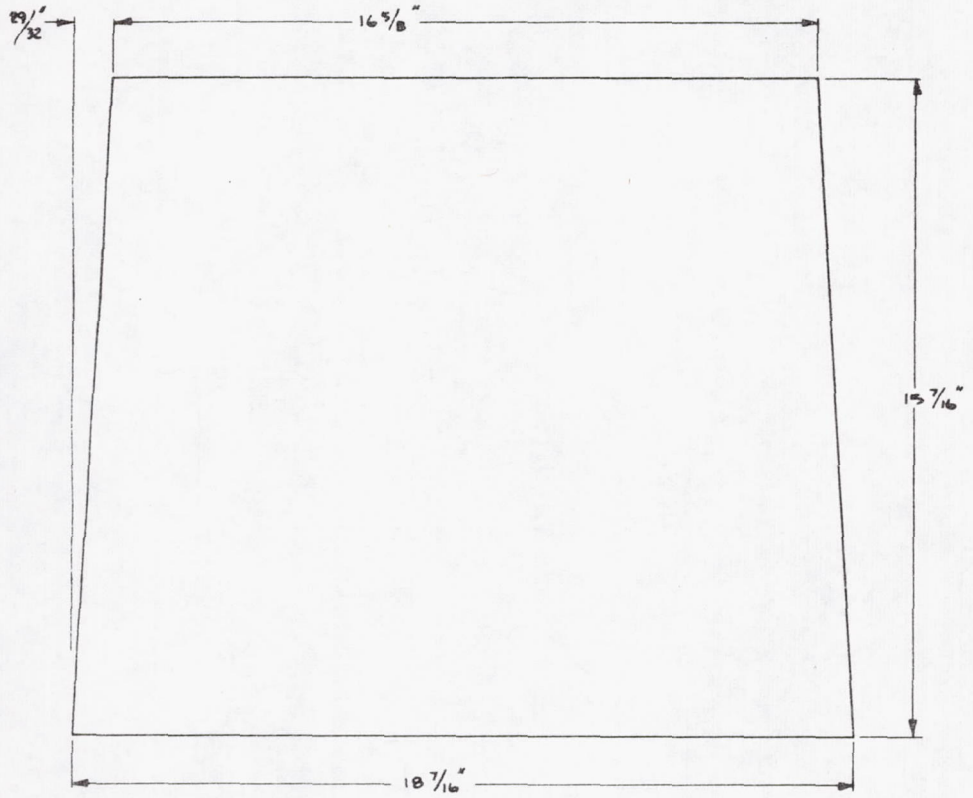

DETAIL -17

1/4" PLEXIGLAS

REVISIONS			
LTR	DESCRIPTION	DATE	APPROVED

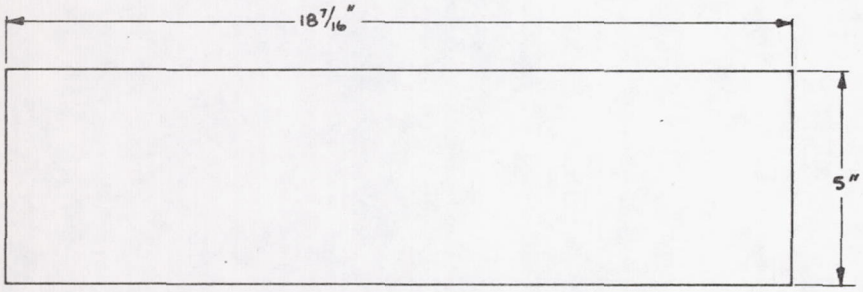

DETAIL -18

1/4" PLEXIGAS

29-50548

FOR PARTS LIST AND APPLICATION DATA SEE PL

DIMENSIONING & TOLERANCING PER ANSI (USASI) Y14.5 UNLESS OTHERWISE SPECIFIED DIMENSIONS ARE IN INCHES TOLERANCES: ANGLES ± DECIMALS .XX ± DECIMALS .XXX ± RIVET & BOLT EDGE MARG ± .05 BEND RADII ± .01 ON .03 & .05 ± .03 ON .09 & GREATER SHEET METAL CORNER RADII INT 1/16 EXT .05 .09	REVIEW & APPROVAL DWG QUAL STRUCT MATL & PRCS CHANGE/ITEM NUMBER	CONTRACT NUMBER DWN BOB NELSON 8/4/75 CHK [illegible] ENGR [illegible] 8-21-75 ORG PROJECT APPROVAL [illegible]	THE BOEING COMPANY CORPORATE OFFICES SEATTLE, WASHINGTON 98124 GAS PLASMA STERILIZER SIZE D CODE IDENT NO. 81205 29-50548 SCALE NONE SH. 9

DWG ORIG BY (ORG) 2-5640

DRAWING RECORDS CLERK:

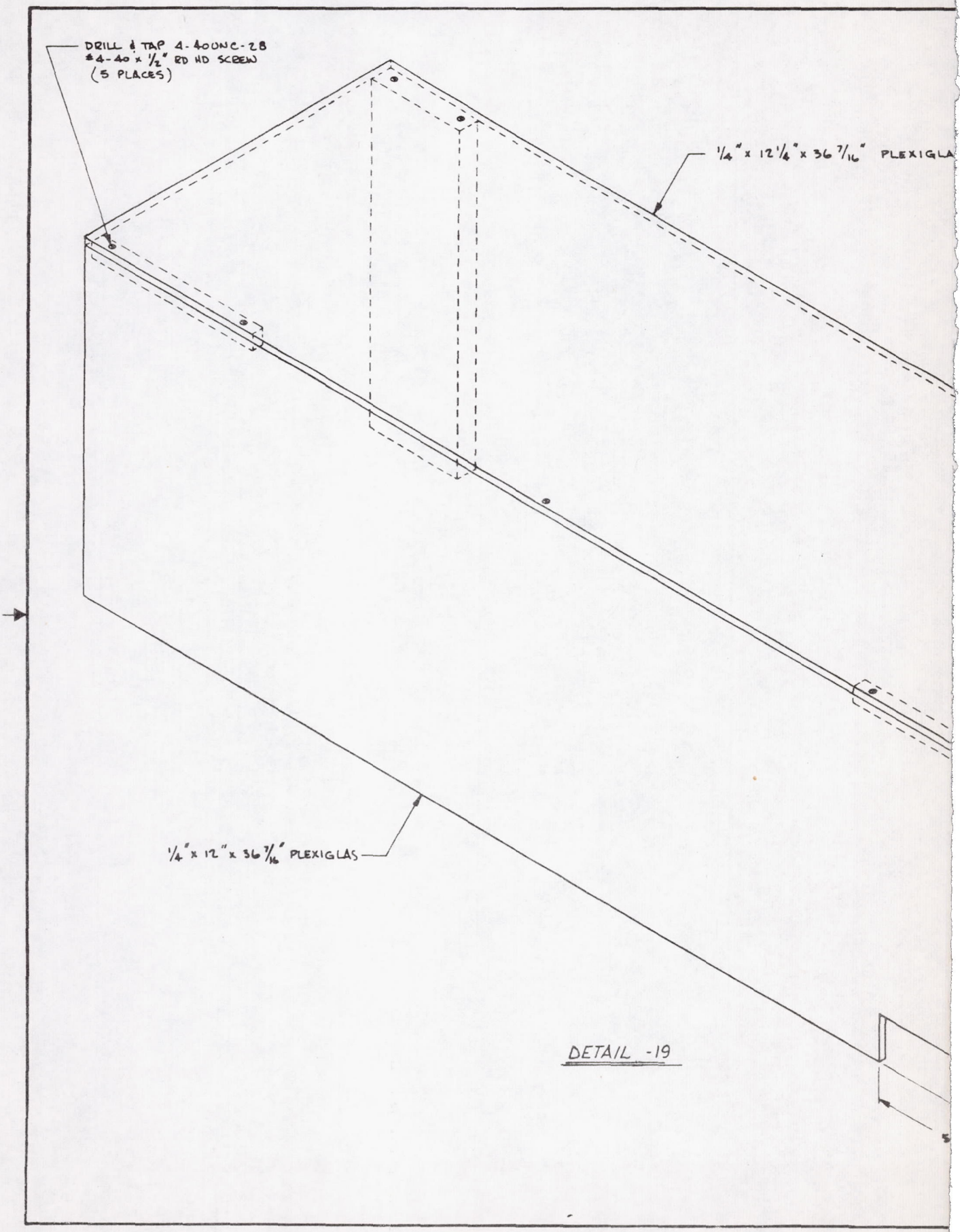
DRILL & TAP 4-40UNC-2B
#4-40 x 1/2" RD HD SCREW
(5 PLACES)
1/4" x 12 1/4" x 36 7/16" PLEXIGLA
1/4" x 12" x 36 7/16" PLEXIGLAS

DETAIL -19

REVISIONS			
LTR	DESCRIPTION	DATE	APPROVED

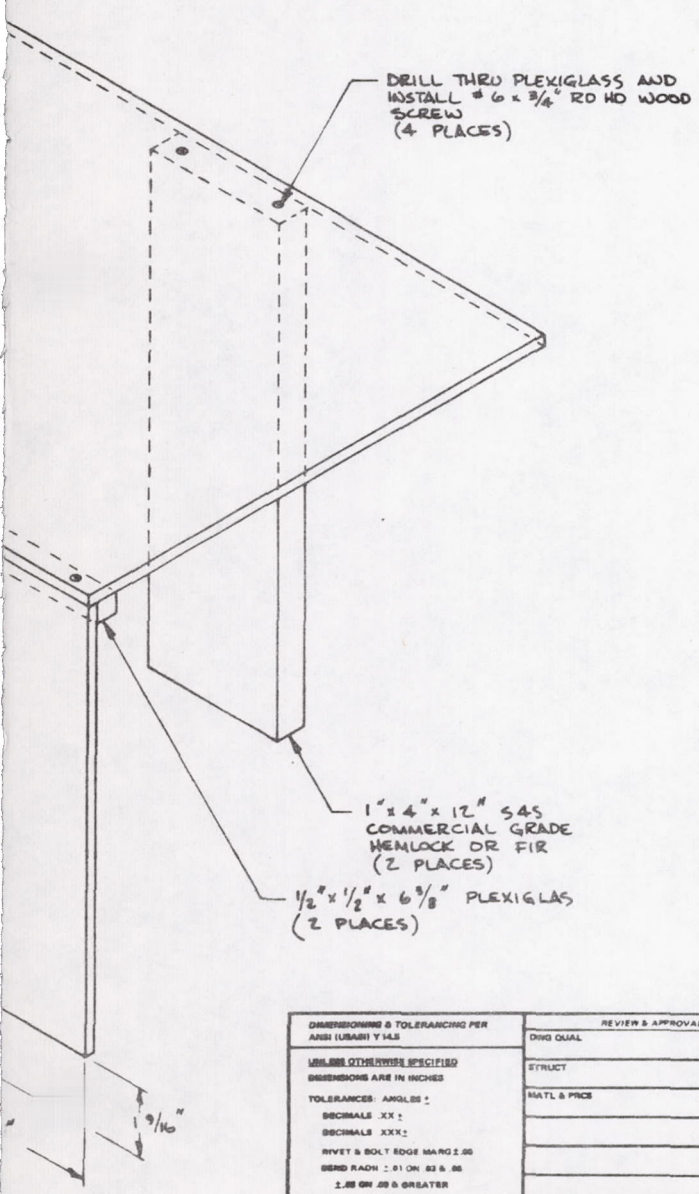

NOTE: BOND PLEXIGLAS PER BAC 5038 USING PS-18 CEMENT, PER MIL-A-25055 CADILLAC PLASTIC & CHEMICAL CO., SAN FRANCISCO, CALIF.

FOR PARTS LIST AND APPLICATION DATA SEE PL

DIMENSIONING & TOLERANCING PER ANSI (USASI) Y 14.5	REVIEW & APPROVAL	CONTRACT NUMBER	THE BOEING COMPANY
UNLESS OTHERWISE SPECIFIED DIMENSIONS ARE IN INCHES	DWG QUAL		CORPORATE OFFICES SEATTLE, WASHINGTON 98124
TOLERANCES: ANGLES ±	STRUCT	DWN BOB NELSON 8/4/75	GAS PLASMA STERILIZER
DECIMALS .XX ±	MATL & PROC	CHK [illegible] 8/21/75	
DECIMALS .XXX ±		ENGR Sheila Fraser 8-21-75	
RIVET & BOLT EDGE MARG ± .06		ORG	
BEND RADII ± .01 ON .03 & .06 ± .05 ON .09 & GREATER		PROJECT APPROVAL [illegible] 8-21-75	
SHEET METAL CORNER RADII INT .10 .16 EXT .25 .06	CHANGE/ITEM NUMBER		SIZE D CODE IDENT NO. 81205 29-50548 SCALE NONE SH. 10

DWG ORIG BY (ORG) 2-5640

DRAWING RECORDS CLOSED

29-50548 REV

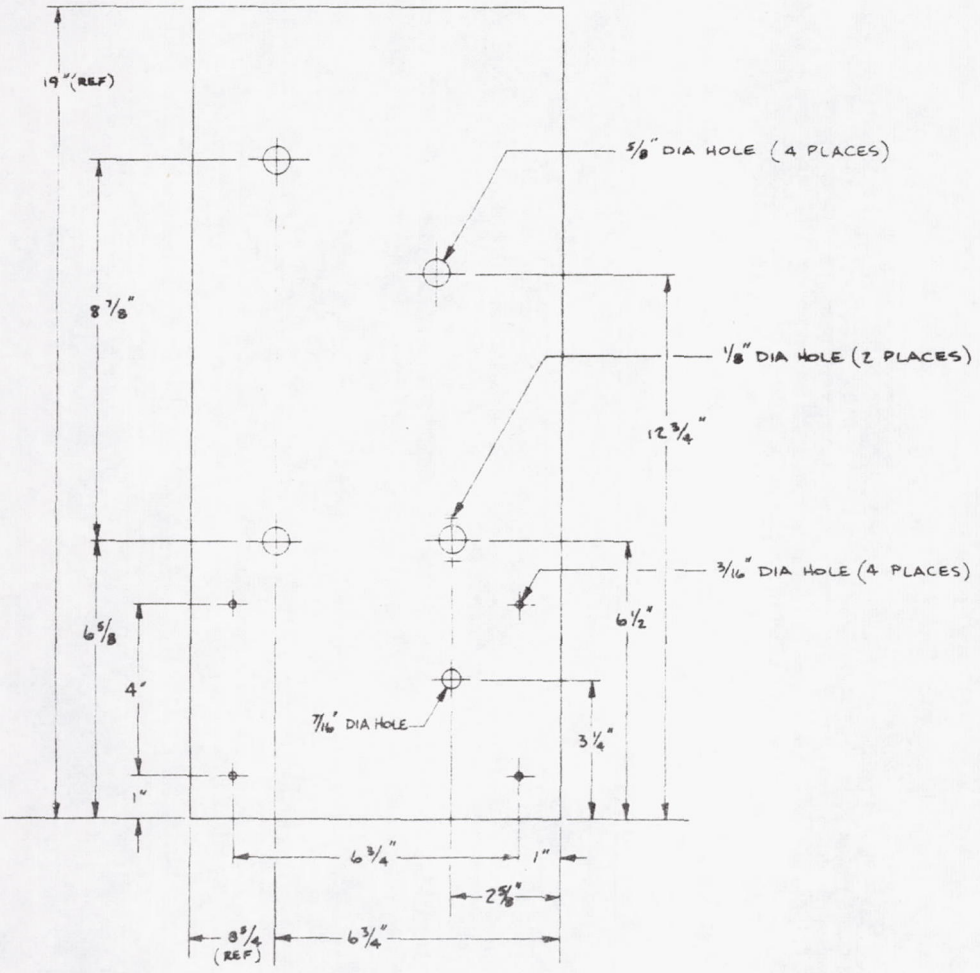

DETAIL -20

(MAKE FROM BUD RADIO PART NO. 1105 NG)

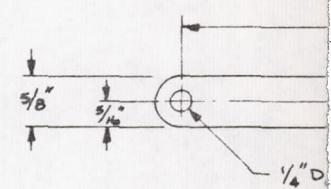

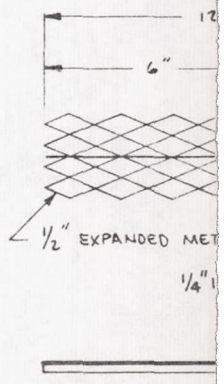

REVISIONS			
LTR	DESCRIPTION	DATE	APPROVED

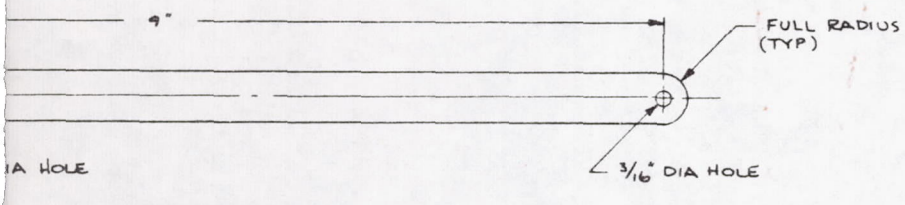

DETAIL -21
(1/16" COPPER SHEET)

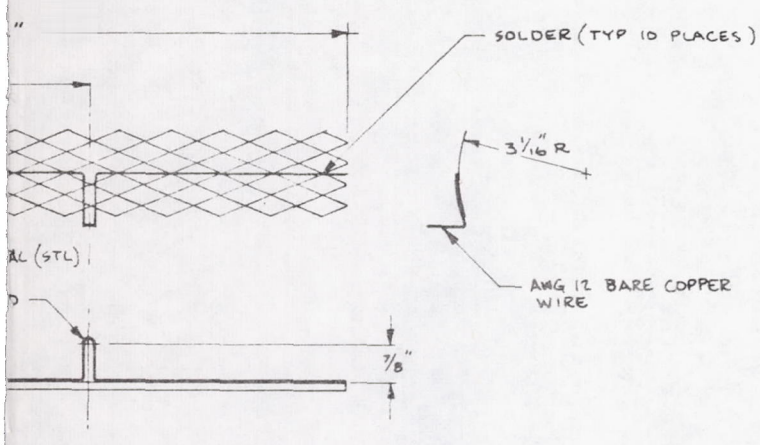

DETAIL -22

FOR PARTS LIST AND APPLICATION DATA SEE PL

DIMENSIONING & TOLERANCING PER ANSI (USASI) Y14.5 UNLESS OTHERWISE SPECIFIED DIMENSIONS ARE IN INCHES TOLERANCES ANGLES ± DECIMALS .XX ± DECIMALS .XXX ± RIVET & BOLT EDGE MARG ± .06 BEND RADII ±.01 ON .06 & .08 ±.02 ON .09 & GREATER SHEET METAL CORNER RADII INT 1/16 EXT .25/.00	REVIEW & APPROVAL DWG QUAL STRUCT MATL & PROC CHARGE/ITEM NUMBER	CONTRACT NUMBER DSGN BOB NELSON 8/4/75 CHK ENGR ORG PROJECT APPROVAL	THE BOEING COMPANY CORPORATE OFFICES SEATTLE, WASHINGTON 98124 GAS PLASMA STERILIZER SIZE D CODE IDENT NO 81205 29-50548 SCALE NONE SH 11

DWG ORIG BY [illegible] 2-5640

29-50548 REV

DD 8000 1228 OR10 4/73

DRAWING RECORD CLERK